Dissertation

Submitted to the

Combined faculties for the Natural Sciences and for Mathematics of the

Ruperto-Carola University of Heidelberg, Germany

For the degree of

Doctor of Natural Sciences

Presented by

Diplom-Biology: Rizos-Georgios Manikas

Born in: Athens, Greece

Oral examination:

Nug1 is a potassium-stimulated GTPase affecting the association of early 60S assembly factors in ribosome biogenesis

Referees: Prof. Dr. E.C. Hurt

Prof. Dr. M. Brunner

To my parents

Acknowledgments

First I would like to thank my supervisor Prof. Dr. Hurt for having me in his lab and trusting me with this PhD work.

Thanks to all members of the Hurt lab, former and new ones, with whom I shared so much time throughout the years. Thanks to Dr. Bebiana Moura and Dr. Nikola Kellner, who read and gave me helpful feedback on my thesis.
Special thanks go to Dr. Emma Thomson for her support, scientific discussions, but mostly for all the help and suggestions she kindly offered in the final steps of the thesis writing. She's not only a lab-buddy, but also a true friend. Thanks to Lucy Dimitrova and her temperament for the fun we had in the lab. Thanks to Roman Teimer, my NPC-buddy and good friend, for the non-scientific discussions and for all the fun we had in and out of the lab. The stories about midget albino elephants living in the Blackwood forest are all true.

Thanks to all the friends I made during my staying in Heidelberg, they made it easier. Special thanks to Thomas Minor for his understanding and genuine support in my life outside the lab. Thanks to Dimitris Liakopoulos my Greek buddy, with whom I've finished a lot of Grauburgunder bottles, while complaining about my project.

Finally, I want to thank my family, my mum and dad and of course my sister for all of the phone calls, messages, Skype sessions and parcels from Greece…but mostly for their unconditional love and support. I'm grateful, thank you.

Table of Contents

Summary

Ribosomes are complex macromolecular machineries responsible for protein synthesis (translation) in all living cells. In yeast, they are composed of four rRNA species assembled with 79 ribosomal proteins to form the small (40S) and the large (60S) subunit. To reach their final translation-competent form, they go through a complex, highly dynamic and coordinated process termed ribosome biogenesis. In eukaryotes, more than 180 transiently associating non-ribosomal factors (assembly factors) and 70 small nucleolar RNAs (snoRNAs) are involved in rRNA processing and modifications, as well as in the assembly of r-proteins (Henras et al., 2008; Lafontaine and Tollervey, 2001; Staley and Woolford, 2009). Several of the 60S ribosome biogenesis factors belong to the superfamily of GTPases, including Nug1. Nug1 is a circularly permuted GTPase and an essential *trans*-acting factor in ribosome biogenesis. It co-purifies with various nucleolar and nucleoplasmic pre-ribosomal particles and exhibits RNA-binding properties (Bassler et al., 2001; Bassler et al., 2006). However, several questions remained open regarding the exact role of Nug1 in ribosome biogenesis, including the regulation of its enzymatic GTPase activity, its binding site on the pre-ribosome, as well as a possible role in the recruitment and/or release of other 60S assembly factors.

During my PhD studies, I performed a series of *in vitro* GTPase and nucleotide binding assays using the *C. thermophilum* (*Ct*Nug1) orthologue to address Nug1's enzymatic activity. With these, I showed that *Ct*Nug1 exhibits a low intrinsic GTPase activity that can be stimulated by potassium ions, rendering Nug1 a cation-dependent GTPase. I've also generated a series of point mutations in the G-domain that specifically inhibit GTP hydrolysis or nucleotide binding. The orthologous mutations in the yeast Nug1 GTPase domain were subsequently tested for their effects on ribosome biogenesis. Early 60S assembly factors including Dbp10, Spb1, Nop2 and Mrt4 associated less with affinity purified pre-ribosomal particles, when the Nug1 nucleotide-binding mutant (D446N) was expressed or when Nug1 was depleted. Interestingly, no growth defects or biochemical differences in pre-ribosomal particle composition were observed for the catalytic

(G339A) mutant, suggesting that the GTP hydrolysis is not essential for Nug1's function.

From the early assembly factors affected, only the essential RNA helicase Dbp10 was genetically linked to Nug1 (Bassler et al., 2001). In collaboration with Dr. Emma Thomson, we identified the binding sites of Nug1 and Dbp10 onto the pre-ribosome using the CRAC technique. Both proteins were found to bind in close proximity to each other on the interface of the 60S subunit at the PTC area. Further, *in vitro* binding assays confirmed a physical interaction between Nug1 and Dbp10.

Together the findings from my PhD thesis show that Nug1 affects the dynamic interplay of assembly factors including those localizing to the PTC area (Dbp10, Sbp1, Nop2, Nsa2), as well as factors involved in the P-stalk formation (Mrt4, Yvh1, Rpp0, Rpl12). In this interplay, the Nug1 binds at the base of helix 89 and may act as a molecular GTPase switch that mediates the crosstalk between the maturation of PTC and the P-stalk, two distinct and essential hallmarks of the 60S subunit.

Zusammenfassung

Ribosomen sind komplexe makromolekulare Maschinen, die für die Proteinbiosynthese (Translation) in allen lebenden Zellen zuständig sind. Die Ribosomen der Hefe setzen sich aus vier RNA-Spezies und 79 ribosomalen Proteinen zusammen, welche die kleine (40S) und große (60S) Untereinheit formen. Um ihre endgültige, translationskompetente Form anzunehmen, müssen sie einen komplexen, hochdynamischen und streng koordinierten Prozess durchlaufen, der Ribosomenbiogenese genannt wird. In Eukaryoten sind mehr als 180 vorübergehend assoziierte, nicht-ribosomale Faktoren (Assemblierungsfaktoren) und 70 small nucleolar RNAs (snoRNAs) an der Weiterverarbeitung und Modifizierung von rRNAs sowie an der Assemblierung von r-Proteinen beteiligt. Mehrere 60S Biogenesefaktoren gehören zur Superfamilie der GTPasen – so auch Nug1. Nug1 ist eine zyklisch permutierte GTPase und ein essentieller *trans*-wirkender Faktor der Ribosomenbiogenese. Es wird mit verschiedenen nukleolären und nukleoplasmischen prä-ribosomalen Partikeln co-aufgereinigt und verfügt über RNA-bindende Eigenschaften. Mehrere Fragen bezüglich der genauen Rolle von Nug1 in der Ribosomenbiogenese blieben bisher jedoch unbeantwortet, darunter die Regulierung der enzymatischen GTPase Aktivität, die Bindestelle auf dem Prä-Ribosom und eine mögliche Rolle in der Rekrutierung und/oder der Freisetzung von anderen 60S Assemblierungsfaktoren.

In meiner Doktorarbeit habe ich eine Reihe von *in vitro* GTPase- und Nukleotid-Bindeassays mit dem *C. thermophilum* Nug1 Ortholog (*Ct*Nug1) durchgeführt, um die enzymatische Aktivität von Nug1 zu untersuchen. Mit diesen Studien konnte ich zeigen, dass *Ct*Nug1 über eine geringe intrinsische GTPase-Aktivität verfügt, die von Kaliumionen stimuliert wird; d.h. Nug1 ist eine Kationen-abhängige GTPase. Ich habe außerdem eine Reihe von Punktmutationen in der G-Domäne generiert, die spezifisch die GTP Hydrolyse oder die Nukleotidbindung inhibieren. Anschließend wurden die orthologen Mutationen in der GTPase-Domäne von Hefe Nug1 erzeugt und ihre Auswirkungen auf die Ribosomenbiogenese untersucht. Frühe Assemblierungsfaktoren wie Dbp10, Spb1 und Mrt4 sind mit geringerer Affinität an aufgereinigte prä-ribosomale Partikel assoziiert, wenn die

Nukleotid-binde-Mutante (D446N) von Nug1 exprimiert wird oder wenn Nug1 zuvor abgereichert wurde. Für die katalytische Mutante (G339A) konnten jedoch keine Wachstumsdefekte oder biochemische Unterschiede in der Zusammensetzung der prä-ribosomalen Partikel gefunden werden. Dies spricht dafür, dass die GTP Hydrolyse für die Funktion von Nug1 nicht essentiell ist.

Von den betroffenen frühen Assemblierungsfaktoren ist nur die essentielle RNA-Helikase Dbp10 genetisch mit Nug1 gekoppelt. In Kollaboration mit Dr. Emma Thomson konnten wir mit Hilfe des CRAC Verfahrens die Bindestellen von Nug1 und Dbp10 am Prä-Ribosom identifizieren. Beide Proteine befinden sich nahe beieinander an der Schnittstelle der 60S Untereinheit im Bereich des PTCs. *In vitro* Bindeassays bestätigten eine physikalische Interaktion zwischen Nug1 und Dbp10.

Zusammen zeigen die Ergebnisse meiner Doktorarbeit, dass Nug1 das dynamische Zusammenspiel der Assemblierungsfaktoren, inklusive der PTC-lokalisierten Faktoren (Dbp10, Sbp1, Nop2, Nsa2) und derjenigen, die an der Ausbildung des P-Stalks beteiligt sind (Mrt4, Yvh1, Rpp0, Rpl12), beeinflusst. In diesem Wechselspiel bindet Nug1 and die Basis von Helix 89 und kann als molekularer GTPase Schalter wirken, der im Dialog der Entstehung von PTC und P-Stalk vermittelt, zweier ausgeprägter und essentieller Merkmale der 60S Untereinheit.

1.The Ribosome

1.1 General

Ribosomes, first observed by electron microscopy (EM) as dense cytoplasmic granules, are complex macromolecular machineries responsible for protein synthesis (translation) in all living cells (Palade, 1955; Brachet and Jean. The Cell-Biochemistry, 1961). They associate together with the messenger RNA (mRNA), amino acylated transfer RNAs (aminoacyl-tRNAs) and a plethora of accessory proteins to form the translation machinery (Moore, 2009; Moore, 2012; Ramakrishnan, 2002). Although ribosomes from bacteria, archaea and eukaryotes (cytoplasmic, mitochondrial and chloroplast) differ in size, ribosomal RNA (rRNA) sequence, structure, and the ratio of protein to RNA, they universally perform the same fundamental function, i.e. converting the information encoded within mRNA into proteins (Moore, 2012) (Figure 1.1).

1.2 Composition of Prokaryotic and Eukaryotic ribosomes

Although ribosomes are characterized as unique macromolecular complexes for their universally conserved function, there are several differences in size and complexity among prokaryotes and eukaryotes. Due to the fact that most of the research in prokaryotic and eukaryotic ribosomes has been performed in *Escherichia coli* (*E. coli*) and *Saccharomyces cerevisiae* (*S. cerevisiae*) respectively, all numbers attributed to ribosome size, nucleotide- and protein-composition in the following sections are referring to those organisms, unless otherwise stated.

A complete ribosome (70S in prokaryotes and 80S in eukaryotes) is made of rRNA and proteins (r-proteins) in approximately a 2:1 ratio. In the complex and dynamic assembly the long rRNA chains form a scaffold upon which the different r-proteins bind (Bashan and Yonath, 2008). Ribosomes can be split into two unequal subunits, namely the large (LSU) and the small subunit (SSU) that differ in their sedimentation coefficients as measured in Svedberg units.

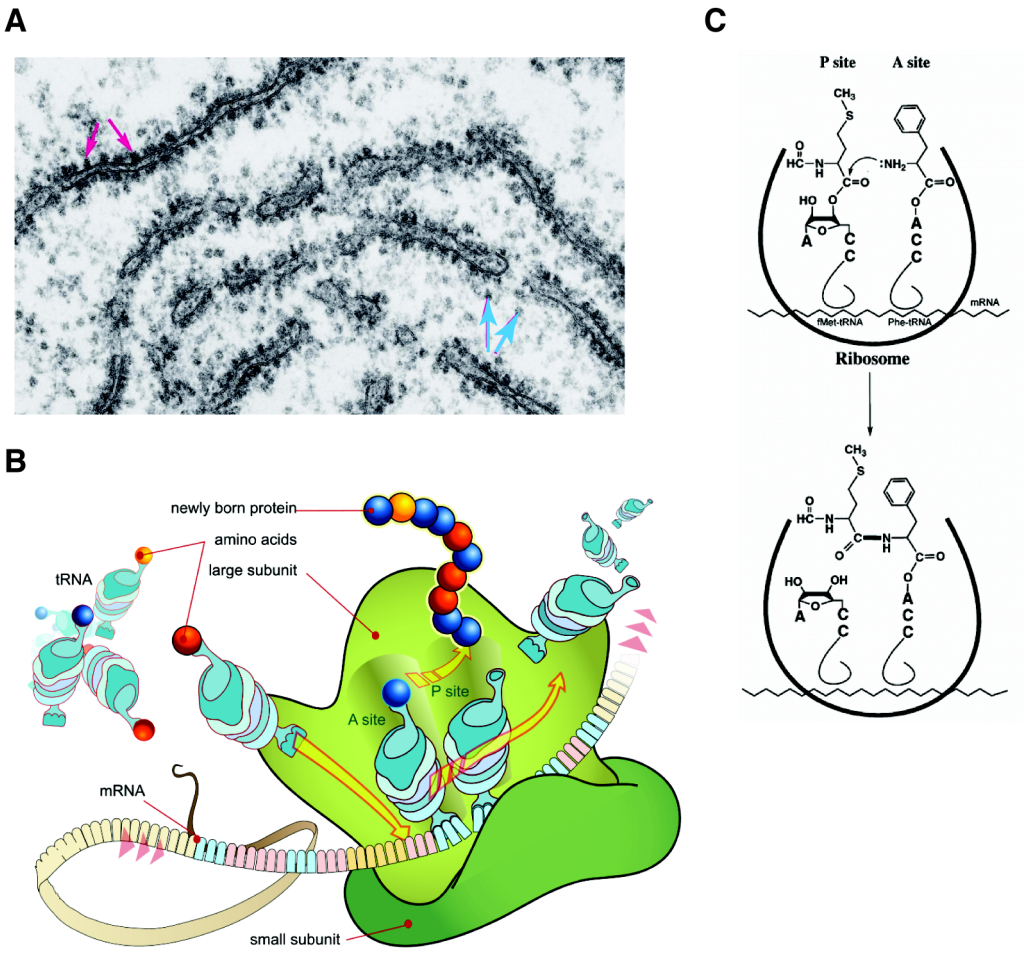

Figure 1.1 The ribosome. **A**) EM picture depicting ribosomes as dense cytoplasmic granules. Cyan and Pink arrows correspond to free and ER-bound ribosomes, respectively. **B**) Cartoon depicting a translating ribosome (adapted from BioBook_mRNA_translation). **C**) Peptide bond formation catalyzed by the ribosome (Zhang and Cech, 1997).

In prokaryotes, the 70S ribosome is about 2.3 MDa with a radius of 200 Å. It has a small subunit (30S) that contains a single rRNA chain the 16S and 21 different r-proteins, whereas the large subunit (50S) has two rRNA chains the 23S and 5S RNA and 34 different r-proteins (Ban et al., 2000; Traub et al., 1967; Yonath, 2002). In eukaryotes, the 80S ribosome is approximately 4 MDa in size with a radius of about 260 Å. It has a small subunit (40S) that contains a single rRNA molecule, the 18S and 33 different r-proteins, whereas the large 60S subunit has three rRNA molecules, the 25S, 5.8S and 5S RNA and 46 different r-proteins (Ben-Shem et al., 2011; Fromont-Racine et al., 2003) (Figure 1.2). In all domains of life the r-protein and rRNA content assemble together to form a very well conserved ribosomal core.

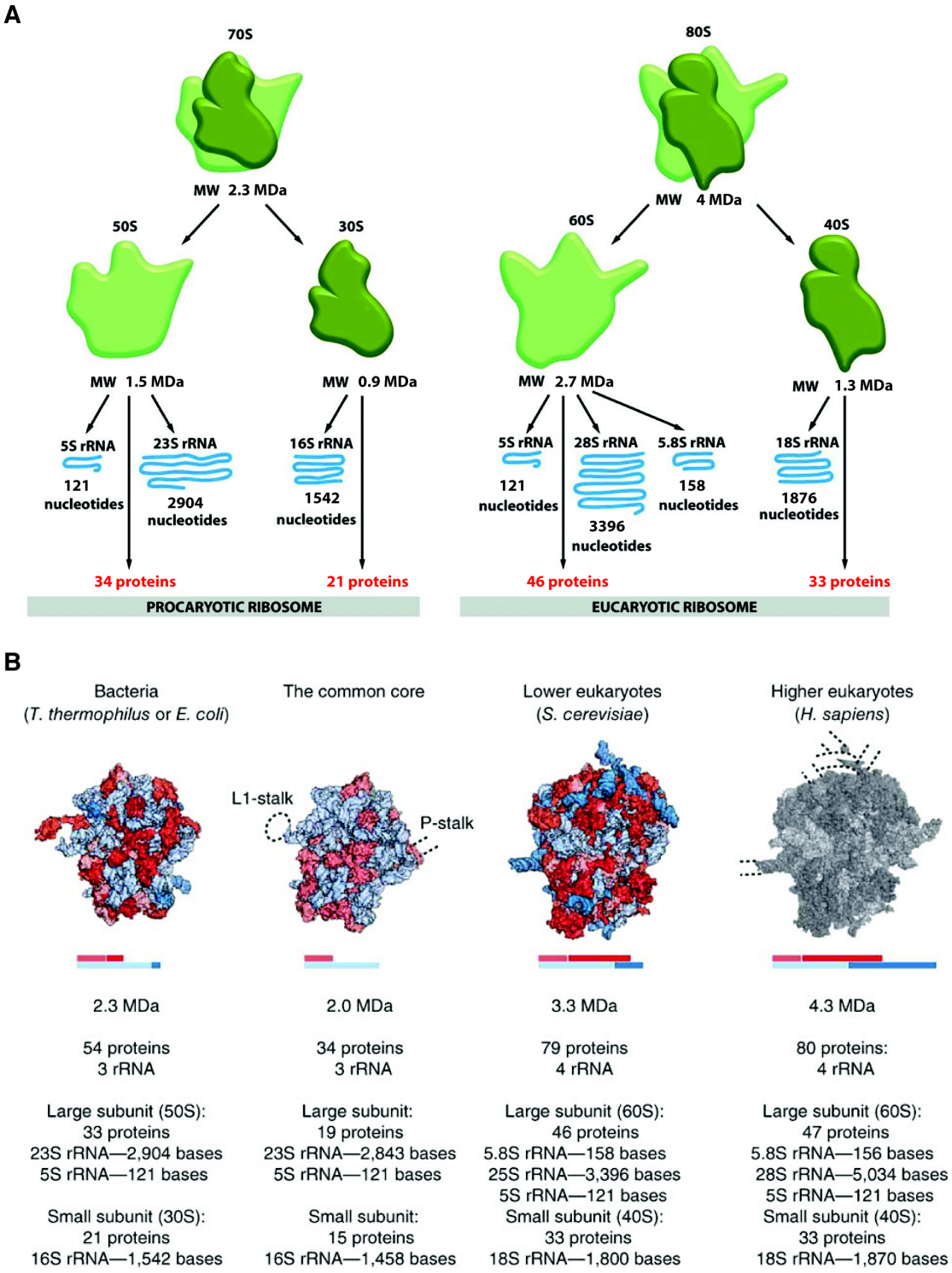

Figure 1.2 Comparison between prokaryotic and eukaryotic ribosome composition. A) The rRNA and protein composition of the ribosome (adapted from StudyblueMolecular exam3). **B**) Comparison between ribosomes from different domains of life (Melnikov et al., 2012).

The size differences between prokaryotic and eukaryotic ribosomes are mostly due to expansions segments (ES) present in the eukaryotic rRNA, as well as to additional ribosomal proteins selected through evolution (Chandramouli et al., 2008; Yokoyama and Suzuki, 2008). Furthermore, several eukaryotic r-proteins that have prokaryotic homologues carry insertions or extensions in their amino acid composition, thus forming eukaryote-specific sequences. These sequences are thought to buffer the additional negative charges of the eukaryotic rRNA ES, thus stabilizing its structure (Ben-Shem et al., 2011). Interestingly, a structural comparison between the *E. coli* and *S. cerevisiae* ribosomes revealed that the ribosomal surface free of eukaryotic specific domains, is actually conserved between all kingdoms of life and includes the G protein–binding platform, the rim of the peptide exit tunnel and the area around the mRNA entry site of the 40S (Ban et al., 2000; Ben-Shem et al., 2010).

1.3 Structural and functional aspects of the ribosome

In all organisms, the two ribosomal subunits are synthesized independently and associate to form functionally active ribosomes for translation. In brief, the small subunit is responsible for mRNA binding, ensuring the correct base pairing between anti-codons of charged tRNAs and codons of mRNAs, thus controlling the translation fidelity. The large subunit is mediating the catalysis of the peptide bond formation between the amino acids loaded onto the peptidyl-and aminoacyl-tRNAs in the peptyl-transferase center (PTC). Additionally, it is involved in the final hydrolysis of the peptidyl-tRNA and the release of the peptide chain. It also contains the exit tunnel through which the nascent polypeptide chains emerge, while it serves as a platform for factors that assist the initiation, elongation, and termination phases of protein synthesis (Ban et al., 2000; Bashan and Yonath, 2008; Steitz, 2008a; Steitz, 2008b).

General features of ribosomes were identified during the 1980's by EM. However it wasn't until atomic resolution crystal structures became available that the details were revealed. The description of the 40S subunit is based on anthropomorphic characteristics. A 'neck' is connecting the 'head' to the 'body', which contains a 'shoulder' and a 'platform'. In the case of the large subunit, a round

base with three almost cylindrical extensions has been described. These extensions are the L1 stalk, the central protuberance (CP) and the P-stalk, which together with the A, P and E site have important functional implications during translation, rendering the ribosome a dynamic machine (Figure 1.3 A)(Ben-Shem et al., 2011).

The L1-stalk is a flexible structural protuberance composed of L1 protein and rRNA helices (H76, H77 and H78) and it is associated with tRNA translocation during which it adopts open and closed conformations (Figure 1.3 B) (Ben-Shem et al., 2011; Trabuco et al., 2010). The P-stalk is a universally conserved lateral protuberance of the 60S subunit serving as a platform upon which translational GTPases bind and promote translation elongation (Figure 1.3 B) (Remacha et al., 1995a; Remacha et al., 1995b). In yeast it is a pentameric protein complex composed of acidic phosphoproteins (P-proteins), more specifically a single P0 bound by two different heterodimers of P1 and P2 (P1a–P2b and P1b–P2a) (Figure 1.3 C) (May et al., 2012) (for stalk assembly see section 1.4.8).

The CP is predominantly made from the 5S rRNA together with the ribosomal proteins Rpl5 on the solvent site of the LSU, Rpl11 and Helix89 on the interior site and the eukaryotic specific protein Rpl6 (Figure 1.3 B). It forms inter-subunit bridges with Rps13 r-protein of the SSU and upon mRNA translocation it undergoes structural rearrangements that are suggested to confer changes at other sites of the 60S subunit, including the L1 stalk (Ben-Shem et al., 2011; Dinman, 2005).

In contrast with the structural landmarks previously discussed, the A, P and E site of the ribosome, are only formed after subunit joining. As the ribosome moves towards the 3' end of the mRNA during translation, these sites are oriented in a 5’ to 3’ direction with respect to the mRNA, as E-P-A. The A site is the point of entry for the aminoacyl-tRNA (except for the first aminoacyl-tRNA, fMet-tRNAfMet, which enters at the P site). The P site is where the peptidyl tRNA is formed in the ribosome. And the E site is the exit site of the uncharged tRNA after offering its amino acid to the growing polypeptide chain (Moore and Steitz, 2003).

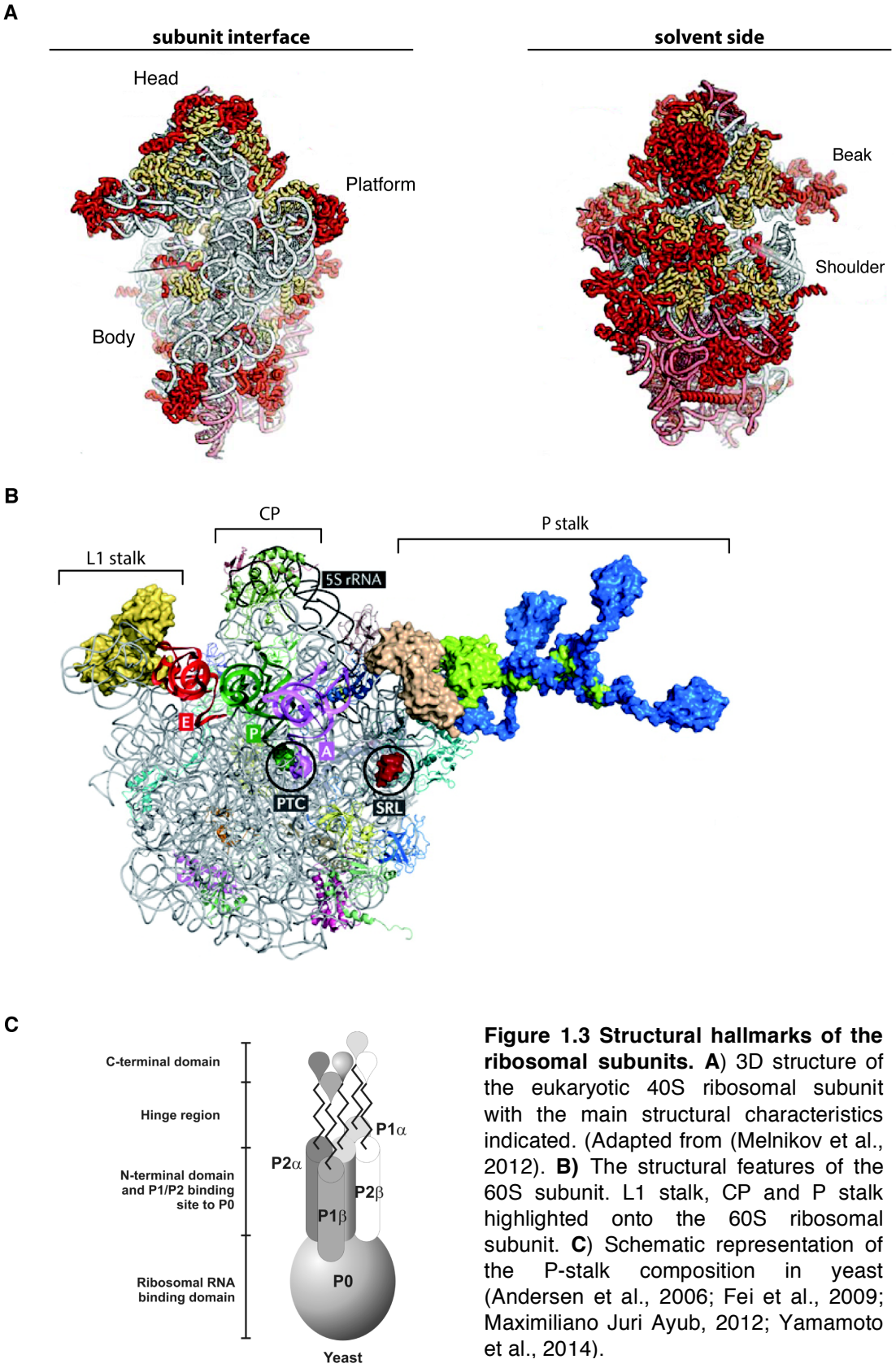

Figure 1.3 Structural hallmarks of the ribosomal subunits. A) 3D structure of the eukaryotic 40S ribosomal subunit with the main structural characteristics indicated. (Adapted from (Melnikov et al., 2012). **B)** The structural features of the 60S subunit. L1 stalk, CP and P stalk highlighted onto the 60S ribosomal subunit. **C**) Schematic representation of the P-stalk composition in yeast (Andersen et al., 2006; Fei et al., 2009; Maximiliano Juri Ayub, 2012; Yamamoto et al., 2014).

1.4 Ribosome biogenesis in *Saccharomyces cerevisiae*

1.4.1 General

Ribosome biogenesis is an essential, highly complex but precisely coordinated process occurring in all cells. Yeast ribosomes are assembled and processed sequentially in a pathway that takes place in different subcellular compartments including the nucleolus, the nucleoplasm and finally the cytoplasm. It begins with the transcription of a large precursor rRNA that is subsequently covalently modified and further processed to yield the mature 18S, 5.8S and 25S rRNAs. Together with the independently transcribed 5S rRNA and the 79 ribosomal proteins they are folded and assembled into functional ribosomes. All these steps take place in large ribonucleoprotein particles (RNPs) called pre-ribosomes. More than 180 transiently associating non-ribosomal factors (assembly factors) and 70 small nucleolar RNAs (snoRNAs) have been identified as being involved in ribosome biogenesis, reflecting its complexity (Henras et al., 2008; Lafontaine and Tollervey, 2001; Staley and Woolford, 2009). Processing, modification and assembly of r-proteins take place within the context of pre-ribosomal particles, containing the numerous transiently associating factors (Figure 1.4).

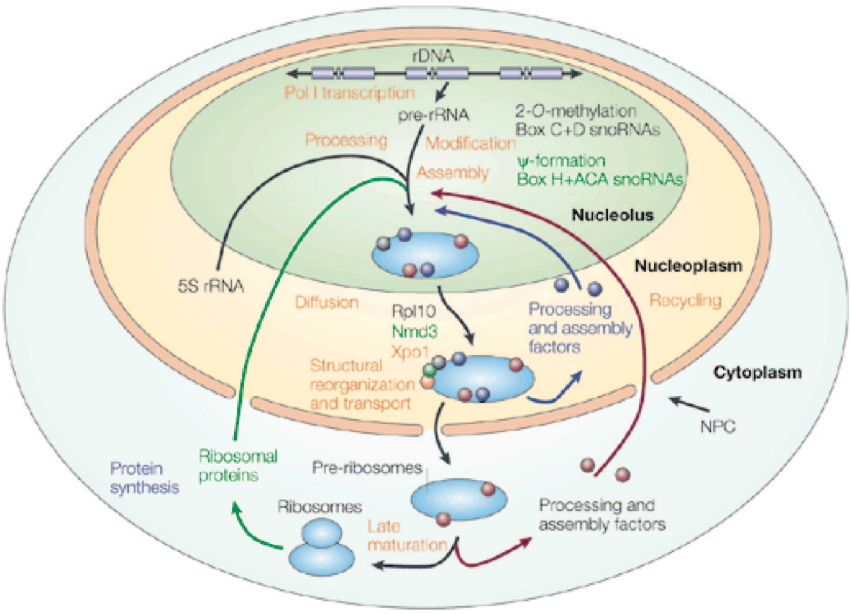

Figure 1.4 Simplified outlook of ribosome biogenesis in yeast. Figure adapted from (Lafontaine and Tollervey, 2001)

1.4.2 rDNA locus and rRNA transcription

In an exponentially growing yeast cell the ratio of RNA to DNA is about 50:1, where approximately 80 % is predicted to correspond to rRNA. This huge amount of rRNA correlates with the estimated number of about 200.000 ribosomes per cell and with a production rate of 2.000 ribosomes per minute (Warner, 1999). In order for yeast cells to meet those rRNA production demands, they have evolved so that 10 % of their entire genome contains ribosomal genes (rDNA) arranged in a single tandem array of 100-200 identical repeats. Together they form a single rDNA locus named *RDN1*, which is located on the right arm of chromosome XII. This single rDNA locus is a unique feature of *S.cerevisae*, as the rDNA loci in higher eukaryotes are scattered forming clusters of repeats, named nucleolar organizer regions (NORs). Due to the repetitive nature of rDNA sequences, recombination events are common; resulting in an increase or decrease of rDNA repeats, easily visualized as expansions and contractions of the nucleolus (Butler and Metzenberg, 1990). To add to the distinctive genomic organization of *S.cerevisae*, the 5S rRNA is also located at the *RDN1* locus, but it is encoded on the opposite strand of each repeat, in contract to other eukaryotes where it is found in separate loci.

Each repeat forms an operon transcribed by RNA polymerase I (RNA pol I), resulting in a large polycistronic precursor rRNA transcript (35S pre-rRNA). This contains the sequences for the mature ribosomal RNAs (18, 5.8S and 25S rRNA), two external transcribed spacers (ETS) and two internal transcribed spacers (ITS). The fourth rRNA species (5S rRNA) is independently transcribed by RNA pol III. Since the polycistronic 35S pre-rRNA contains rRNA sequences of both the large and small subunit, it results in equal production of 40S and 60S subunits (Granneman and Baserga, 2004) (Figure 1.5).

This 35S primary transcript is covalently modified at numerous sites and subjected to many endo- and exonucleolytic processing steps and finally correctly folded along with the r-proteins, to produce the mature subunits. These steps require a series of non-ribosomal *trans*-acting factors that include RNA helicases, endo- and exo-nucleolytic RNAses, potential RNA chaperones, as well as rRNA methyltransferases, pseudo-uridine synthases and finally several snoRNAs (Henras et al., 2008; Kressler et al., 2010).

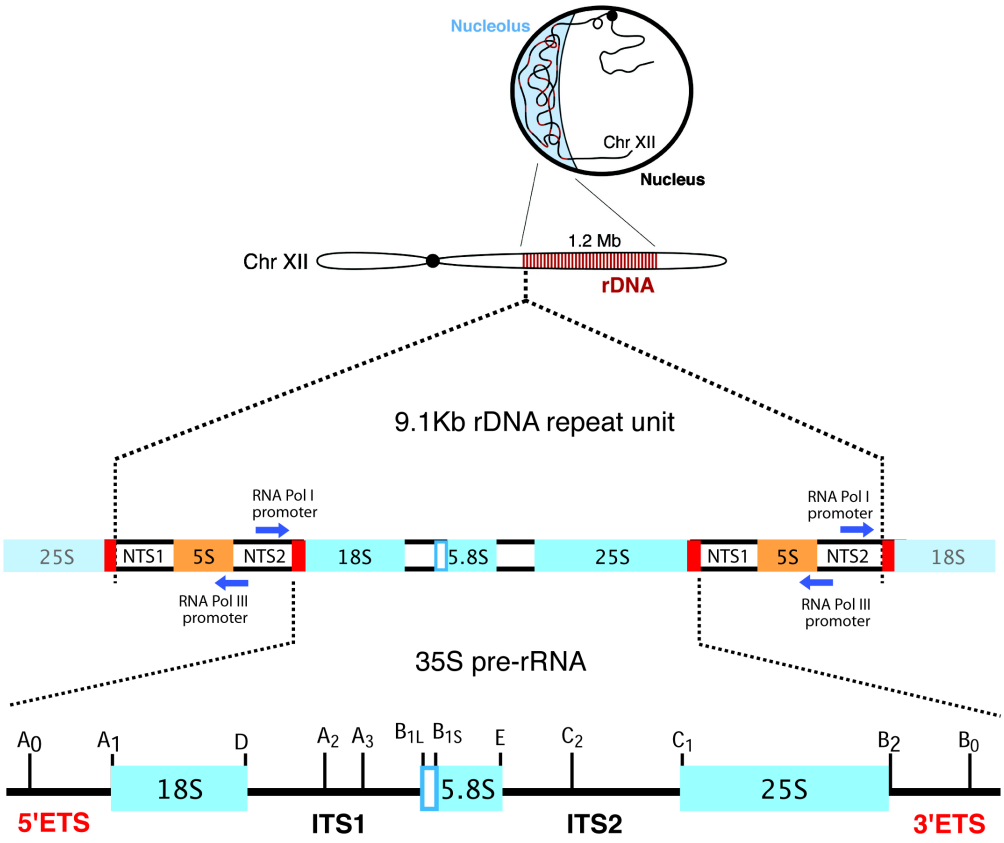

Figure 1.5 Schematic representation of the rDNA operon in yeast. Each rDNA repeat contains the 35S and 5S rRNA genes. The colored boxes denote the mature rRNA species. NTS (non transcribed sequence); ITS (internal transcribed spacer); ETS (External transcribed spacer). A_0 to C_2 denote cleavage sites (Eckert-Boulet and Lisby, 2009).

1.4.3 pre-rRNA modifications

The 35S pre-rRNA undergoes multiple modifications at different residues prior to its maturation. These modifications include 45 pseudouridylations (isomerization of uridine to pseudouridine Ψ), 55 2'-*O*-ribose methylations and about 10 base methylations (Decatur et al., 2007).To date it has been suggested that none of these modifications are important individually, but together they are believed to affect RNA conformation, stability and the translational activity of ribosomes via non-canonical base pairing and altered steric properties (Nissen et al., 2000; Ofengand, 2002).

Two groups of snoRNPs, namely the box C/D and the box H/ACA mediate the methylation and pseudouridylation reactions respectively (Figure 1.6) (Reichow et al., 2007). In each snoRNP family the protein components are common and include Nop1, Nop56, Nop58 and Snu13 for the C/D box and Cbf5, Gar1, Nhp2 and

Nop10 for the H/ACA box snoRNPs, with Nop1 exhibiting the 2'-*O*-methyltransferase activity and Cbf5 the pseudouridine synthase activity (Lafontaine et al., 1998; Tollervey et al., 1993). The methylation and pseudouridylation target sites are dictated by RNA base-pairing between snoRNAs and the pre-rRNA sequence to be modified.

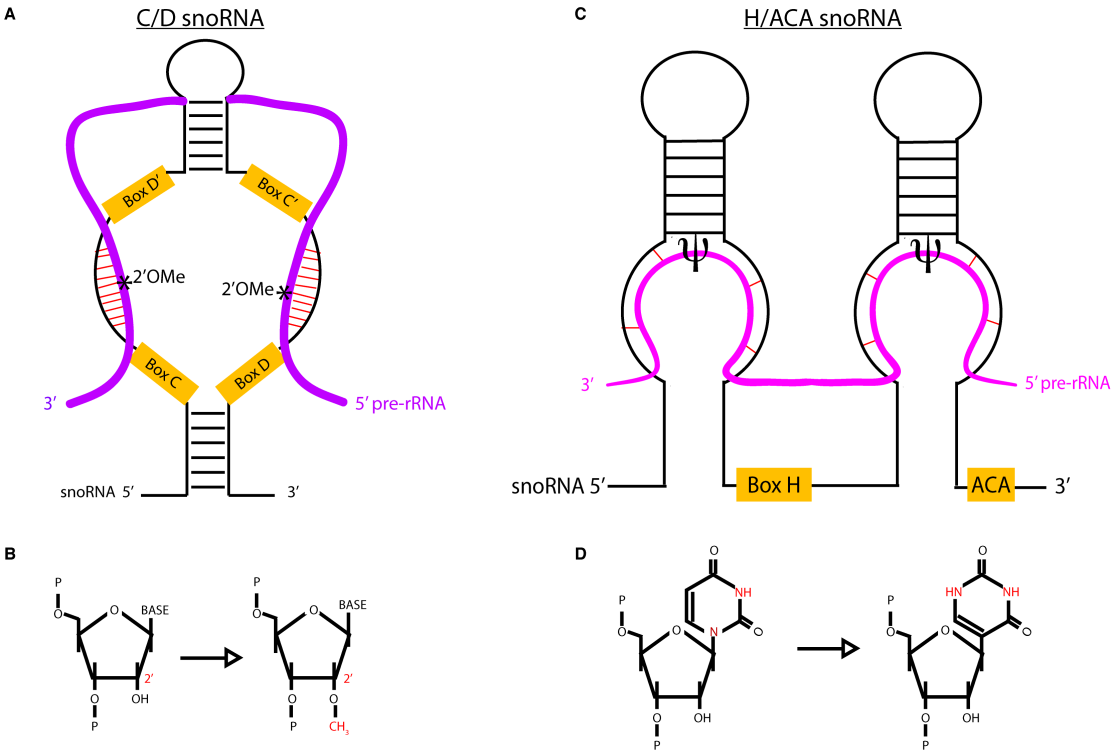

Figure 1.6 Schematic representation of C/D and H/ACA box snoRNAs. A) The C/D box snoRNP structure and its function in 2'-*O*-ribose methylation (**B**). The H/ACA box snoRNP (**C**) pseudouridylates (Ψ) its substrates by rotating (isomerization reaction) the uracil about 120° (**D**) (Reichow et al., 2007).

1.4.4 pre-rRNA processing

The first detectable pre-rRNA intermediate in *S. cerevisiae*, named 35S pre-rRNA, contains the mature 18S, 5.8S and 25S rRNA sequences separated by two internal transcribed spacers (ITS1 and ITS2) and flanked by two external transcribed spacers (5' and 3' ETS) (Figure 1.5). The processing begins with the co-transcriptional release of the 90S pre-particle that contains the 35S pre-rRNA cleaved in the 3'-ETS (B_0) by the Rnt1 endonuclease (Kufel et al., 1999). This pre-rRNA is subsequently cleaved in the 5'-ETS at site A_0 (generating the 33S pre-rRNA), at site A_1 that corresponds to the 5' end of the mature 18S rRNA (generating

the 32S pre-rRNA) and at site A_2 in ITS1 (generating the 20S and $27SA_2$ pre-rRNAs) (Figure 1.7). The last processing step of the 20S rRNA takes place in the cytoplasm after export, where the cleavage at site D by Nob1 generates the 3'-end of the mature 18S rRNA (two non essential base dimethylations also contribute to the final mature 18S rRNA) (Fromont-Racine et al., 2003; Lafontaine et al., 1998).

The maturation of $27SA_2$ pre-rRNA to mature 5.8S and 25S rRNAs is far more complex and involves several nuclear steps and two alternative pathways. In yeast about 85 % of the $27SA_2$ population is cleaved at site A_3 in ITS1 by the essential endonuclease RNase MRP (Henry et al., 1994), rapidly followed by 5' to 3' RNA trimming by Rat1-Xrn1 to form site B_{1S}; the remaining 15 % of $27SA_2$ is formed by cleavage directly at site B_{1L}. The two alternative pathways result in long (L) and short (S) forms of 5.8S rRNA with about 7- 8 nucleotides difference in length. While two forms of the 5.8S are found in all eukaryotes the functional distinction been them remains elusive. Maturation of the 3' end of the 25S (site B_2) occurs following the cleavage at site B_1. The two forms of 27SB ($27SB_S$ and $27SB_L$) are matured following identical pathways involving initial processing at the C_2 site, an event that effectively separates the precursors of 5.8S from 25S. Subsequently the 5' end of the 25S is matured (from C_2 towards C_1), and requires the 3' to 5' exonucleolytic activity of Rat1-Xrn1. In parallel the 3' end of the 5.8S is matured in a complex series of processing steps requiring multiple exonucleases, including the exosome complex (Figure 1.7) (Fromont-Racine et al., 2003; Henry et al., 1994; Schmitt and Clayton, 1993; Venema and Tollervey, 1999).

The independently transcribed 5S rRNA has a small extension at the 3' end (about 10 nucleotides), which is removed by the Rex1 exonuclease in a single step (van Hoof et al., 2000). The pre-factors Rpf2 and Rrs1 recruit 5S rRNA together with the ribosomal proteins Rpl5 and Rpl11 into early pre-60S particles (Zhang et al., 2007), which is a prerequisite for 35S pre-rRNA processing (Dechampesme et al., 1999).

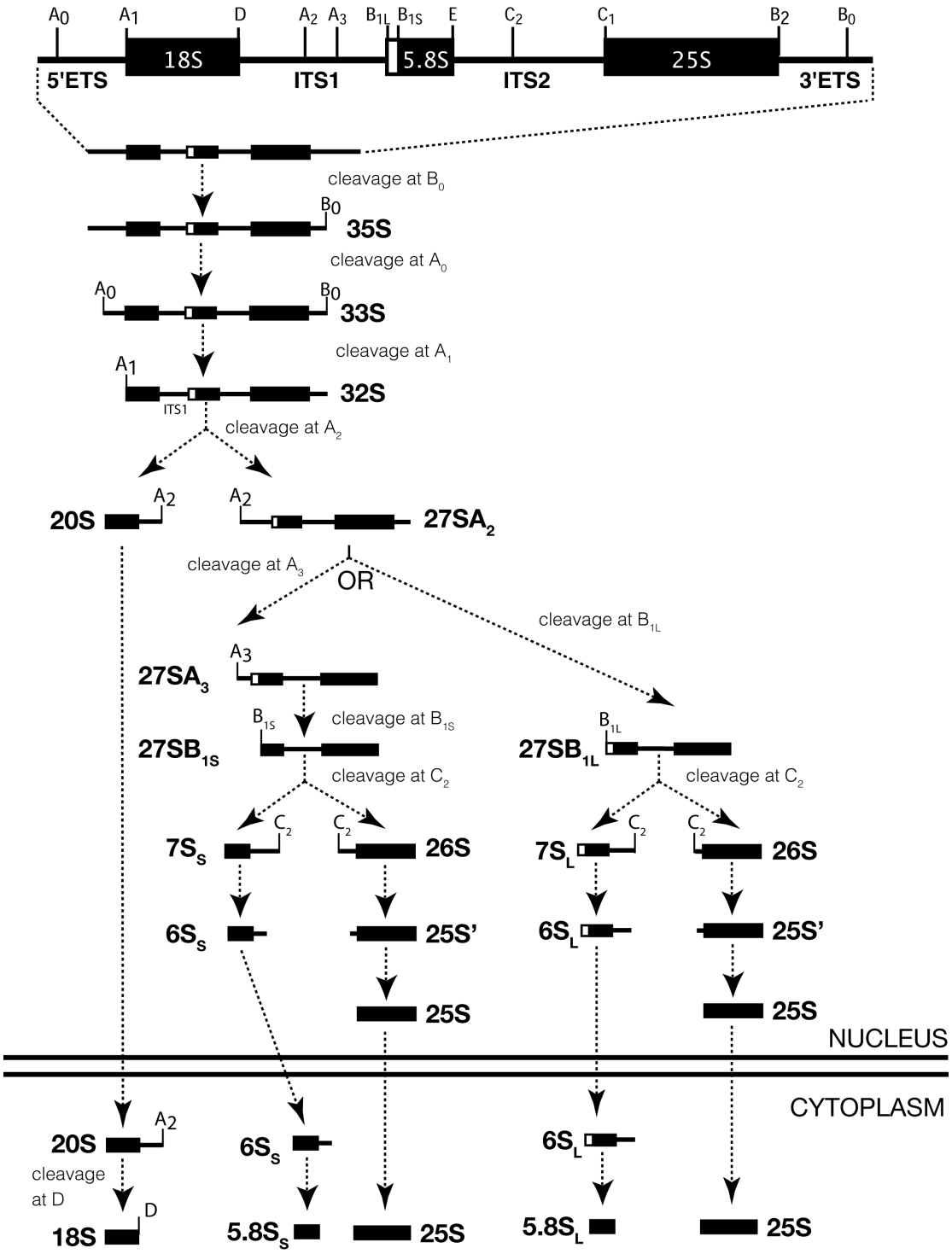

Figure 1.7 Schematic representation of 35S rRNA processing (see text for details).

1.4.5 Ribosomal proteins

As described above (see section 1.2) ribosomal proteins comprise the second component of the ribosome, unevenly coating its surface with only a few of them present at the inter-subunit area or the peptidyl-transferase center (Ben-Shem

et al., 2011; Dresios et al., 2006). Except from being well conserved among different kingdoms of life, the r-proteins are small in size (10-45 KDa in yeast) and contain a large number or Arg and Lys residues, rendering them very basic. This basic character is suggested to act as a buffer neutralizing the negative charges of the rRNA (Wilson and Nierhaus, 2005).

In an exponentially growing *S. cerevisiae* cell, almost 50 % of RNA pol II transcription is devoted to ribosomal genes (Warner, 1999), 59 of which are duplicated (not all of them are functional equivalent, as seen in the case of P1 and P2 proteins) (Deutschbauer et al., 2005; Remacha et al., 1995a; Remacha et al., 1995b). Additionally, the yeast r-protein genes are frequently interrupted by introns (Spingola et al., 1999), providing an additional level of regulation and quality control during the splicing event (Parenteau et al., 2011).

The *in vivo* role of many r-proteins (except those participating in translation) is still elusive, but it has been suggested that they function as RNA chaperons during ribosome biogenesis, facilitating the folding of pre-rRNAs, as well as stabilizing the rRNA structures on the mature ribosome. Both of the suggested functions rely upon the long extensions present on r-proteins, forming intertwined networks with the rRNA molecules and thus contributing to the tight packing of the ribosome (Caldarola et al., 2009).

Finally, it has been shown that some r-proteins have additional roles besides their function onto the ribosome. Such roles, termed extra-ribosomal functions include DNA repair, development and apoptosis, as well as cancer (Lindstrom, 2009; Warner and McIntosh, 2009; Wool, 1996).

1.4.6 Pre-ribosome assembly and *trans*-acting factors

Unlike bacteria where ribosomes can assemble *in vitro* (Shajani et al., 2011), the eukaryotic ribosome requires numerous and mostly essential non-ribosomal *trans*-acting factors. These factors include ATPases, GTPases, helicases, kinases or nucleases that have been shown or suggested to participate in modification, processing and folding of rRNA, as well as the sequential recruitment of r-proteins (Kressler et al., 2010; Thomson et al., 2013).

Early experiments in the 1970s using sucrose gradient analysis of radiolabelled ribosomes, identified pre-particles corresponding to 90S, 66S and 43S species containing not only rRNA and r-proteins but also a plethora of accessory proteins (Kruiswijk et al., 1978; Trapman et al., 1975; Udem and Warner, 1972). Subsequently, with the use of genetic screens (high copy suppressors or synthetic lethality screens) many *trans*-acting factors have been identified (Kressler et al., 2010; Venema and Tollervey, 1999). However, a significant breakthrough in the field was the advent of the tandem affinity purification (TAP) method, with which pre-ribosomes were isolated under native conditions and their composition was analyzed by mass spectrometry (Rigaut et al., 1999). The systematic isolation and identification of several assembly intermediates showed that the composition of pre-particles is highly dynamic, thus contributing to the complexity of the process itself (Granneman and Baserga, 2004; Nissan et al., 2002; Schafer et al., 2003; Tschochner and Hurt, 2003).

1.4.7 The 90S pre-ribosome (SSU processome) and 40S subunit maturation

As RNA pol I transcription of the rDNA genes ensues, ball-like structures are formed at the 5' end of the emerging nascent transcripts, as visualized by chromatin spreads (Miller and Beatty, 1969) (Figure 1.8 A). This structure is believed to be the earliest nascent pre-ribosome, named small subunit processome (SSU) or 90S pre-ribosome (Dragon et al., 2002; Grandi et al., 2002) wherein the early processing, modification and assembly steps take place.

This pre-ribosome is a large multi-subunit particle formed stepwise with the initial co-transcriptional incorporation of the tUTP subcomplex (transcription U three protein) (Gallagher et al., 2004; Granneman and Baserga, 2005). This first nucleating step is required for the subsequent downstream assembly of two independent (but not mutually exclusive) assembly lines that require the multi-component complexes U3 snoRNP/UTP-B and Rrp5/UTP-C, respectively (Figure 1.8 B) (Perez-Fernandez et al., 2011; Perez-Fernandez et al., 2007). It is worth mentioning that these early pre-ribosomes contain, almost exclusively, biogenesis

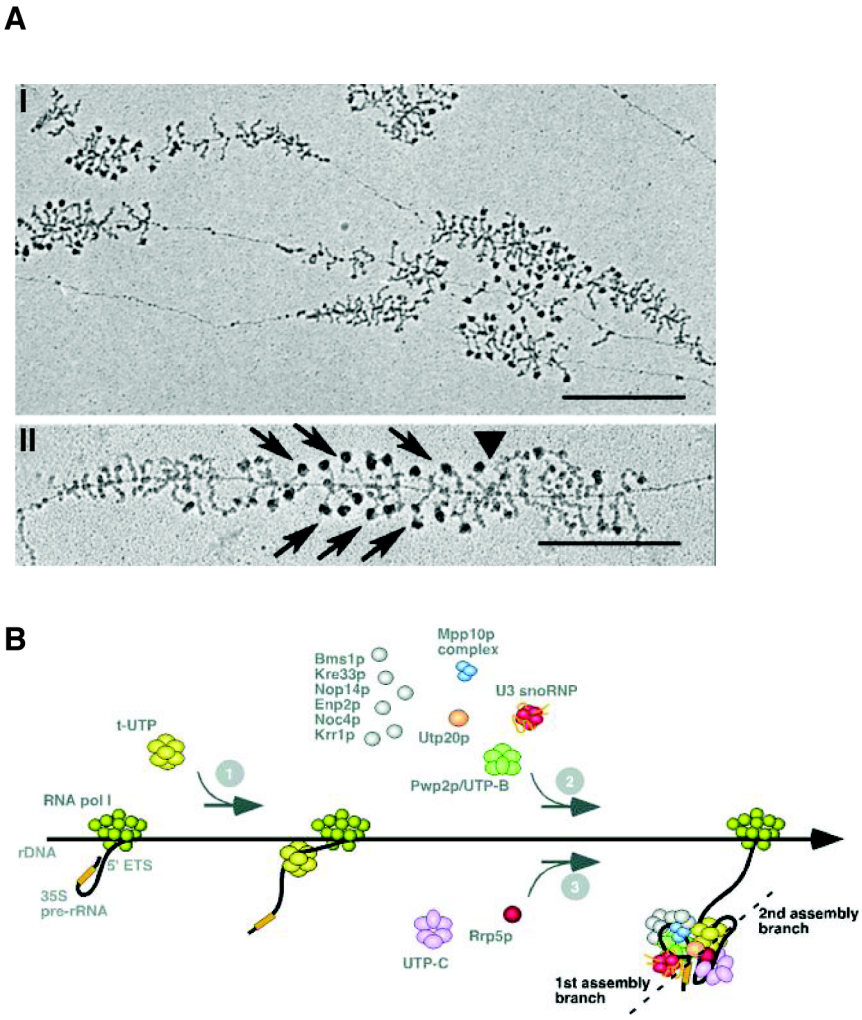

Figure 1.8 Early steps in ribosome biogenesis, the 90S pre-particle. A) Electron micrographs of pre-rRNA transcription, visualized as 'Christmas trees'. Arrows indicate the terminal knobs. Scale bar corresponds to 1.0 µm in (I) and 0.5 µm (II). Adapted from (Raska et al., 2006). **B**) A model for the stepwise assembly of the 90S pre-ribosomes and the formation of the terminal knobs. For details go to section 1.4.7. Adapted from (Perez-Fernandez et al., 2007)

factors required for the synthesis of the 40S and ribosomal proteins of the small subunit and are lacking r-proteins and processing factors required for the 60S subunit (Dragon et al., 2002; Grandi et al., 2002). Consequently these early assembly and processing steps are essential for the biogenesis of the small, but not the large subunit.

Following cleavage at A_2, which effectively separates pre-40S from pre-60S assembly, most of the early trans-acting factors are released. Additionally, it is suggested that this step triggers the association of 60S assembly factors that will

form the first pre-60S particle together with the $27SA_2$ rRNA (Hage and Tollervey, 2004; Ofengand, 2002; Schafer et al., 2003; Tschochner and Hurt, 2003).

Following the A2 cleavage, the pre-40S particles contain only a handful of trans-acting factors (Dim1, Dim2, Enp1, Hrr25, Nob1, Prp43, Rrp12 and Tsr1) with only a few more (Ltv1, Pfa1, Rio1 and Rio2) incorporated together with r-proteins in the subsequent steps (Figure 1.9) (Lebaron et al., 2005; Schafer et al., 2003; Vanrobays et al., 2004). These pre-40S particles display already the typical 'head', 'platform' and 'body' landmarks (described in section 1.3) of the mature 40S subunit and are rapidly exported in the cytoplasm. The formation of the characteristic 40S 'beak', as well as the stable incorporation of Rps3 result from ATP-dependent phosphorylation and de-phosphorylation events. The main factors involved in these events include Rps3, Enp1 and Ltv1 that get phosphorylated by Hrr25 (isoform of casein kinase I) and de-phosphorylated by an unknown phosphatase (Schafer et al., 2006). Moreover, RNA-protein crosslinking and EM studies have shown that Enp1 and Ltv1 have proximal binding sites to Rps3, suggesting that the stable association of Rps3 protein can only occur when these factors are released (Figure 1.9) (Granneman et al., 2010; Strunk et al., 2011).

The last maturation step in the 40S biogenesis pathway takes place in the cytoplasm and includes the dimethylation reactions on the 20S rRNA, catalyzed by Dim1, and its cleavage at the D site to form the mature 18S rRNA, by Nob1 together with Prp43 and Pfa1 (Fatica et al., 2004; Lamanna and Karbstein, 2009; Lebaron et al., 2009). Finally, a possible role for several of the remaining *trans*-acting factors associated with the 40S pre-ribosome, is to inhibit the premature association with the 60S subunit thus preventing the assembly of a faulty translation machinery (Granneman et al., 2010; Strunk et al., 2011).

1.4.8 The 60S pre-ribosome maturation

Following the emergence of 40S and 60S pre-ribosomes, pre-60S particles must undergo more extensive maturation events compared to the small subunit. Consequently more 60S intermediate particles have been identified, corresponding to numerous nucleolar, nucleoplasmic and cytoplasmic intermediates containing

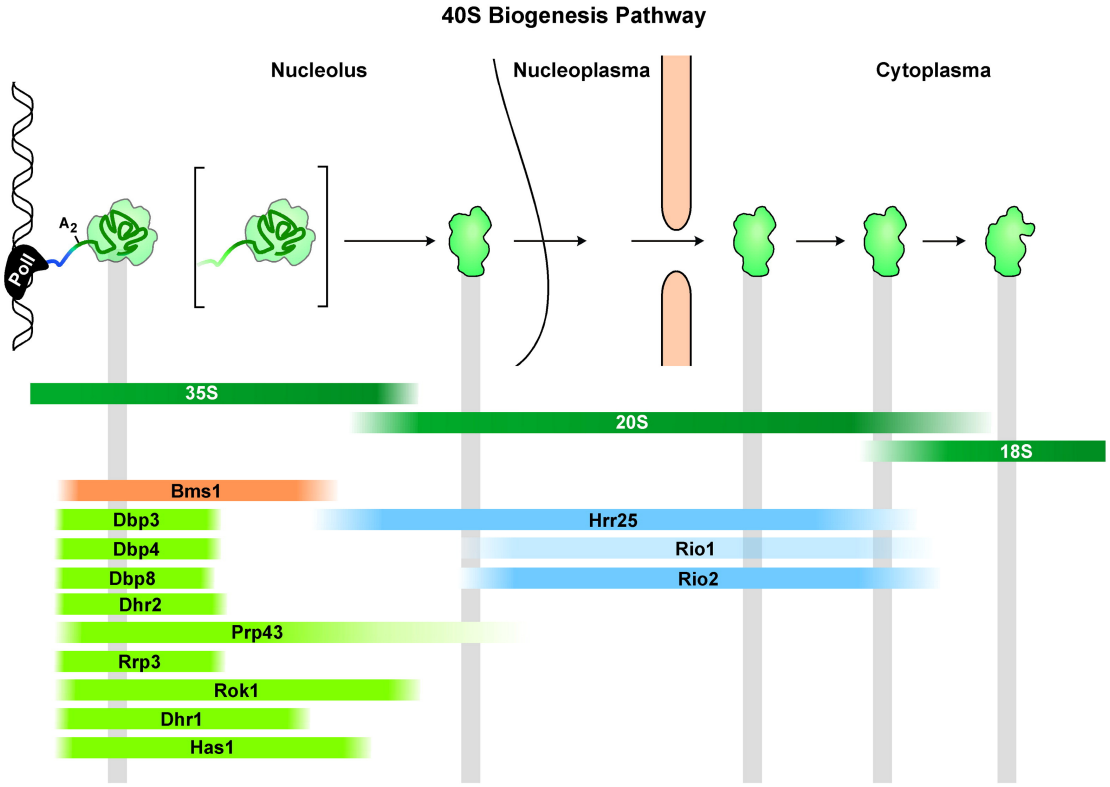

Figure 1.9 The 40S subunit maturation. Cartoon depicting *trans*-acting factors involved in the 40S subunit pathway and their rRNA content (dark green). DExD/H-box ATPases are in green, kinases in light blue and Bms1 GTPase in orange. Adapted from (Kressler et al., 2010)

different, but overlapping sets of proteins. The information gathered from these affinity purifications has allowed a spatial and temporal map of 60S subunit biogenesis to be established, which reflects the dynamic character of this pathway (Figure 1.10) (Bassler et al., 2001; Fatica et al., 2004; Harnpicharnchai et al., 2001; Saveanu et al., 2001). Whilst many particles have been isolated, examples of well-characterized intermediates are discussed below.

The Ssf1 pre-particle is suggested to be the earliest pre-60S particle composed of a mixture of 27SA and 27SB pre-rRNAs, ribosomal proteins, and about 30 trans-acting proteins, including Noc1 and Rrp5 (Fatica et al., 2004; Kressler et al., 2008). Further downstream, the Nsa1 nucleolar intermediate contains besides 5S rRNA almost exclusively 27SB rRNA. Additionally, the Ytm1-Erb1-Nop7 sub-complex, involved in the formation of the $27SA_3$ pre-rRNA together with Rat1 and Xrn1 is also present in this pre-particle (Holzel et al., 2005; Tang et al., 2008; Ulbrich et al., 2009), whereas the Noc1-Noc2 complex has already been

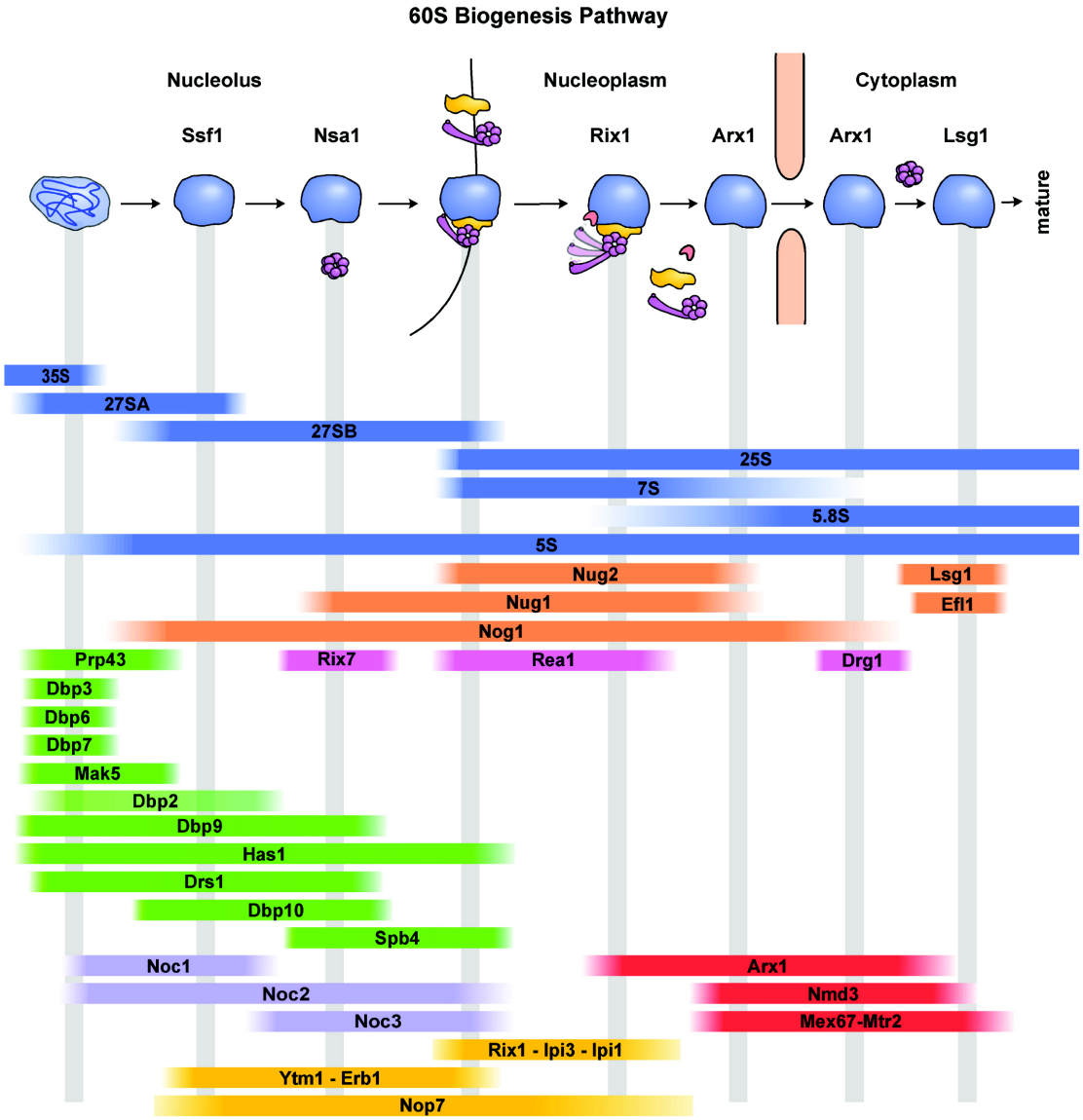

Figure 1.10 A simplified view of the complex and dynamic pre-60S ribosome maturation. Different pre-60S particles as indicated on the top of the figure are depicted together with their rRNA content (blue). GTPases are in orange, DExD/H-box ATPases in green, AAA-ATPases in magenta, sub-complexes in purple/yellow, and export factors in red. Adapted from (Kressler et al., 2010)

exchanged for the Noc2–Noc3 module (Kressler et al., 2008; Milkereit et al., 2001).

Furthermore, the Rpf2 factor has been found present in both Ssf1 and Nsa1 pre-particles, suggesting that it together with Rrs1 promotes the incorporation of the 5S RNP (5S rRNA in complex with Rpl5 and Rpl11) within these early pre-60S particles (Zhang et al., 2007). Additionally, it has recently been shown by cryo-EM using Rsa4-containing Arx1 pre-particles, that the 5S RNP has not yet adopted its

mature conformation, suggesting that additional rearrangements must take place (Leidig et al., 2014).

The Rix1 pre-particle reflects the transition from the nucleolus to the nucleoplasm, and compared to the earlier Nsa1 pre-ribosome, has lost many factors including Spb1, Erb1, Nop2, Puf6, Ebp2, Ytm1, the Noc2-Noc3 module and the DExD/H-ATPases Dbp10, Drs1, Spb4, Dbp9, and Has1(Kressler et al., 2008). Nevertheless, it is enriched with new factors, including Rea1, the Rix1-Ipi3-Ipi1 sub-complex, the Arx1-Alb1 module, Rsa4, Sda1, and Nug2. Moreover, EM studies showed that the Rix1 pre-ribosome exhibits a tadpole-like structure, where the "tail" corresponds to the gigantic AAA-ATPase Rea1 (Nissan et al., 2004; Ulbrich et al., 2009). The AAA domains of Rea1 bind near the CP of the 60S, proximal to the Rix1-Ipi3-Ipi1 sub-complex. Rea's MIDAS domain (metal ion-dependent adhesion site) is positioned at the tip of a hinge-like structure that contacts the biogenesis factors Ytm1 and Rsa4. These two pre-factors are subsequently released in an ATP-dependent manner (Bassler et al., 2010; Ulbrich et al., 2009). Although the functional roles of Ytm1 and Rsa4 remain unclear, it is known that they reside on distinct pre-ribosomes. Ytm1, along with Nop7 and Erb1, are released from nucleolar particles (Bassler et al., 2010), whereas Rsa4 together with Rea1 itself have been shown to dissociate from a later nucleoplasmic pre-ribosome (Ulbrich et al., 2009).

The Rea1 mediated release of factors has been proposed to restructure the pre-60S particle. Such conformational rearrangements are suggested to stimulate the GTPase activity of Nug2. Furthermore, the Nug2 GTPase has recently been shown to have a 'proofreading' role in the pre-60S biogenesis prior to export (Matsuo et al., 2014). RNA-protein crosslinking experiments showed that the Nug2 binding sites on the pre-60S ribosome overlap with the nuclear export adaptor Nmd3. Catalytically inactive Nug2 is retained on pre-particles and thus prevents the recruitment of Nmd3, inhibiting nuclear export (Matsuo et al., 2014). Once the exchange of Nug2 to Nmd3 has taken place, export-competence is achieved. In such an export competent particle the essential Xpo1 export receptor can be recruited in addition to the Mex67-Mtr2 heterodimer (see section 1.5.3).

The exact composition of the export-competent pre-60S ribosome is yet to be

precisely defined. However, the Arx1-containing particles have been found in both the nucleoplasm and cytoplasm, indicating that they travel through the nuclear pore complex (NPC) (Bradatsch et al., 2007; Yao et al., 2007) (for details on ribosome export see section 1.5.3)

Following export, a hierarchical series of cytoplasmic maturation events take place that include the release and recycling of *trans*-acting factors and the concomitant incorporation of late-associating r-proteins. These steps are driven by a number of different NTPases (Figure 1.11) (for details on individual NTPases see section 1.6).

Drg1 is an exclusively cytoplasmic AAA-ATPase that has been shown to interact with NPC filaments (Kappel et al., 2012). Consequently it has been implicated in some of the first steps of cytoplasmic maturation. Indeed depletion or mutation of Drg1 prevents the release of Nog1 and Rlp24 and the incorporation of Rpl24 protein (Pertschy et al., 2007). After the release of Nog1-Rlp24 module, the recruitment of Rei1 and Jjj1 promotes the release of Arx1 and Alb1 from cytoplasmic pre-60S ribosomes (Demoinet et al., 2007; Greber et al., 2012; Hung and Johnson, 2006; Lebreton et al., 2006; Meyer et al., 2007; Pertschy et al., 2007)

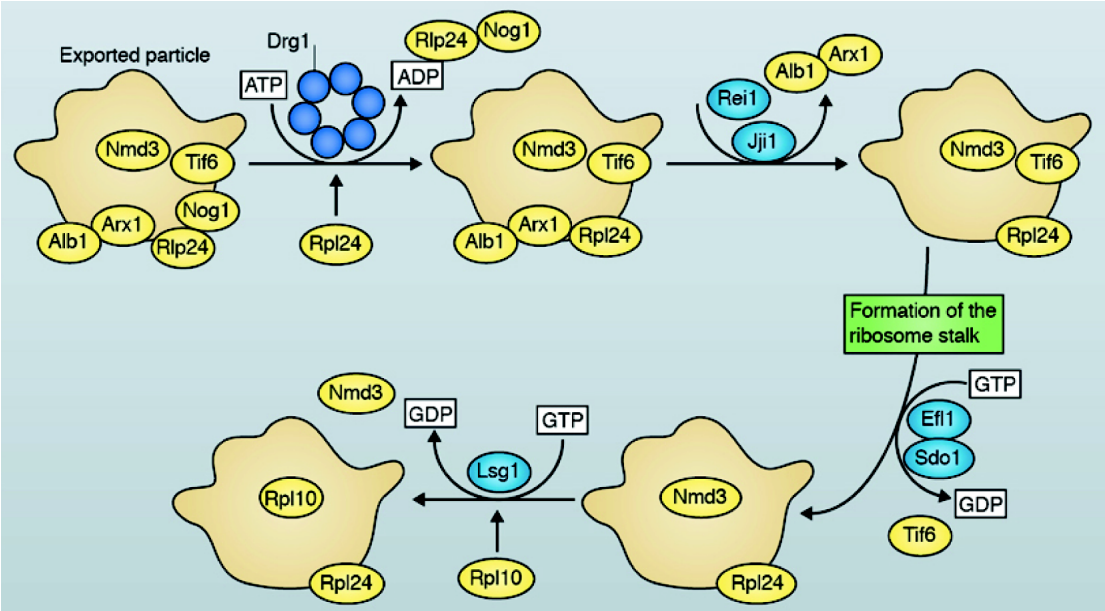

Figure 1.11 Schematic representation of the last cytoplasmic events covering the 60S maturation. The release of Nog1-Rlp24 by Drg1, is followed by that of Arx1-Alb1 module mediated by Rei1-Jjj1.The ribosome subunit anti-association factor Tif6 is released by Efl1-Sdo1, subsequently triggering the stable incorporation of the Rpl10 and the release of the export adaptor protein Nmd3 (for details see text). Adapted from (Thomson et al., 2013).

The release of Arx1-Alb1 module is followed by the formation of the 60S stalk (P-stalk), which is an essential cytoplasmic maturation event. Formation of the P-stalk is a complex process involving multiple pre-factors including Mrt4 and Yvh1, as well as the incorporation of the multiple ribosomal proteins (Rpp0, Rpp1, Rpp2 and Rpl12). The dual-specificity phosphatase Yvh1 facilitates the exchange of Mrt4 for the ribosomal protein Rpp0 (Figure 1.12) (Kemmler et al., 2009; Lo et al., 2009; Rodriguez-Mateos et al., 2009a; Rodriguez-Mateos et al., 2009b). Mrt4, itself a non-essential acidic paralogue of Rpp0, is suggested to bind early to the pre-ribosome at approximately the same position as Rpp0 does in the mature 60S, thus preventing the pre-mature association of Rpp0. The precise timing of these events is debated, however the current model favors the sequential association of these factors starting with the early incorporation of Mrt4 and the late exchange event catalyzed by Yvh1 that lead to Rpp0 entry and the formation of a translation-competent ribosome (Kemmler et al., 2009; Lo et al., 2009; Rodriguez-Mateos et al., 2009a; Rodriguez-Mateos et al., 2009b).

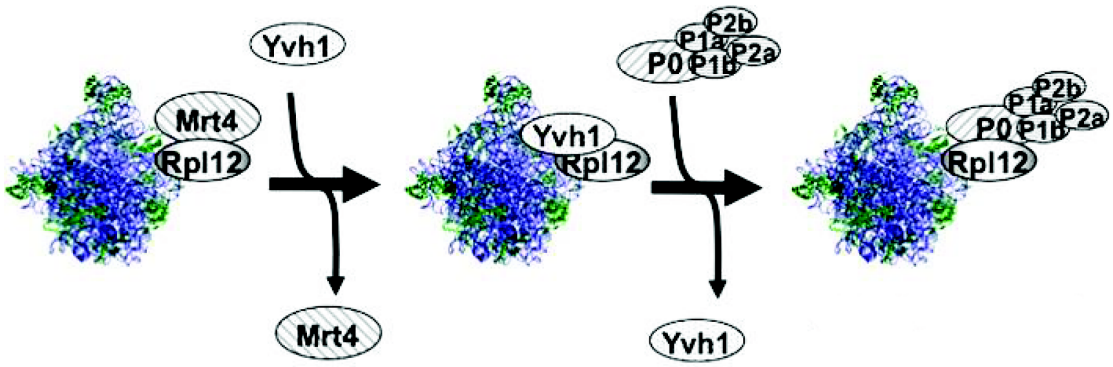

Figure 1.12 Schematic representation of the P-stalk formation during 60S subunit maturation. Mrt4 and Rpl12 are incorporated early during ribosome biogenesis in the nucleolus. Yvh1 to the pre-particle and leads to the release of Mrt4. Subsequently, Yvh1 is displaced as the stalk assembles onto the 60S subunit, by Rpp0 and the rest of the P-proteins. Adapted from (Lo et al., 2009) (see text for more details).

Following stalk formation Tif6 and Nmd3 must be removed from the pre-ribosome, although the order of release is unclear. The removal of Nmd3 is coupled to the incorporation of Rpl10 and requires the GTPase activity of Lsg1 (Hedges et al., 2005; West et al., 2005), while the release of Tif6 utilizes the GTPase activity of

Efl1 and its partner Sdo1 (Senger et al., 2001). Interestingly, Tif6 exhibits a subunit anti-association activity during biogenesis, thus preventing pre-mature subunit joining, rendering its release a checkpoint for translation initiation (Menne et al., 2007; Senger et al., 2001).

1.5 Nucleocytoplasmic transport during ribosome biogenesis

As described above, the final maturation steps of both subunits take place in the cytoplasm and pre-ribosomes must be exported there through the nuclear pore complex (NPC). Although the precise details governing export competence remain unclear, the export process itself is tightly regulated to prevent immature ribosomal subunits from being exported. In addition to export, ribosome biogenesis also depends on the import of trans-acting factors, as well as ribosomal proteins.

1.5.1 The nuclear pore complex (NPC)

A general characteristic of all eukaryotic cells is the presence of the nucleus, a membrane-bound organelle that encloses the genomic material. The nucleus is spatially defined by a lipid bilayer, the nuclear envelope (NE), which forms a barrier preventing free transport of macromolecules between the nuclear interior and the cytoplasm. The nuclear pore complexes (NPCs) first identified in the 1950s (Gall, 1967), are proteinaceous assemblies forming aqueous channels that penetrate the NE at areas where the inner nuclear membrane fuses with the outer one. NPCs form a doughnut-shaped structure with a characteristic eight-fold radial symmetry. More specifically, the transport channel is formed by the central spoke complex, which serves as a scaffold and is in turn sandwiched between a nuclear and a cytoplasmic ring. Filaments from the outer ring protrude into the cytoplasm, whereas the fibrils in the nuclear ring are joining to form the nuclear basket (Figure 1.13) (Aitchison and Rout, 2012; Wente and Rout, 2010).

The yeast NPC is about 60 MDa, 50 nm in height with a total diameter of 100 nm and approximately 50 nm of inner diameter (Aitchison and Rout, 2012). Despite their large molecular mass, NPCs are composed of a set of approximately only 30 different evolutionary conserved proteins, collectively termed nucleoporins

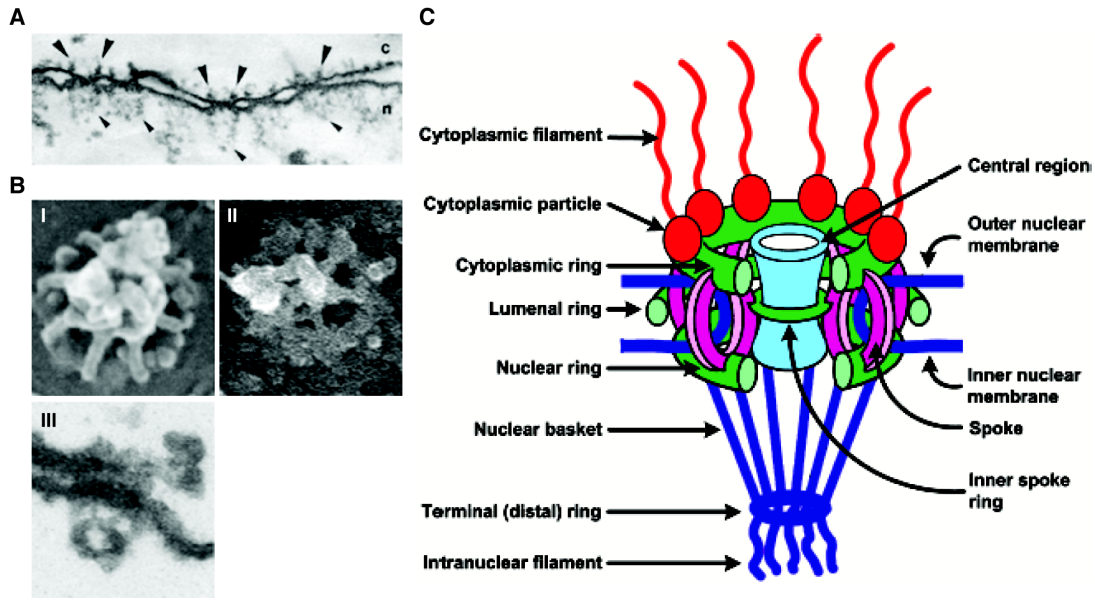

Figure 1.13 The nuclear pore complex. A) Electron micrographs of NPCs. Embedded and thin-sectioned nuclei from *Xenopus laevis*. Big and small arrowheads denote the cytoplasmic filaments and the nuclear basket respectively. (n for nucleus and c for cytoplasm) adapted from (Gall, 1967). **B**) View of the nuclear basket of isolated nuclei from *Xenopus* oocytes prepared by critical point drying and field emission scanning electron microscopy (I), quick-freeze/freeze-drying/rotary metal shadowing (II) and thin-sectioning and transmission electron microscopy (III). Adapted from Martin Goldberg (www.dur.ac.uk/m.w.goldberg/). **C**) Cartoon depicting the main substructures of the NPC. Adapted from (Sorokin et al., 2007).

(Hoelz et al., 2011). Each nucleoporin is found in multiple copies, with the majority found to associate in stable sub-complexes, resulting in ~500–1,000 protein molecules in the fully assembled pore. However, despite great effort, the absolute stoichiometry of all nucleoporins within a single NPC remains unknown (Cronshaw et al., 2002; Rabut et al., 2004; Rout et al., 2000).

Nucleoporins can be subcategorized into three broad groups. The first group contains those with trans-membrane domains believed to anchor the NPC to the NE. The second group is composed of the central scaffold nucleoporins that have been shown to contain alpha-solenoids, beta-propellers and coiled-coil domains. Finally, the last group comprises of phenylalanine-glycine rich repeats (FG-repeats) nucleoporins (Denning et al., 2003; Devos et al., 2006; Isgro and Schulten, 2007; Mansfeld et al., 2006; Patel et al., 2007; Stavru et al., 2006). These FG rich stretches made of 4-48 GLFG, FxFG, PxFG or SxFG repeats, are thought to adopt long natively unfolded conformations that form the meshwork-like permeability

barrier of the NPC (Peters, 2005; Peters, 2009; Terry and Wente, 2009; Tran and Wente, 2006).

1.5.2 Nucleocytoplasmic transport, Karyopherins and Ran-cycle

The NPC barrier (described in section 1.5.1) is freely permeable for small molecules (30-50 KDa, or 5 nm in size) that diffuse following concentration gradients. In contrast, import and export of molecules larger than the passive diffusion limit are coordinated energy-dependent processes involving specialized transport receptor proteins, termed karyopherins (Cook et al., 2007; Pante and Kann, 2002). The majority of nucleocytoplasmic transport receptors belong to the karyopherin β family, also known as importin β-like proteins (Mosammaparast and Pemberton, 2004; Strom and Weis, 2001). Karyopherins have an average size of 90-150 KDa and are characterized by multiple HEAT/ARM repeats (for β- or α-importins, respectively) which form extended alpha helical structures and bind to the Ran GTPase (Gsp1 in yeast). As karyopherins mediate nuclear import or export, they are addressed as importins or exportins, respectively (Figure 1.14 A). They associate with their cargo either directly or indirectly (via an adaptor protein) and translocate through the NPC via transient interactions with nucleoporins (Cingolani et al., 2002; Riddick and Macara, 2005). For the transport of proteins importins recognize and bind to the nuclear localization signal (NLS) of the cargo and translocate it to the nucleus, whereas exportins bind to leucine-rich nuclear export sequence (NES) and ensure its transport to the cytoplasm (Cook et al., 2007).

The directionality of the transport process is achieved by the Ran GTPase, which can exist in a GTP- or a GDP- bound form. The nucleotide load of Ran is the result of compartmentalization of GTPase regulatory proteins (Figure 1.4 B). Guanine-nucleotide exchange factor (RanGEF) is restricted to the nucleus and the GTPase-activating protein (RanGAP) is found in the cytoplasm. The function of these regulatory proteins is to generate a Ran GTP::GDP gradient across the NE, with Ran loaded with GTP inside the nucleus and GDP in the cytoplasm (Dasso, 2002; Weis, 2003) (Cook et al., 2007; Nilsson et al., 2002; Vetter et al., 1999).

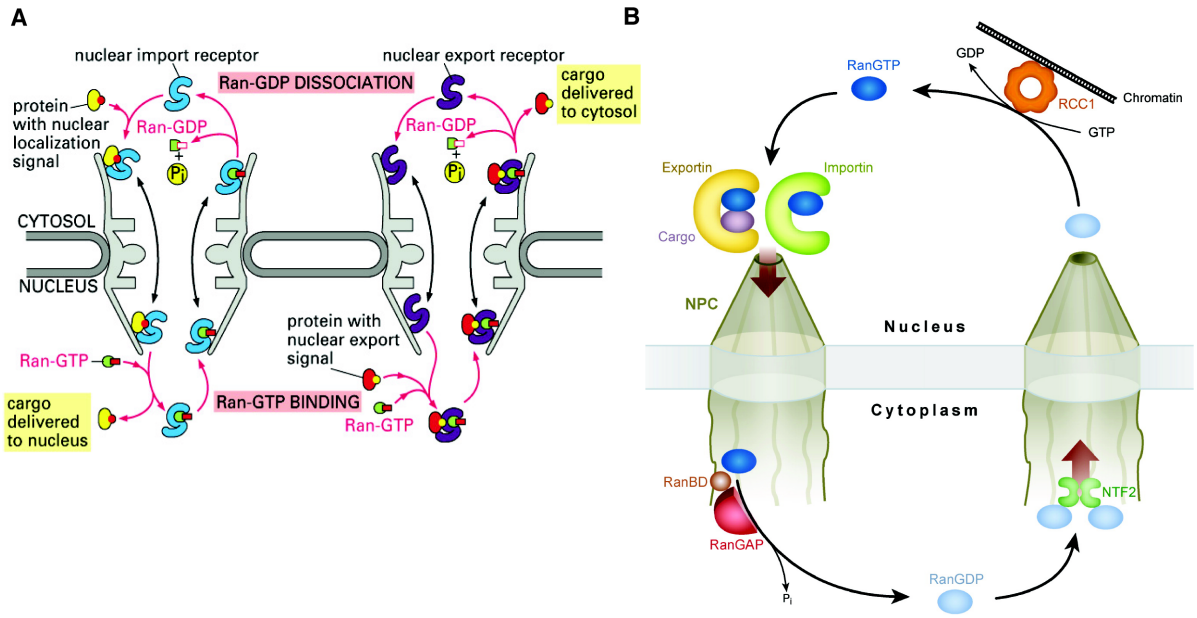

Figure 1.14 Nuclear export of pre-40S and pre-60S particles. Schematic representation of the translocation process mediated by *trans*-acting factors (yellow) (for details see text). Adapted from (Thomson et al., 2013).

1.5.3 Export of pre-ribosomal subunits

Early work from the 1970s, based on radiolabeling experiments, suggested that the export of the 40S and 60S pre-ribosomes is independent of each other (Gleizes et al., 2001; Trapman and Planta, 1976; Trapman et al., 1976; Udem and Warner, 1973). Additional work that utilized GFP-tagged r-proteins along with FISH experiments, supported these results and further showed that the export of both subunits is Ran- and Xpo1 (exportin one)- dependent (Bataille et al., 1990; Gadal et al., 2001b; Gleizes et al., 2001; Hurt et al., 1999; Moy and Silver, 1999; Moy and Silver, 2002; Stage-Zimmermann et al., 2000; Zemp and Kutay, 2007).

In the case of the pre-60S subunits, Xpo1 binds to the NES provided by the export adaptor Nmd3 (Figure 1.15). This essential biogenesis factor associates with the export-competent pre-60S, shuttles between nucleoplasm and cytoplasm and has been recently shown (by CRAC experiments) to bind at a distinct area of the inter-subunit region (Gadal et al., 2001b; Ho and Johnson, 1999; Ho et al., 2000a; Ho et al., 2000b; Matsuo et al., 2014; Nissan et al., 2002).

Since the kinetics of translocation through the NPC are considerably slower for larger cargos (Ribbeck and Gorlich, 2002), it was suggested that several nuclear

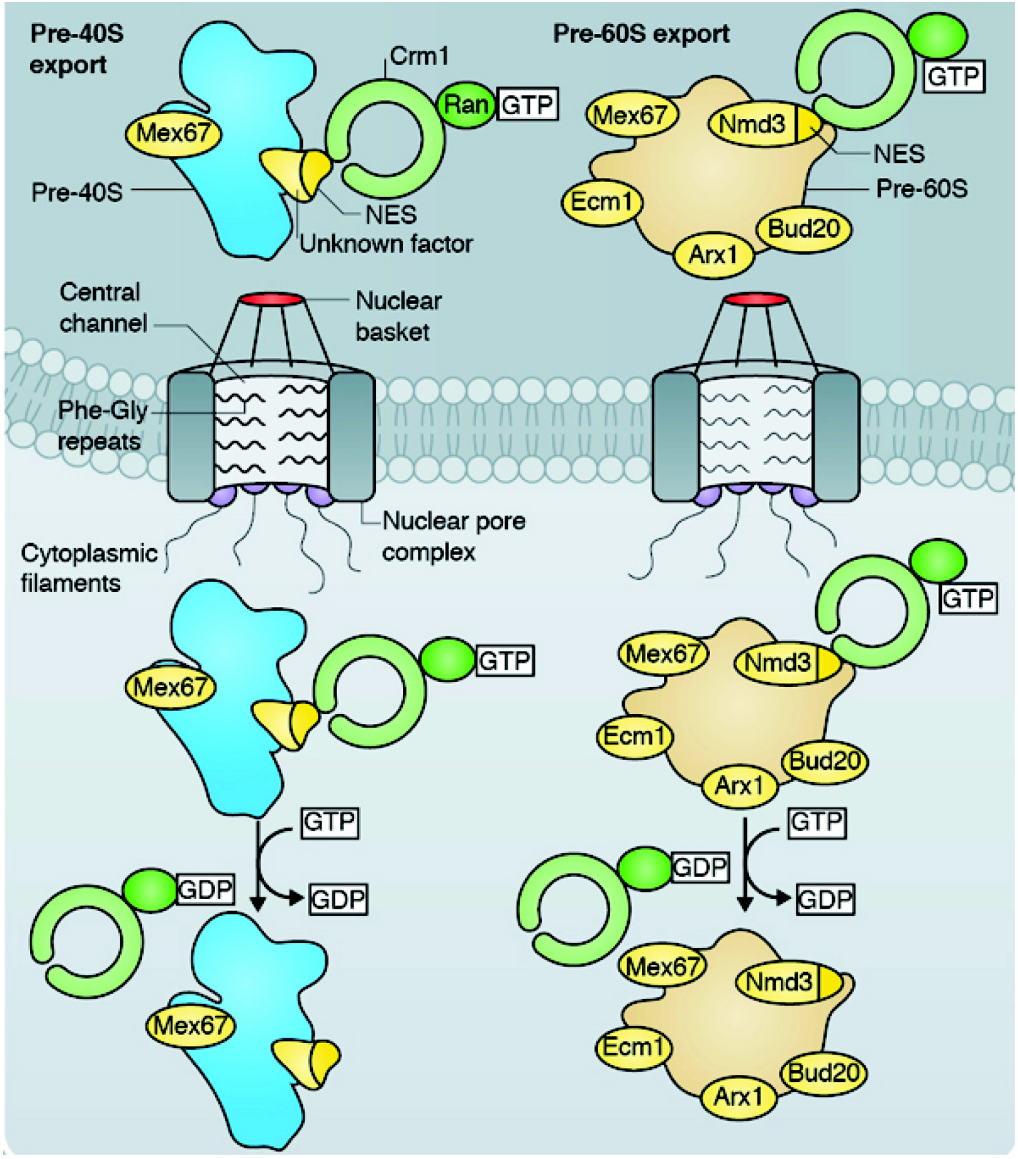

Figure 1.15 Nucleocytoplasmic transport is mediated by specialized translocating proteins. **A**) Importins and exportins are responsible for the import and export of molecules respectively, through the NPCs (for details see text) (adapted from Molecular biology of the cell, Alberts 4th Edition). **B**) The Ran GTase is a key component of the translocation process. The compartmentalization of GTPase regulatory proteins (RanGEF restricted in the nucleus and RanGAP in the cytoplasm), creates a RanGTP gradient across the nuclear envelop that is responsible for the directionality of the process (Cook et al., 2007).

export receptors are involved in the 60S subunit export. Indeed, additional factors have been shown to facilitate the 60S subunit export, including Arx1, Ecm1, Bud20 and Npl3 (Bassler et al., 2012; Bradatsch et al., 2007; Hackmann et al., 2011; Yao et al., 2010). Furthermore, the general mRNA export receptor Mex67-Mtr2 and the HEAT-repeat-containing protein Rrp12 have been shown to be involved in the

export of both subunits (Figure 1.15) (Faza et al., 2012; Ofengand, 2002; Yao et al., 2007).

In contrast to the large subunit, the source(s) of NES within the pre-40S remains elusive. Despite the essential role played by Xpo1, no single factor has been identified to directly mediate the export of pre-40S ribosomes. However, a number of candidates have been suggested including several r-proteins (Rps15, Rps10, Rps26, Rps2, Rps0 and Rps3) (Ferreira-Cerca et al., 2005; Leger-Silvestre et al., 2004) and trans-acting factors (Rio2, Ltv1) (Schafer et al., 2006; Schafer et al., 2003; Seiser et al., 2006; Zemp et al., 2009). Despite the work performed thus far, it is difficult to distinguish those factors directly required for export and those that make pre-ribosomes competent for export.

1.6 Energy-dependent enzymes and ribosome biogenesis.

Ribosome biogenesis requires the concerted activity of several essential ATP- or GTP-consuming enzymes. These energy-consuming enzymes include 19 DExD/H-box ATPases, seven GTPases, three AAA-ATPases, three kinases, and two ABC proteins. Such enzymes are believed to play a regulatory role during the assembly process, providing the energy required and thus confer directionality and accuracy during the maturation process (Kressler et al., 2010; Strunk et al., 2011). It has been shown that most of the DExD/H-box proteins are engaged in early nucleolar events (Bernstein et al., 2006; Granneman et al., 2006a), whereas the AAA-ATPases and GTPases seem to be predominantly involved in later steps of pre-60S biogenesis.

1.6.1 The ATP-binding cassette (ABC) enzymes

The ATP-Binding Cassette Family (ABC Superfamily) is the largest transport protein family that includes several hundred different membrane proteins. More than 100 ABC transporters are distributed from prokaryotes to humans (Choi, 2005). This family of proteins harness the energy stored in ATP to transport diverse cargos across the cell membrane, against their concentration gradient (Locher, 2009).

Two members of this family, Rli1 and Arb1, which localize to both the

nucleoplasm and cytoplasm, have been shown to be essential for ribosome assembly (Dong et al., 2005; Dong et al., 2004; Yarunin et al., 2005). Interestingly, despite the fact that Arb1 appears to associate with the 60S pre-ribosomes, its depletion causes a 40S biogenesis defect (Dong et al., 2005), whereas Rli1 depletion affects both 40S and 60S export (Kispal et al., 2005; Yarunin et al., 2005). Despite this preliminary characterization, the precise roles of Arb1 and Rli1 in ribosome assembly remain to be elucidated.

1.6.2 DExD/H-ATPases

DEAD-, DEAH- and DExH-box families (collectively referred to as DExD/H-box proteins ATPases or so-called RNA helicases) belong to the SF2 superfamily of helicases and constitute the largest class of NTPases involved in ribosome biogenesis (Gorbalenya and Koonin, 1993). Members of the SF2 family are required for the metabolism of many different RNPs, including ribosome biogenesis, pre-mRNA splicing, mRNA export, translation initiation, and RNA turnover (Bleichert and Baserga, 2007; Cordin et al., 2006). While it is difficult to generalize about the properties of all helicases, *in vitro* analysis of multiple helicases have shown them capable of RNA-dependent ATP hydrolysis. For some helicases additional activities have been shown including ATP-dependent RNA binding, unwinding of RNA or RNA/DNA duplexes and disruption of RNA-protein complexes (Cordin et al., 2006; Jankowsky and Bowers, 2006; Jankowsky and Fairman, 2007; Linder, 2006).

Structurally, the DExD/H-box proteins are composed of a ‘helicase’ core, which is formed by two similar domains (RecA-like helicase domains) joined by a flexible linker that adopts open or closed conformations (figure 1.16 A). Furthermore, most helicases contain additional domains of variable length and composition flanking the ‘helicase’ core. This helicase core of about 400 amino acids, contains eight conserved sequence motifs (figure 1.16 B) (Cordin et al., 2006; Rocak and Linder, 2004; Walker et al., 1982) that are suggested to be involved in ATP binding, ATP hydrolysis, RNA binding, and/or joining of the two domains (both domains are needed to form the RNA binding surface). Interestingly, since the hydrolysis of ATP is not always required for RNA unwinding, RNP remodeling

and/or release of RNA-binding proteins, it has been proposed that it might be solely required for the recycling of the helicase (Liu et al., 2008).

In *S. cerevisiae* 37 DExH/D-box proteins have been identified, with 19 being involved in ribosome biogenesis. More specifically, seven are involved in 40S subunit maturation, while ten are required for 60S assembly. Only two helicases Has1 and Prp43 are implicated in the assembly of both subunits (Figure 1.16 C).

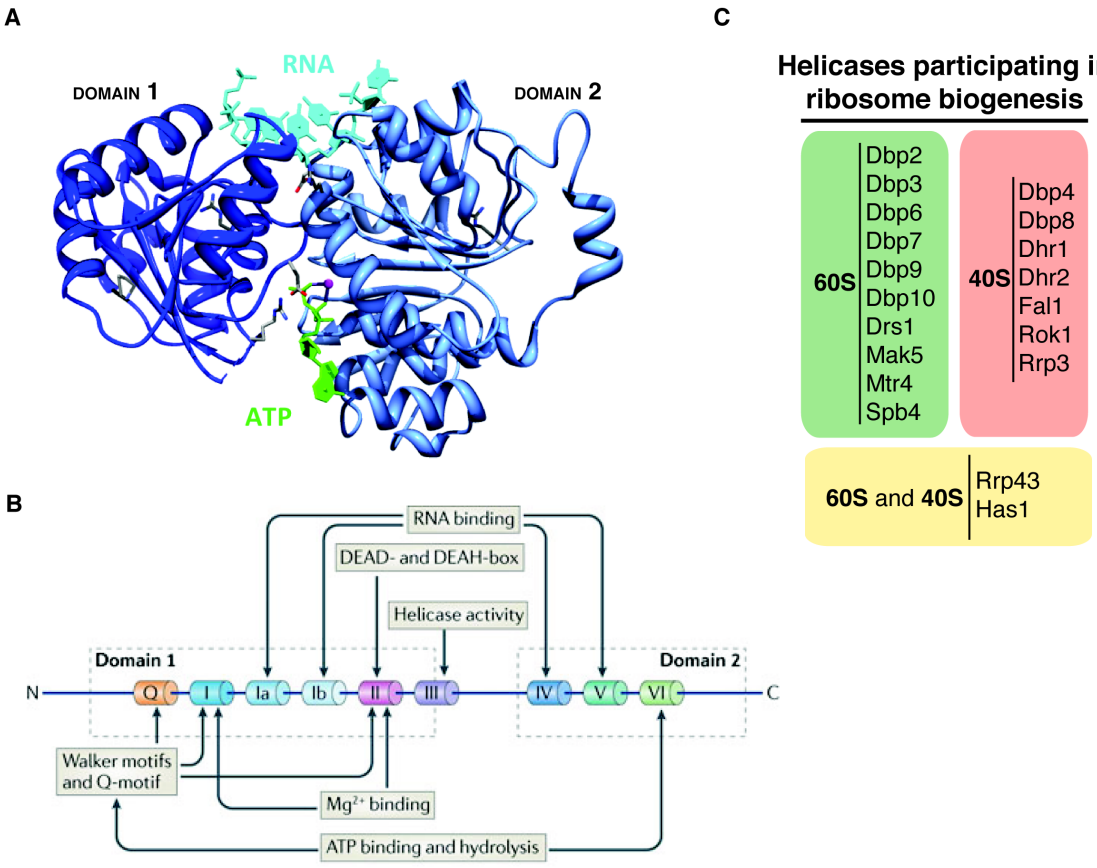

Figure 1.16 ATP-dependent RNA helicases. A) Crystal structure of a helicase (Mss116), depicting the two domain architecture as well as the ATP and RNA binding sites. Adapted from (Pugh et al., 2012). **B**) DEAD- and DEAH-box families of helicases contain amino- and carboxy-terminal domains (domain 1 and domain 2, respectively) and eight characteristic motifs within these domains (depicted here as boxes I–VI, plus the Q motif). The known or proposed functions of each motif are indicated. Motif II forms interactions with the β-phosphate and γ-phosphate of ATP through Mg^{2+} and is required for ATP hydrolysis. Adapted from (Parsyan et al., 2011). **C**) List of RNA helicases participating in ribosome biogenesis (for details see text).

Furthermore, while experimental data suggest that the DExD/H-box proteins indeed act as ATPases (Bernstein et al., 2006; Garcia and Uhlenbeck, 2008; Granneman et al., 2006a; Granneman et al., 2006b; Rocak and Linder, 2004), their

precise molecular function in ribosome biogenesis remains elusive. Nevertheless, some potential remodeling activities have been proposed that would confer structural rearrangement on the pre-ribosome and thus promote ribosome biogenesis. Such activities include priming the rRNA for cleavage, disrupting protein-RNA interactions and promoting the release of snoRNA following modification.

1.6.3 AAA-ATPases

The AAA-ATPases (ATPases Associated with diverse cellular Activities) form a large, but functionally diverse protein family belonging to the ring-shaped P-loop NTPases. AAA-ATPase members are found in all organisms (Hanson and Whiteheart, 2005) and they are essential for many cellular functions, including DNA replication, protein degradation, membrane fusion, microtubule severing, peroxisome biogenesis, signal transduction and the regulation of gene expression, as well as ribosome biogenesis (Hanson and Whiteheart, 2005; Iyer et al., 2004; Neuwald et al., 1999; Tucker and Sallai, 2007; Ulbrich et al., 2009; Vale, 2000).

A common feature of all these proteins is the structurally conserved ATPase domain (about 250 amino acids) that contains the Walker A and Walker B motifs (Erzberger and Berger, 2006). Despite the fact that these ATPases can harbor one (type I), two (type II) or six AAA domains, they assemble into mostly hexameric rings that undergo structural changes during the ATPase cycle (Figure 1.17 A and B) (Hanson and Whiteheart, 2005; Vale, 2000). Hence, they couple chemical energy provided by ATP hydrolysis to conformational changes, which are subsequently transduced into mechanical force exerted on macromolecular substrates. Thus, it is suggested that AAA-ATPases remodel, release or translocate their substrates (Frickey and Lupas, 2004; Iyer et al., 2004).

Three essential AAA-ATPases, namely Rix7, Rea1 and Drg1 have been identified as playing a role in 60S ribosome biogenesis, with each one of them removing specific non-ribosomal factors from the pre-particles. Rix7 (type II AAA-ATPase) was the first AAA-ATPase identified to participate in the 60S biogenesis

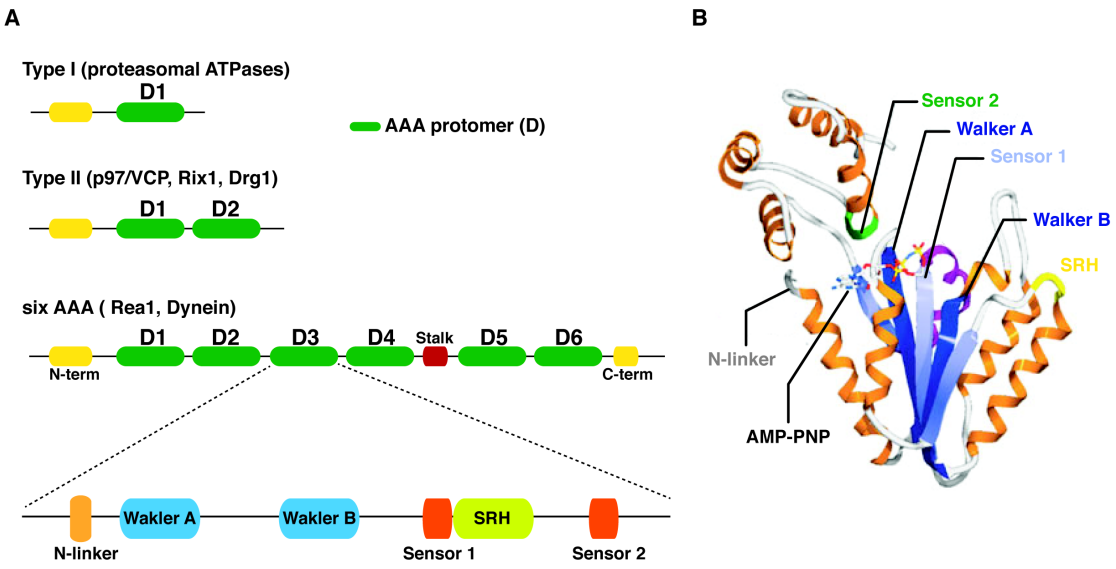

Figure 1.17 Domain organization and structure of an AAA-ATPase. A) The domain architecture of the three types of AAA-ATPases together with an enlarged view of a D domain containing the characteristic sequence motifs (for details see text). **B**) Approximate positions of the key elements on the D2 AAA domain of NSF (PDB 1D2N) (SRH: second region of homology; AMP-PNP: nucleotide analogue coordinated by Mg^{2+}). Adapted from (Hanson and Whiteheart, 2005).

pathway (Gadal et al., 2001a). It was shown to interact with Nsa1, a WD protein and is required for Nsa1 release from the nucleolar pre-particles (Kressler et al., 2008). The timing of this release is unclear, as is the question of whether Rix7 is directly or indirectly influencing the release of Nsa1. Interestingly, since Rix7 is the closest homologue of Cdc48, a factor that recognizes ubiquitinated substrates, it was suggested that Rix7 might also act on modified substrates and indeed Nsa1 was found to be poly-ubiquitinated (Jentsch and Rumpf, 2007; Panse et al., 2006).

The second AAA-ATPase involved in ribosome formation is Rea1, the largest protein found in yeast (about 560 KDa). Rea1 was identified as a component of the Nug1 and Rix1 particles (Bassler et al., 2001; Nissan et al., 2002) and is involved in 60S subunit maturation and ITS2 processing (Galani et al., 2004). This ATPase has six AAA domains that form a ring structure (with only protomer 2, 3, 4, and 5 being active) (Garbarino and Gibbons, 2002) (Garbarino and Gibbons, 2002; Neuwald et al., 1999; Ulbrich et al., 2009). As described in an earlier section (see 1.4.8) Ytm1 and Rsa4 represent the two known substrates of Rea1 and are removed in two successive, but independent, energy-consuming steps (Bassler et al., 2010; Ulbrich

et al., 2009).

The third AAA-ATPase Drg1 contains two (type II) AAA domains (D1 and D2) with the D2 domain mediating its oligomerization into hexameric rings (Zakalskiy et al., 2002). The AAA-ATPase Drg1 mediates the removal of Nog1 GTPase and its binding partner Rlp24 (ribosome-like protein 24) (Kappel et al., 2012; Pertschy et al., 2007), which leads to the stable association of Rpl24 in the pre-60S particle (see section 1.4.8).

1.6.4 Kinases

To date, almost all kinases identified in ribosome biogenesis are involved predominantly in the 40S subunit maturation. As mentioned in section 1.4.7, Hrr25 is a component of late pre-40S particles that together with the sub-complex of Ltv1-Enp1-Rps3 participates in the 'beak' formation of the 40S subunit (Schafer et al., 2006; Schafer et al., 2003). Interestingly, Hrr25 has also been implicated in 60S biogenesis as it has been shown to phosphorylate Tif6 (Basu et al., 2003; Schafer et al., 2006). Accordingly, depletion of Hrr25 results in 40S and 60S processing defects (Ray et al., 2008).

Rio1 and Rio2 belong to a family of atypical serine protein kinases, found to associate with pre-40S particles and are involved in the cytoplasmic processing of the 20S pre-rRNA (Geerlings et al., 2003; Vanrobays et al., 2003; Vanrobays et al., 2001). Although auto-phosphorylation of Rio1 and Rio2 can be detected, the recently solved structures together with biochemical data revealed that both proteins function predominantly as ATPases (Ferreira-Cerca et al., 2014; Ferreira-Cerca et al., 2012).

It has also been recently shown that two isoforms (δ and ε) of the human casein kinase 1 (CK1) participate in the cytoplasmic maturation of pre-40S particles. Despite their partially redundant roles in the process, they are both required for the recycling of several 40S trans-acting factors (Enp1, Ltv1, Rrp12, Dim2, Rio2 and Nob1), as well as for processing of 18S pre-rRNA (Zemp and Kutay, 2007; Zemp et al., 2014).

1.6.5 GTPases

1.6.5.1 General overview

GTPases form a superclass of functionally diverse enzymes that are able to bind and hydrolyze the nucleotide guanosine triphosphate (GTP). This superclass can be sub-divided into two large classes, the TRAFAC (after translation factors) and SIMIBI (after signal recognition particle, MinD, and BioD) class. These two classes exhibit subtle differences in the organization of the G-domain, and together contain over 20 distinct families that can be further subdivided into 57 subfamilies on the basis of conserved sequence motifs, shared structural features, and domain architectures (Leipe et al., 2002; Verstraeten et al., 2011).

Major families include the small monomeric GTPases Rho, Ras, Ran, Rab and Arf, the hetrotrimeric G-proteins (GPCRs), the large motor GTPases like Dynamin, the initiation and elongation factors participating in translation, the SRP/SR family and finally the ribosome biogenesis GTPases (Leipe et al., 2002). These enzymes are involved in diverse cellular functions, including signal transduction, protein biosynthesis, protein translocation, growth control and differentiation, various vesicular processes (endocytosis, vesicular transport, organelle division) and cytoskeletal reorganization (Bourne et al., 1990; Hall, 1990; Takai et al., 2001; Vetter and Wittinghofer, 2001).

A common feature of all GTPases is the presence of the so-called G-domain, which is composed of five conserved sequence motifs (G1 to G5) (Figure 1.18 A). The G1 or Walker A motif [GxxxxGK(S/T)] forms the P-loop and directly interacts with the oxygen of the α- and β- phosphates of the GTP, thus coordinating the nucleotide binging. The G2 motif, also known as the effector region, contains a conserved threonine [T] that contacts the γ- phosphate of the GTP and the water molecule that is in line for the nucleophilic attack. This region often shows large structural differences between the GTP- and GDP-bound states and is therefore also referred to as switch I region. The G3 or Walker B motif [DxxG] interacts with the γ- phosphate and coordinates the catalytic Mg^{2+} ion. The nucleotide state of the GTPase affects also this motif causing structural rearrangements and is thus named switch II region. The G4 motif [(N/T)KxD] forms hydrogen bonds with the guanine

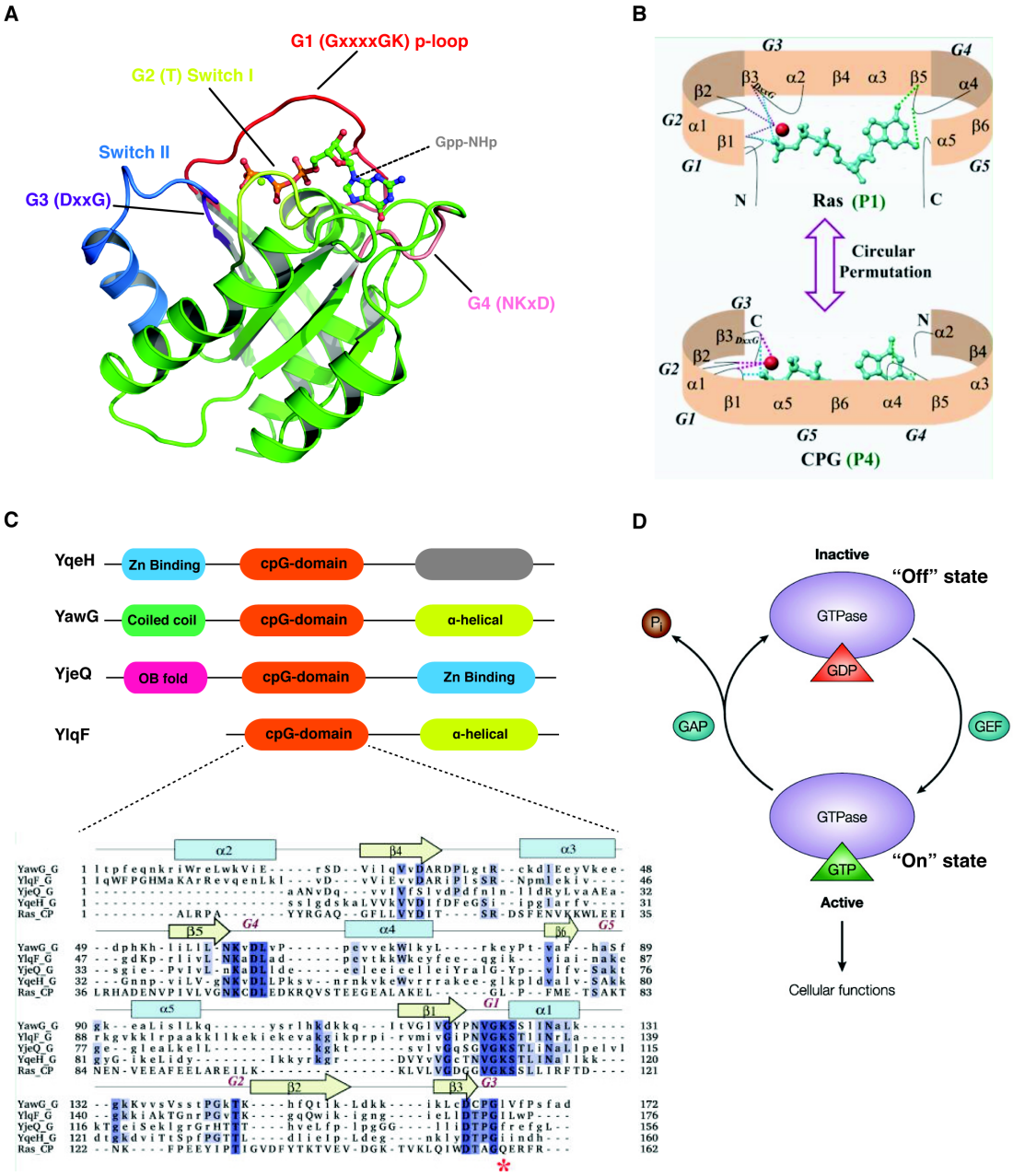

Figure 1.18 General overview of the G domain organization. A) The crystal structure of p21 Ras depicting the characteristic G domain motifs (for details see text). **B**) The comparison between a canonical and a circularly permutated GTPase indicates that the structural features essential for GTP binding and hydrolysis are preserved in both. **C**) The four distinct subfamilies of cpGTPases. Cartoon depicts the domain organization and the alignment shows the conserved G motifs. Adapted from (Anand et al., 2006). **D**) Schematic representation of the switch-like function of GTPases. The GTP-bound "on" and GDP-bound "off" state of the GTPase results in active or inactive form of the enzyme. Adapted from (Anand et al., 2006).

conferring nucleotide specificity. Finally, the G5 motif interacts with the guanine ring, via water-mediated hydrogen bonds, but is poorly conserved, especially in GTPases

involved in ribosome biogenesis (Verstraeten et al., 2011; Vetter et al., 1999; Vetter and Wittinghofer, 2001). Some of these GTPases are characterized by a unique DAR motif that is not present in small Ras-like GTPases, however it is suggested to play a similar role as the G5 motif (Hill et al., 2006).

Interestingly, the aforementioned conserved order of G motifs has in some GTPases been circularly permuted, resulting in a reordered [(G5/DAR)-G4-G1-(G2)-G3] pattern (Figure 1.18 B). These atypical circularly permuted GTPases (cpGTPases) are represented by distinct subfamilies including YlqF (*Bacillus subtilis*), YqeH (*B.subtilis*), YjeQ (*Escherichia coli*) and YawG (*Schizosaccharomyces pombe*) (Figure 1.18 C) (Leipe et al., 2002). However, despite such variation in the motif order that could potentially cause alterations in secondary structure elements, the three dimensional G-domain structure is well preserved as seen in YlqF (New york Structural Genomics Research Consortium) and YjeQ cpGTPases (Levdikov et al., 2004; Shin et al., 2004). This supports the view that folding and the final structure adopted by the G-domain is a well-conserved defining feature of all GTPases. Furthermore, unlike the canonical GTPases, little is known about cpGTPases and their functions. It has been suggested that they share a close evolutionary relationship to a set of bacterial ribosome-binding GTPases that couple guanine nucleotide binding and an RNA-binding function (Anand et al., 2006). Although it is not clear whether the RNA binding regulates the GTP binding or vice versa, it is worth mentioning that cpGTPases also carry a hydrophobic substitution after the G3 motif suggesting an alternative catalytic mechanism (Kim do et al., 2008). Another feature of cpGTPases is the presence of additional domains flanking the GTPase core. These are proposed to stabilize the permuted G-domain and are believed to propagate intra-molecular conformational changes (Anand et al., 2006).

Functionally GTPases can be characterized as molecular switches that cycle between a GTP-bound “on” state and a GDP-bound “off” state (Figure 1.18 D). However, it is the intrinsic properties of each GTPase that determine the duration of the GTP, GDP, and apo states during this cycle. Nevertheless, other proteins provide additional levels of regulation and help them accomplish their function. Among these protein factors are the GTPase-activating proteins (GAPs) that

promote GTP hydrolysis, the guanine nucleotide exchange factors (GEFs) that catalyze the exchange of GDP for GTP, as well as the guanine nucleotide dissociation inhibitors (GDIs) that inhibit the release of GDP (Barr and Lambright, 2010; Bos et al., 2007; Cherfils and Chardin, 1999; Iwashita and Song, 2008; Sprang, 1997; Vetter and Wittinghofer, 2001).

1.6.5.2 GTPases in ribosome biogenesis

To date, yeast ribosome assembly requires seven GTPases. Only Bms1 and eIF5b (Fun12) are involved in the 40S biogenesis pathway, whereas Nog1, Nug1, Nug2, Lsg1 and Efl1 are participating in the maturation of the 60S subunit (for Efl1 role, see section 1.4.8).

Bms1 is essential for 40S biogenesis and mediates the incorporation of Rcl1 into the nucleolar 90S particles (Gelperin et al., 2001; Karbstein et al., 2005; Wegierski et al., 2001). Furthermore, it is suggested that the C-terminal domain of Bms1 acts as an intra-molecular GTPase activator (GAP) that subsequently triggers its own release from pre-particles (Karbstein and Doudna, 2006; Karbstein et al., 2005). The GTPase eIF5b (fun12) is involved in the last steps of the 40S subunit maturation where it is suggested to facilitate the Nob1-dependent cleavage of the 20S rRNA to 18S (Lebaron et al., 2012; Strunk et al., 2012).

The GTPases implicated in the biogenesis of the large subunit associate and act at different times during biogenesis. Nog1 is an evolutionarily conserved, essential GTPase that has been shown to associate with various pre-particles from the nucleolus to the cytoplasm (Kressler et al., 2008; Pertschy et al., 2007; Saveanu et al., 2001). It interacts genetically and physically with the ribosomal-like protein Rlp24 (Saveanu et al., 2001) with which it is released in the cytoplasm in a Drg1-dependent manner (Pertschy et al., 2007). However, the exact function of Nog1 in 60S biogenesis is not clear.

The other three GTPases Nug1, Nug2 and Lsg1 belong to the group of circularly permuted GTPases (cpGTPases) with their G-domains being highly homologous to the prokaryotic YlqF/RbgA cpGTPases. Work performed with the YlqF protein, showed that its activity could be stimulated by free 50S subunits and thus supported a role of this GTPase in 50S ribosome assembly (Matsuo et al.,

2006; Matsuo et al., 2007; Uicker et al., 2006). Earlier work revealed that Nug1 exhibits GTPase activity *in vitro*, but was only recently shown for Nug2 (Bassler et al., 2006; Hedges et al., 2005; Matsuo et al., 2014; Saveanu et al., 2001). Further, mutations within the G-domain of all three GTPases disrupt ribosome biogenesis (Bassler et al., 2006; Hedges et al., 2005; Matsuo et al., 2014; Saveanu et al., 2001). In contrast to the prokaryotic cpGTPases, the eukaryotic Nug1, Nug2, and Lsg1 contain extended N-terminal and C-terminal domains and they have been recently classified by *in silico* analysis in the group of cation-dependent GTPases (Ash et al., 2012).

As mentioned in section 1.4.8, Nug2 associates with nucleoplasmic pre-60S particles and is suggested to inhibit the export of pre-ribosomes by preventing the binding of the export adaptor Nmd3 (Matsuo et al., 2014). In contrast, Lsg1 localizes exclusively to the cytoplasm and is involved in the incorporation of the Rpl10 protein onto the pre-60S particles. It is suggested that Rpl10 in complex with its chaperone Sqt1, binds to the export-competent pre-60S particle in proximity to Nmd3 and that Nmd3 together with Sqt1 are released by the GTPase activity of Lsg1 (Hedges et al., 2005; West et al., 2005).

1.6.5.3 Nug1 GTPase

The Nug1 GTPase was first identified as a component linked to 60S ribosomal subunit export (Bassler et al., 2001). Genetic screens revealed synthetic lethal relationships with Ecm1, Mtr2, Dbp10, Noc2 and Noc3 (Bassler et al., 2001). Furthermore, GFP-tagged Nug1 was found to localize to the nucleolus and nucleoplasm, which agrees with the biochemical data showing that Nug1 co-purifies with various nucleolar and nucleoplasmic pre-ribosomal particles (Bassler et al., 2001; Bassler et al., 2006).

The predicted domain architecture of Nug1 revealed an N-, a middle- and a C-terminal domain (Figure 1.19 A and B). The N-terminal domain, which is only present in eukaryotic orthologues, is rich in positively charged amino acids and predicted to be highly flexible. The middle domain corresponds to the GTPase-domain, that contains the circularly permuted G motifs (DAR-G4-G1-G2-G3) and together with the C-terminal domain are conserved from bacteria and archaea to

eukaryotes (Ash et al., 2012). Interestingly, the N-terminus of Nug1 is essential for nucleolar targeting and association with pre-60S particles, but it has also been shown to exhibit rRNA binding activity (Bassler et al., 2006). In contrast, little is known about its C-terminal domain, which is well conserved and essential for cell viability, but with no characteristic fold.

Moreover, it has been suggested that nucleostemin (NS), guanine nucleotide binding protein-like 3 (GNL3L) and the Ngp1 protein constitute the vertebrae homologues of Nug1. These factors share a common domain composition and subcellular localization with Nug1, but little primary sequence similarity. They are composed of a charged N-terminal RNA-binding domain, followed by a coiled-coil, a permuted G-domain and an extra coiled-coil domain in the C-terminus. These three proteins shuttle between the nucleolus and nucleoplasm, but differ in their sub-nuclear dynamics (Meng et al., 2007). Further, each of these proteins has been shown to display tissue and development specific patterns of expression. Functionally, they are all involved in the stabilization of p53 and correspondingly have been implicated in cell-cycle arrest (Ma and Pederson, 2008).

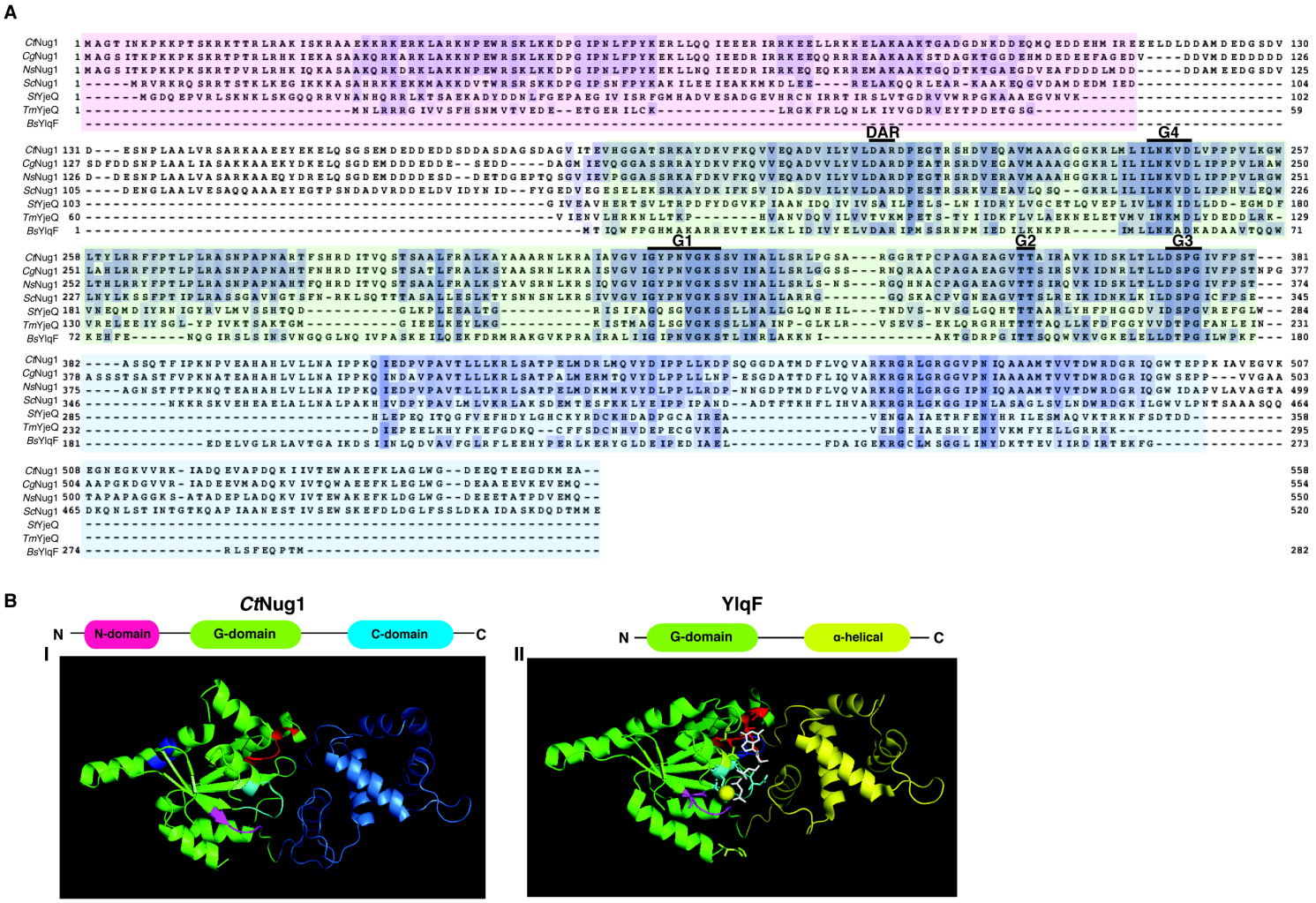

Figure 1.19 Domain organization of Nug1. **A**) Alignment between the homologous sequences of Nug1 from *Chaetomium thermophilum* (*Ct*), *Chaetomium globosum* (*Cg*), *Neurospora crassa* (*Nc*), *Saccharomyces cerevisiae* (*Sc*), YjeQ from *Thermotoga maritima* and *Slamonella enterica* (St) and YlqF from *Bacillus subtilis*. The domain architecture is depicted with the N-terminus being pink, the G domain green and the C-terminus blue. **B**) Comparison between the crystal structure of YlqF (PDB 1PUJ) and the predicted structure of *Ct*Nug1 (phyre2 software). The G domain is colored in green, whereas the C-terminal domain is in yellow for YlqF and blue for *Ct*Nug1. The predicted structure of *Ct*Nug1 is missing the N-terminus and a part of the C-terminus [ΔN(1-194)/ ΔC(452-557]. The G-domain motifs are color-coded: G1 in cyan, G2 in yellow, G3 in magenta, G4 in red and G5 (DAR) in dark blue.

2. Aims of the study

The exact role(s) of Nug1 GTPase and related homologous proteins (YlqF, GNL3L) in ribosome biogenesis remain unknown. It is clear in yeast that the Nug1 GTPase associates with several pre-60S particles in the nucleolus and nucleoplasm, exhibits RNA-binding properties and is essential for the 60S subunit maturation (Bassler et al., 2006). However, it remained unclear how the enzymatic GTPase activity of Nug1 is regulated and how it is involved in ribosome biogenesis. Like other GTPases (Barr and Lambright, 2010; Bos et al., 2007; Cherfils and Chardin, 1999; Iwashita and Song, 2008; Sprang, 1997; Vetter and Wittinghofer, 2001) it could participate in signal transduction, behaving as a sensor for structural rearrangements. Alternatively, it could use its enzymatic activity to recruit or release other *trans*-acting factors or to trigger changes within the rRNA itself. GTP hydrolysis and the nucleotide-binding/exchange could thus stimulate or inhibit the progression of pre-ribosomal particles in the biogenesis pathway.

In order to further elucidate the role of Nug1, I sought to first characterize its GTPase activity *in vitro.* To this end, I will generate mutants in the GTPase domain of Nug1 and assess their nucleotide binding and GTP hydrolysis. Using these *in vitro* data, I could address the role of Nug1 mutants and their effects on ribosome biogenesis *in vivo*, utilizing complementary biochemical and cell biology approaches. The combination of these approaches could help elucidate the significance of Nug1's GTPase activity in 60S subunit assembly.

3. Results

3.1 *Chaetomium thermophilum* Nug1 exhibits a low intrinsic GTPase activity, which can be stimulated by potassium ions.

Nug1 is a circularly permuted GTPase and an essential *trans*-acting factor in ribosome biogenesis (Bassler et al., 2006). In order to elucidate its function I first analyzed its enzymatic GTPase activity *in vitro*. As the recombinant yeast Nug1 protein purifies poorly these studies were performed using the *Chaetomium thermophilum* homologue of Nug1 (*Ct*Nug1). *C. thermophilum* is a thermophilic fungus found in soil, dung, or rotting plants and belongs to the group of filamentous ascomycetes (Ascomycota). It has an optimum growth temperature of around 55°C and participates in the breakdown of cellulose at the high-temperature decomposing and compostation phase (La Touche, 1948). Compared to their mesophilic counterparts, thermophilic proteins often exhibit higher protein stability, less aggregation and thus purify better (Amlacher et al., 2011; Hakulinen et al., 2003). Due to these superior properties we identified and cloned the homologue of Nug1 from a cDNA library of *C. thermophilum.*

To first address whether the thermophilic Nug1 can complement the loss of the yeast homologue, the yeast Nug1 shuffle strain (*nug1*Δ + Rps316-P.*NUG1*::*NUG*1) was transformed with a centromeric plasmid (YCplac22) harboring *ScNUG1* or *CtNUG1* under the control of the yeast Nug1 promoter (P_{NUG1}). Transformants were spotted on SDC+ 5'FOA plates in 10-fold serial dilutions and grown at 30 °C for four days (Figure 3.1 A). 5'FOA-containing plates support the growth of strains that have lost the *URA3*-containing plasmid (pRS316-Nug1) and are used as an indication of complementation. This test showed that *Ct*Nug1 complemented the otherwise non-viable *nug1*Δ strain. Additionally, the growth behaviour of the transformants was further analyzed by spotting them on Yeast Peptone Dextrose plates (YPD) in 10-fold dilution steps at various temperatures (Figure 3.1 B). No differences in growth were observed between the thermophilic (*Ct*Nug1) and yeast Nug1 (*Sc*Nug1) at 30°C or 37°C, but a slight slow growth phenotype was observed at 23°C. This could be due to misfolding of the thermophilic protein when grown at a low temperature. Thus this growth analysis

showed that the *Ct*Nug1 could complement the loss of *Sc*Nug1, suggesting that these two proteins are functionally interchangeable.

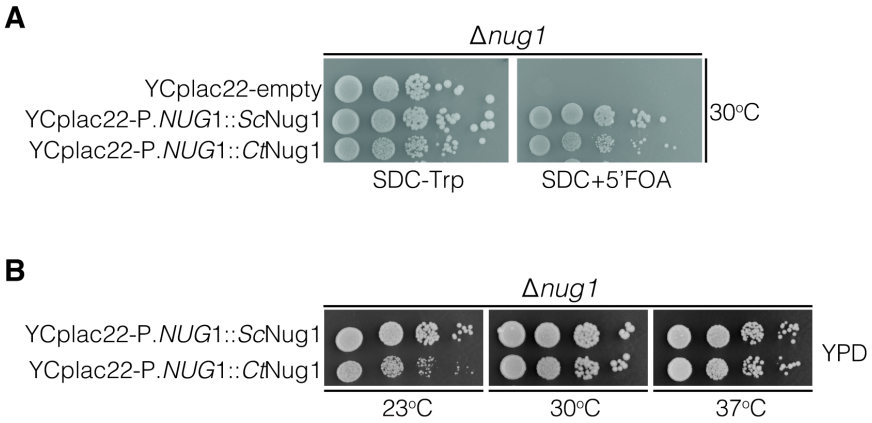

Figure 3.1 *Ct*Nug1 complements the otherwise lethal *nug1*Δ strain. (A) Complementation test of the Nug1 shuffle strain (W303 *MATa nug1::kanMX6, pRS316-NUG1*) transformed with empty plasmid, yeast *Sc*NUG1 or *C. thermophilum Ct*NUG1. The yeast (*Sc*) and the thermophilic (*Ct*) Nug1 ORFs were introduced into the centromeric YCplac22 plasmid and expressed under the control of the native *NUG*1 promoter (P.*NUG*1). Cells were spotted in 10-fold serial dilutions on SDC-Trp and SDC+5'FOA plates and grown at 30°C for 3 days. SDC-Trp plates were used as a control and SDC+5'FOA as test for complementation. Empty Ycplac22 plasmid serves as a negative control for cell viability in the case of SDC+5'FOA plates. **(B) *Ct*Nug1 displays similar growth behavior to *Sc*Nug1**. Growth analysis of the yeast *nug1*Δ strain complemented by Ycplac22-P.*NUG1*::*Sc*Nug1 or Ycplac22-P.*NUG1*::*Ct*Nug1. Transformants were spoted in serial dilution steps (as described above) on YPD plates and grown at different temperatures (23, 30, 37 °C) for 2 days.

Having established that *Ct*Nug1 could complement the *nug1*Δ strain, *in vitro* analysis of *Ct*Nug1's GTPase activity was performed. *Ct*Nug1 was expressed in *E. coli* and purified as described in the Materials and Methods (see section 5.3.3.3). The IPTG-induced protein was soluble and could be purified in a series of purification steps, including cation exchange (SP sepharose), Ni-NTA-affinity purification and a final step utilizing size-exclusion chromatography. This purification process resulted in highly pure *Ct*Nug1 with a yield in the mg range (20 mg/ml) (Figure 3.2 A, top and bottom). Using purified *Ct*Nug1 protein, a series of GTPase assays (single turnover assays) were performed with [γ-^{32}P]-labeled GTP (Figure 3.2 B, top and bottom). In a single-turnover assay the enzyme is in excess over the substrate to allow direct observation of the conversion of substrate to product. In our experiments the ^{32}Pi (free phosphate) released after the GTP hydrolysis was separated from the [γ-^{32}P]-GTP by thin layer chromatography and subsequently

visualized by phosphorimager analysis. Quantification of the phosphorimager data using ImageJ software allowed for the calculation of the ratio between hydrolyzed phosphate (Pi) to total GTP (GTP + Pi).

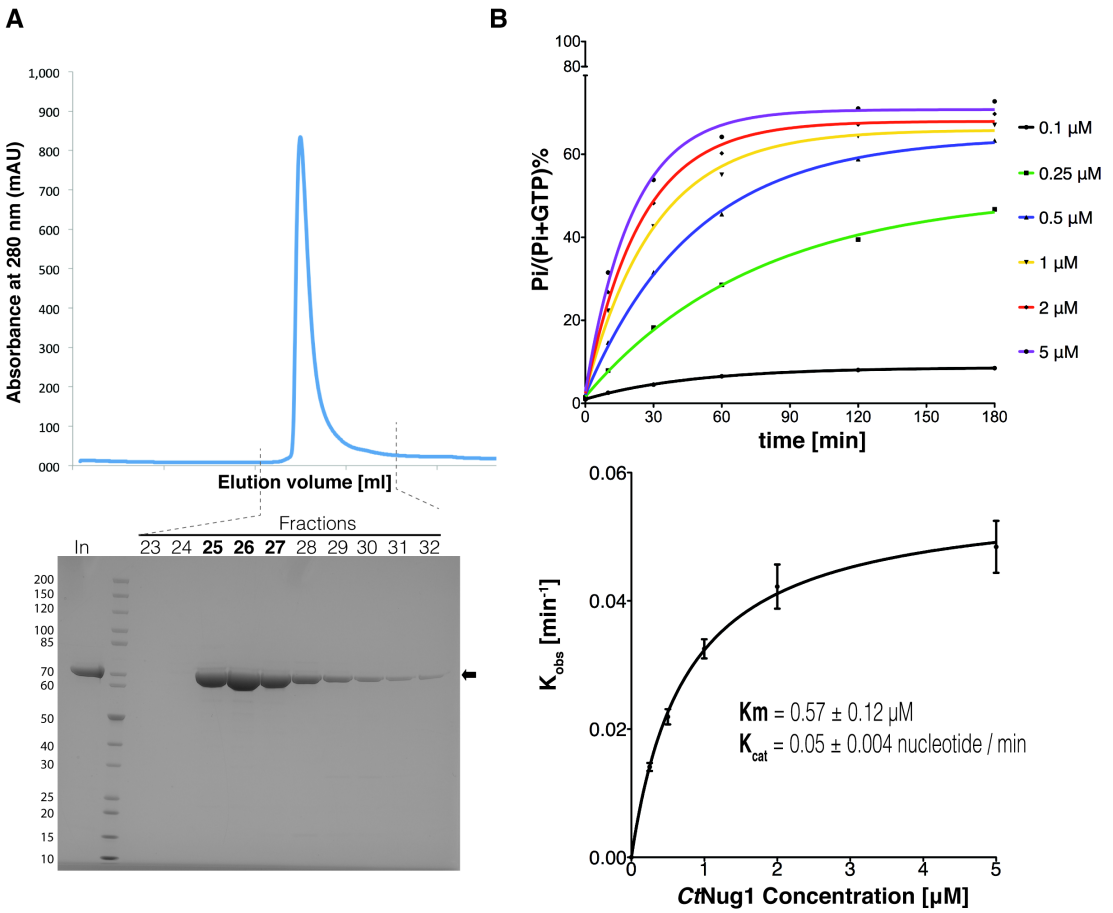

Figure 3.2 Nug1 exhibits an intrinsic GTPase activity *in vitro*. (A) The recombinantly expressed *Ct*Nug1 can be purified in high yields (20 mg/ml). top: chromatogram from size-exclusion chromatography (Superdex200 10/300). Y-axis indicates the protein absorbance at 280 nm, expressed in absorbance units (mAU) and X-axis the elution volume in ml; bottom: The size-exclusion chromatography fractions were analyzed by SDS-PAGE and Coomassie staining. Black arrow indicates *Ct*Nug1. The numbers on top of the gel correspond to the gel-fitration fractions, and "In" denotes the input. **(B) Characterization of *Ct*Nug1's GTPase activity using [γ-^{32}P]-labeled GTP.** Recombinantly expressed *Ct*Nug1 was subjected to single-turnover GTPase assays (see text). The enzymatic reaction was carried out with a final concentration of 100 nM GTP containing 750 nCi of γ^{32}P-labeled GTP (6000 Ci/ mmol) (for details see section 5.3.4). Phosporimager analysis was performed using ImageJ software; top: graph shows the ratio of hydrolyzed phosphate (Pi) to total GTP (GTP+ Pi) plotted against time (t=0, 10, 30, 60, 120 and 180 min) for the different protein concentrations of *Ct*Nug1 (0.1, 0.25, 0.5, 1, 2, 5 µM). For each of the curves obtained in this GTPase assay the observed rate constants (K_{obs}) were calculated and plotted against the different concentrations of *Ct*Nug1 (shown in the bottom graph). Nonlinear regression and the standard enzyme kinetics equations of GraphPad software were used to calculate the indicated Km and K_{cat} values.

With these assays, the ratio of hydrolyzed phosphate (Pi) to total GTP (GTP + Pi) was plotted against time for each of the different concentrations of *Ct*Nug1 and the respective K_{obs} values (the observed rate constants of each reaction) were calculated using the equations described in Materials and Methods (see section 5.3.4). Under the conditions tested, *Ct*Nug1 was able to hydrolyze GTP with a Km of 0.57 ± 0.12 µM and a Kcat = 0.05 ± 0.004 nucleotide / min (Figure 3.2 B, bottom). The turnover rate (K_{cat}) value of *Ct*Nug1 is comparable to those observed for other GTPases, including members of the Rab and Ras subfamilies that exhibit K_{cat} values of 0.02- 0.08 nucleotide /min (Barr and Lambright, 2010; Bos et al., 2007; Cherfils and Chardin, 1999; Iwashita and Song, 2008; Sprang, 1997; Vetter and Wittinghofer, 2001). The enzymatic activity of these GTPases is stimulated in the presence of GTPase Activating Proteins (GAPs) and thus raised the question whether *Ct*Nug1's GTPase activity could be regulated.

For most of the small monomeric GTPases, GTP activating proteins (GAPs) and guanine nucleotide exchange factors (GEFs) have been identified to regulate the GTPase activity (see Introduction). However, it is unlikely that Nug1 is regulated in the same way as it is a member of the HAS (hydrophobic amino acid substitution) subfamily of GTPases. In this subfamily, the catalytic glutamine following the G3 motif [DxxG**Q**] has been replaced by a hydrophobic amino acid (in the case of *Ct*Nug1, *Sc*Nug1, YlqF and YqeH an isoleucine [DxxG**I**] suggesting an alternative catalytic mechanism.

Interestingly, a new group of GTPases, termed 'cation-dependent' has been recently described that exhibit enhanced activity when certain cations are present (Ash et al., 2012). Based on a multiple-sequence alignment of cation-dependent GTPases (CD-GTPases) (Ash et al., 2012), *Ct*Nug1 was found to contain the conserved residue within the G1 motif (N322) predicted to coordinate the cation (Figure 3.3 A, left panel). Further, atomic structures of CD-GTPases, such as the bacterial MnmE (involved in tRNA modification) (Scrima and Wittinghofer, 2006) and FeoB (involved in iron transfer) (Ash et al., 2011a; Ash et al., 2011b) suggested that there is a restriction in the radius of the cation, to allow it to fit properly into the enzymatic pocket (Figure 3.3 A, right panel). To assess whether the same was true for *Ct*Nug1, GTPase assays were performed in the presence of cations with

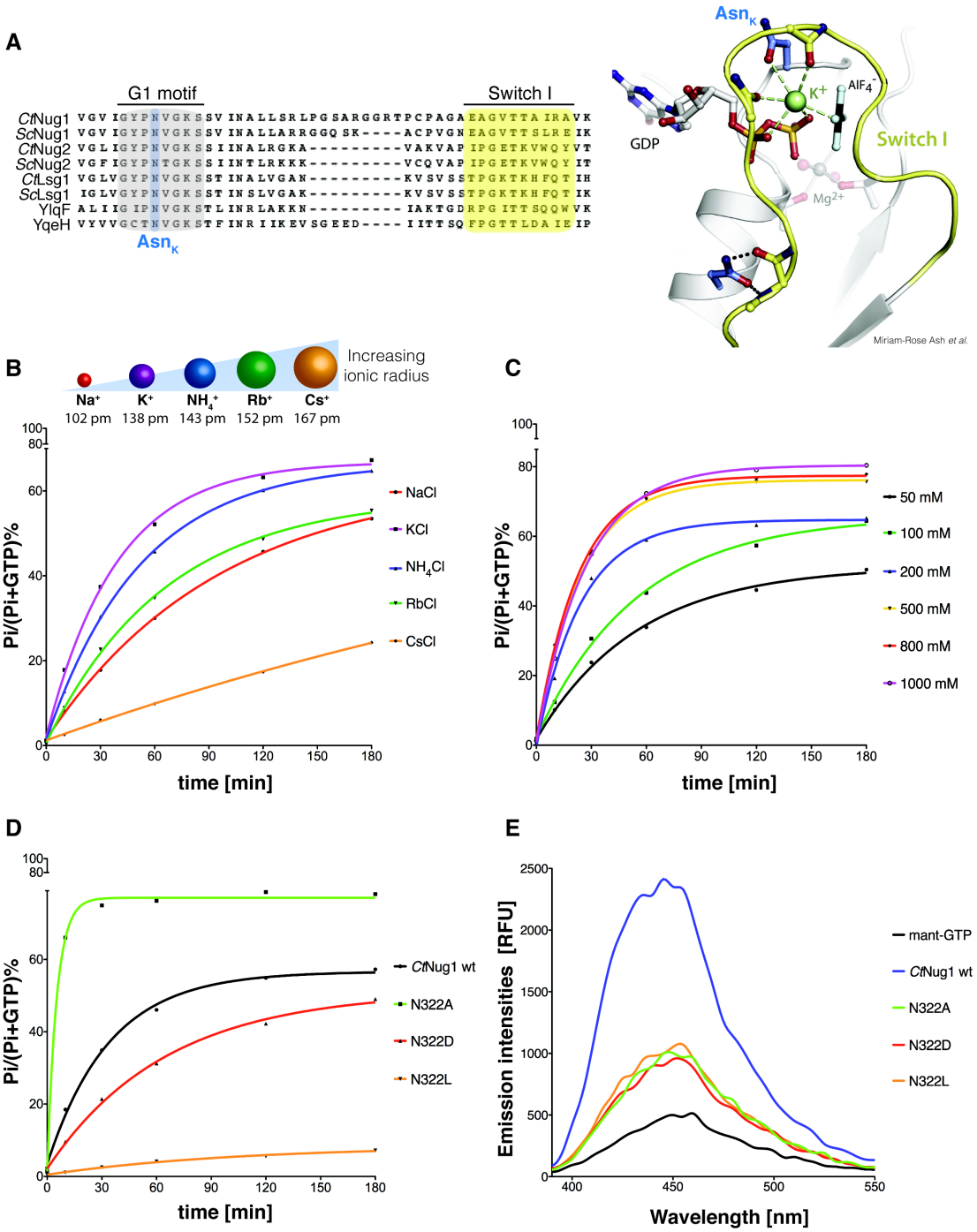

Figure 3.3 The GTPase activity of *Ct*Nug1 is stimulated by potassium ions. (A) The conserved asparagine in the G1 motif is the residue involved in cation coordination. left panel: multiple-sequence alignment showing the conserved G1 motif and Switch I region between cation-dependent GTPases including the thermophilic (*Ct)* and yeast (*Sc*) Nug1, Nug2 and Lsg1, as well as the *B. subtilis* YlqF and YqeH. The alignment was performed with ClustalW (Larkin et al., 2007) based on the complete protein sequences and visualized with Jalview (Waterhouse et al., 2009). G1 [GxxNxGKS] and Switch I (G2) motifs are highlighted in grey and yellow boxes, respectively. The conserved asparagine residue (Asn_K) is highlighted in blue; right panel: the Asn_K participates in potassium coordination together with backbone residues from the Switch I region. Magnified view of the GTPase domain of the cation-dependent *Streptococcus thermophilus* FeoB in complex with potassium and GDP·AlF_4^- (PDB ID: 3SS8) (Miriam-Rose Ash *et al.*). Asn_K is indicated and highlighted in blue, Switch I region in yellow and the rest of the G1 motif is shown in transparent grey. **(B) The ionic radius of the catalytic cation affects the *Ct*Nug1 GTPase activity.** top: cartoon depicting the increasing ionic radius of Na^+: 102 pm, K^+: 138 pm, NH_4^+: 143 pm, Rb^+: 152 pm

and Cs^+: 167 pm. The indicated ionic radii correspond to coordination number VI (the presence of water molecules forming a cell around the ions in solution is not calculated); bottom: Single-turnover GTPase assays were performed as previously described (see figure 3.2) for *Ct*Nug1 in the presence of the above-mentioned cations (200 mM). The graph shows the ratio of hydrolyzed phosphate (Pi) to total GTP (GTP+ Pi) plotted against time (t=0, 10, 30, 60, 120 and 180 min) for the different cations. **(C) Increasing concentrations of potassium ions can stimulate *Ct*Nug1's GTPase activity *in vitro*.** The graph depicts the GTPase activity *Ct*Nug1 WT in the presence of increasing concentrations of KCl (50, 100, 200, 500, 800 and 1000 mM). **(D) The conserved asparagine (N322) in the G1 motif is involved in the coordination of the potassium ion.** The graph shows the GTPase activity of WT *Ct*Nug1 compared to the K^+-loop mutants (N322A, N322D, N322L) (for details see text). **(E) The K^+-loop mutants are able to bind mant-GTP**. Reactions of 100 μl were performed in 96-well plates, with 1 μM of recombinant protein incubated with 0.5 μM of mant-nucleotide for 10 min at 30°C. The reaction mixture was then excited at 355 nm and emission spectra (385 and 600 nm) were recorded with spectrophotometer. The graph shows the emission spectra (intensities in relative fluorescence units, RFU) of mant-GTP when incubated with *Ct*Nug1 WT or the indicated K^+-loop mutants. Both GTPase and nucleotide binding assays were performed at least twice, yielding highly reproducible data sets.

increasing ionic radii (Na^+: 102 pm, K^+: 138 pm, NH_4^+: 143 pm, Rb^+: 152 pm, Cs^+: 167 pm) (Figure 3.3 B). Of the different ions tested, a maximal stimulation of *Ct*Nug1's GTPase activity was observed in the presence of potassium ions, whereas the lowest enzymatic activity (approximately three times less) was obtained for the caesium, the largest ion tested. Additionally, we tested whether increasing the concentration of potassium ions (50 - 1000 mM) could further stimulate the enzymatic activity of *Ct*Nug1 (Figure 3.3 C). These experiments showed that the GTPase activity of *Ct*Nug1 increased as the concentration of potassium rose up to 500 mM KCl. However, above 500 mM of KCl no further stimulation on GTPase activity could be observed.

To confirm that the enhanced activity observed for *Ct*Nug1 was due to cation stimulation, mutants were generated with the aim of disrupting ion binding. Therefore, the conserved asparagine in the G1 motif [Gxx**N**xGKS] was substituted with an uncharged alanine (N322A), a charged aspartic acid (N322D) and a hydrophobic leucine (N322L) (referred thereafter as K^+-loop mutants). These mutants were subsequently purified and tested for GTP hydrolysis and nucleotide binding using single-turnover GTPase (Figure 3.3 D) and fluorescence-based assays (Figure 3.3 E), respectively. The K^+-loop mutants tested exhibited decreased GTPase activity when compared to wild-type *Ct*Nug1 (Figure 3.3 D), except for the N322A mutant, which showed increased activation compared to the WT protein (see Discussion). The loss of GTPase activity seen in *Ct*Nug1 G-domain

mutants could either be due to failure in GTP hydrolysis or inability to bind nucleotide. To distinguish between these two possibilities, fluorescence-based nucleotide-binding assays were performed. In these experiments wild-type and mutant versions of *Ct*Nug1 were incubated with mant-GTP (Figure 3.3 E) (see also section 5.3.5). mant-GTP is a fluorescent GTP analog that does not emit light when it is in solution due to inter- and intra-molecular quenching by the solvent and the guanine base, respectively. Upon binding to protein, mant-GTP emits light (the fluorescence quantum yield increases significantly) rendering it a sensitive sensor for protein-nucleotide interactions.

When tested for nucleotide binding, all three K^+-loop mutants (N322A, N322D and N322L) were found to bind guanine nucleotide, as their emission spectra were higher in relative fluorescence units (RFUs) than the background level (mant-GTP alone). However, when compared to the wild-type *Ct*Nug1, they exhibited a decrease in nucleotide binding ability (Figure 3.3 E). Together our *in vitro* studies show that *Ct*Nug1 displays an intrinsically low GTPase activity that can be stimulated in the presence of potassium ions that are coordinated by the asparagine (N322) residue in the G1 motif.

3.2 Mutations within the GTPase-domain of *Ct*Nug1 result in impaired nucleotide binding or hydrolysis.

With the aim of identifying Nug1 mutants that are defective in nucleotide binding and/or GTPase activity, we generated a series of point mutations within each of the conserved motifs (G1 to G3) that comprise the *Ct*Nug1 GTPase domain (K325A, T356A/T357A, D372N and G375A) (Figure 3.4 A). Mutations in the conserved lysine of the G1 [GxxxxG**K**S] or in the aspartate of G3 [**D**xxG] motif are predicted to impair nucleotide binding in the enzymatic pocket. Additionally, mutations in the conserved threonine of the Switch I region (G2 motif) or in the glycine of the G3 [Dxx**G**] motif are predicted to affect the hydrolysis of GTP (Bourne et al., 1990; Hall, 1990; Takai et al., 2001; Vetter and Wittinghofer, 2001).

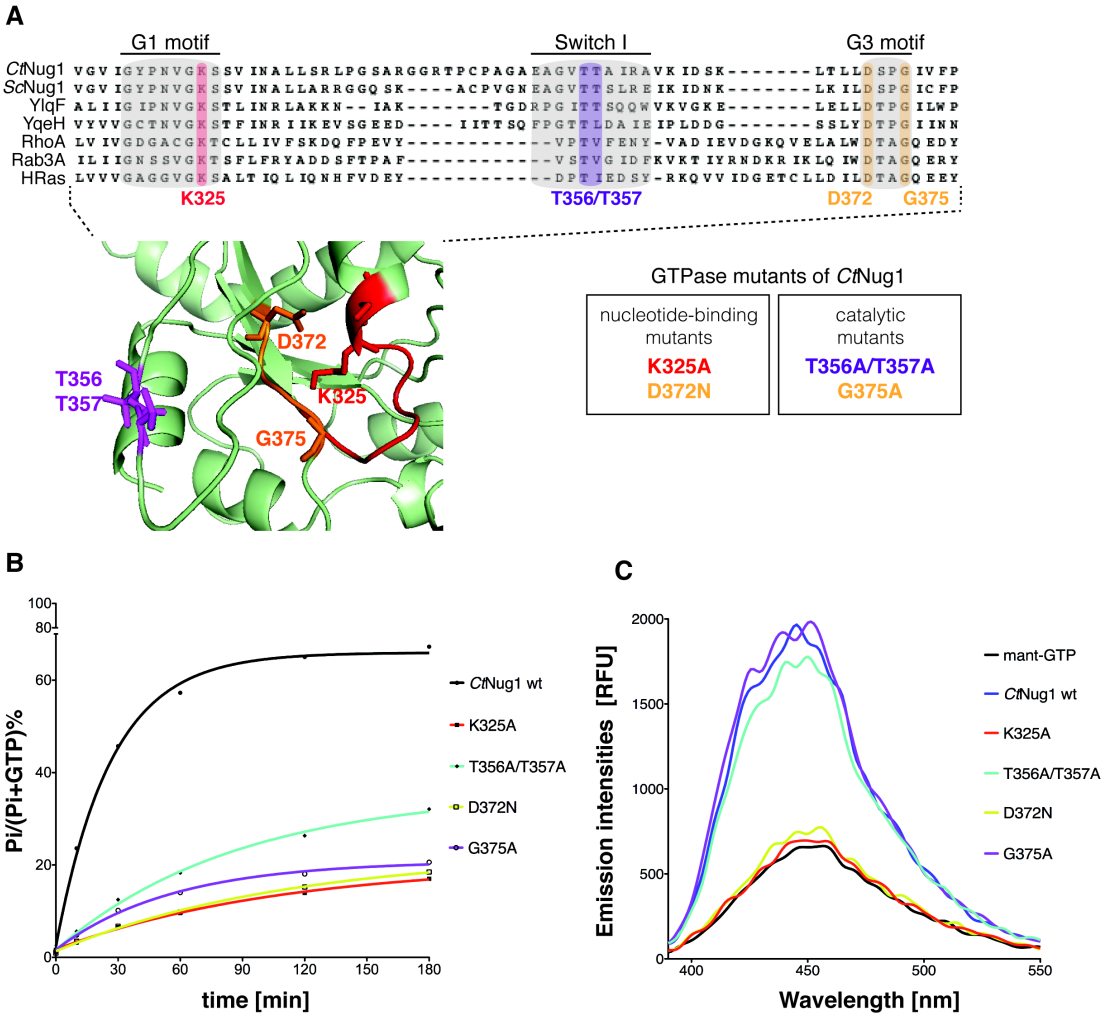

Figure 3.4 The G-domain mutants of *Ct*Nug1 are impaired in nucleotide binding and/or hydrolysis. (A) *Ct*Nug1 contains the conserved residues important for GTP binding and hydrolysis. top: multiple-sequence alignment of the G-domain of different GTPases including the thermophilic (*Ct)* and yeast (*Sc*) Nug1, the *B. subtilis* YlqF and YqeH and the human small GTPases Rho1A, Rab3A and HRas. The alignment was performed with ClustalW (Larkin et al., 2007) based on the complete protein sequences and visualized with Jalview (Waterhouse et al., 2009). G1 [GxxxxGKS], Switch I (G2) and G3 [DxxG] motifs are highlighted in grey boxes. The conserved residues subsequently mutagenized are highlighted in red, purple and orange for G1, Switch I and G3 motif, respectively; bottom left: magnified view of *Ct*Nug1 GTPase-domain modeled based upon the crystal structure of the *B. subtilis* YlqF (PDB ID: 1puj) homologue using the Phyre2 software (Kelley and Sternberg, 2009). The predicted model *Ct*Nug1 is missing the N-terminus (1-199 aa) and part of its C-terminal end (452-558 aa). The remaining protein sequence shares 27 % identity with YlqF and the modeled structure exhibits 100 % confidence. The residues involved in nucleotide binding and/or hydrolysis are color-coded as in the alignment; bottom right: table indicating the mutations generated in the GTPase domain of *Ct*Nug1 together with their predicted function. **(B) The G-domain mutants of *Ct*Nug1 exhibit lower enzymatic activity compared to the WT protein.** Radioactivity-based GTPase assays were performed as previously described (see figure 3.2) using 1 µM of recombinantly expressed protein. The graph shows the ratio of hydrolyzed phosphate (Pi) to total GTP (GTP+ Pi) plotted against time (t=0, 10, 30, 60, 120 and 180 min) for the various GTPase mutants (K325A, T356A/T357A, D372N and G375A). **(C) *Ct*Nug1 WT and catalytic mutants T356A/T357A and G375A are able to bind to fluorescent GTP analogue, mant-GTP.** Fluorescence-based nucleotide binding assays were performed as described in figure 3.3 E. The graph shows the emission spectra (intensities in relative fluorescence units, RFU) of mant-GTP when incubated with *Ct*Nug1 WT or the indicated G-domain mutants. Both GTPase and nucleotide binding assays were performed at least twice, yielding highly reproducible data sets.

Each GTPase mutant was expressed in *E. coli* and purified following the same purification procedure as performed for the wild-type *Ct*Nug1. The yield of these mutant proteins was significantly lower, when compared to the WT *Ct*Nug1, requiring an additional concentration step before comparable GTPase and fluorescence-based nucleotide binding assays could be performed. The GTPase assays (Figure 3.4 B) revealed that each of the mutants generated exhibited an inhibition of activity when compared to WT *Ct*Nug1. Interestingly, the mutants predicted to be involved in nucleotide binding (K325A and D372N) exhibited the greatest decrease in enzymatic activity (approximately 7 times less than the WT *Ct*Nug1). The loss of GTPase activity in the G-domain mutants of *Ct*Nug1, confirms that the enzymatic activity observed in the GTPase assays can be attributed to *Ct*Nug1 and not to contaminants.

Further, fluorescence-based nucleotide-binding assays (Figure 3.4 C) showed that the K325A and D372N mutants are indeed inhibited in nucleotide binding, as their emission spectra were similar to background (fluorescent analog alone). This finding supports the idea that their low hydrolysis rates observed in the GTPase assays were due to their inability to bind nucleotide. In contrast, the G375A and T356A/T357A mutants defective in GTP hydrolysis could bind mant-GTP at the same levels as the WT *Ct*Nug1. Thus, the mutants generated can be divided into 2 categories: i) nucleotide-binding mutants (K325A, D372N) that exhibit a defect in GTP hydrolysis, only as a consequence of an inability to bind nucleotide and ii) hydrolysis mutants (G375A, T356A/T357A) that retain the ability to bind GTP. Hence, we have generated Nug1 mutants that effectively separate nucleotide binding from hydrolysis.

3.3 The *S. cerevisiae* Nug1 nucleotide-binding mutant (D336N) causes defects in 60S subunit maturation.

To gain *in vivo* insight into the role-played by Nug1's nucleotide binding and GTP hydrolysis the orthologous yeast G-domain mutants were generated. Due to the high sequence similarity between the *C. thermophilum* and *S. cerevisiae* Nug1

GTPase domain, I could identify the residues in the yeast Nug1 that were shown for *Ct*Nug1 to be involved in catalysis (T320, T321, G339), GTP- binding (K293, D336), as well as potassium coordination (N290) (see previous section). Hence, the *nug1K283A, nug1T320A/T321A, nug1D336N*, *nug1G339A*, *nug1N290A, nug1N290L* and *nug1N290D* yeast mutants were generated and tested for complementation using the Nug1 shuffle strain (*nug1*Δ + Rps316-P.*NUG1*::*NUG*1).

C. thermophilum	*S. cerevisiae*	Function
K325A	K293A	Nucleotide Binding
T356A/T357A	T320A/T321A	GTP hydrolysis
D372N	D336N	Nucleotide Binding
G375A	G339A	GTP hydrolysis
N322A/D/L	N290A/D/L	Potassium coordination

Table1: The orthologous mutations generated in the GTPase domain of *Ct*Nug1 and *Sc*Nug1 together with their predicted function.

All mutants were expressed from a centromeric plasmid (YCplac22) under the control of the endogenous yeast Nug1 promoter (P.*NUG1)* and subsequently transformed in the shuffle strain of Nug1 for growth analysis (Figure 3.5 A) (see also section 3.1). While all Nug1 mutants complemented the non-viable *nug1*Δ strain, their growth behavior differed. The Nug1 constructs carrying mutations shown *in vitro* to affect nucleotide binding (K293A, D336N) exhibited significantly slower growth when compared to the WT Nug1. In contrast, growth appeared to be unaffected in mutants defective in GTP hydrolysis (T320A/T321A, G339A) or in the K^+-loop mutants (N290A, N290D and N290L).

To exclude that the growth phenotypes observed for the different Nug1 mutants were not due to variations in protein expression levels, the amounts of Nug1 WT or mutants was tested in whole cell lysate by SDS-PAGE and Western blotting. Since all constructs were C-terminally TAP-tagged, it was possible to detect them using an anti-pA antibody (Figure 3.5 B). This analysis showed no difference in protein levels when Nug1 WT was compared to nucleotide-binding or hydrolysis mutants. As Nug1 is involved in ribosome biogenesis we sought to investigate if the growth defects observed here would reflect impaired ribosome assembly.

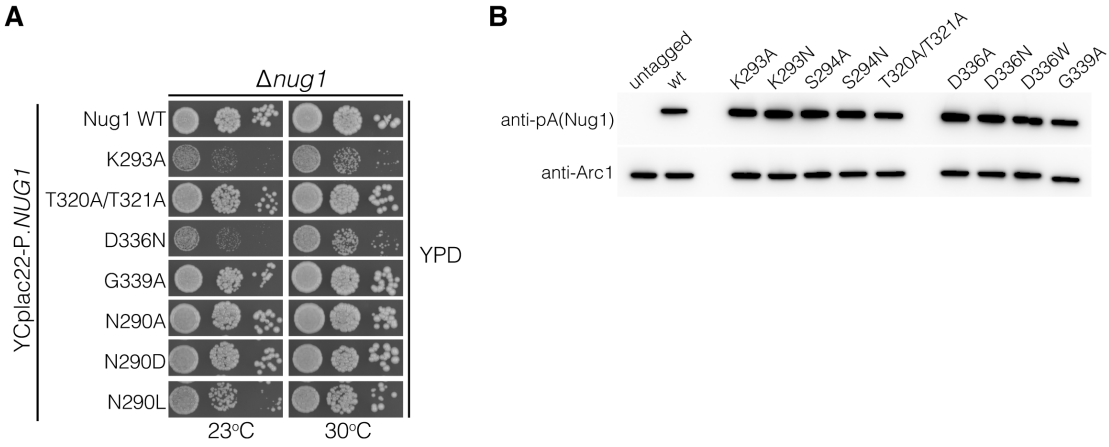

Figure 3.5 The Nug1 nucleotide-binding mutants exhibit show growth phenotypes. (A) Growth analysis of the yeast *nug1*Δ strain complemented by *NUG*1 or *nug*1 K293A, T320A/T321A, D336N, G339A, N290A, N290D and N290L expressed from a centromeric plasmid (YCplac22) under the control of the native *NUG*1 promoter (P.*NUG*1). Ten-fold serial dilutions of the indicated strains were spotted on YPD plates for 2 days at 23 and 30°C. **(B) The expression levels of the Nug1 GTPase mutants are not affected *in vivo.*** Whole cell lysates were prepared (see materials and methods section 5.3.1) from exponentially growing cells for each of the indicated mutants. Samples were analyzed on SDS-PAGE and the protein levels of the Nug1 constructs were determined by western blotting using antibodies against the C-terminal TAP-tag. The anti-Arc1 western blot served as loading control and untagged Nug1 served as negative control.

To assess the impact of representative nucleotide-binding (D336N) and GTP hydrolysis (G339A) mutants on ribosome biogenesis, ribosomal subunits and polysomes were analyzed by sucrose density gradient centrifugation (Figure 3.6 A, top). This analysis revealed that compared to the wild-type protein or the catalytic G339A mutant, the Nug1 impaired in nucleotide-binding (D336N) exhibited a substantial decrease in 60S and an increase in 40S subunits. As a result of 60S subunit decrease, 80S was also reduced and the appearance of “halfmers” was observed. The “halfmer” polysomes correspond to 40S subunit together with mRNAs that are stalled in translation initiation complex, as the 60S subunit is missing. To investigate potential differences in the association with pre-ribosomal particles of Nug1 WT and mutants, fractions from the sucrose gradient centrifugation were analyzed by SDS-PAGE and western blotting (Figure 3.6 A, bottom). In this analysis we observed that *nug1* D336N and G339A proteins were efficiently assembled into pre-60S subunits, suggesting that the 60S defects seen for the D336N mutant were not due to impaired recruitment with pre-ribosomes.

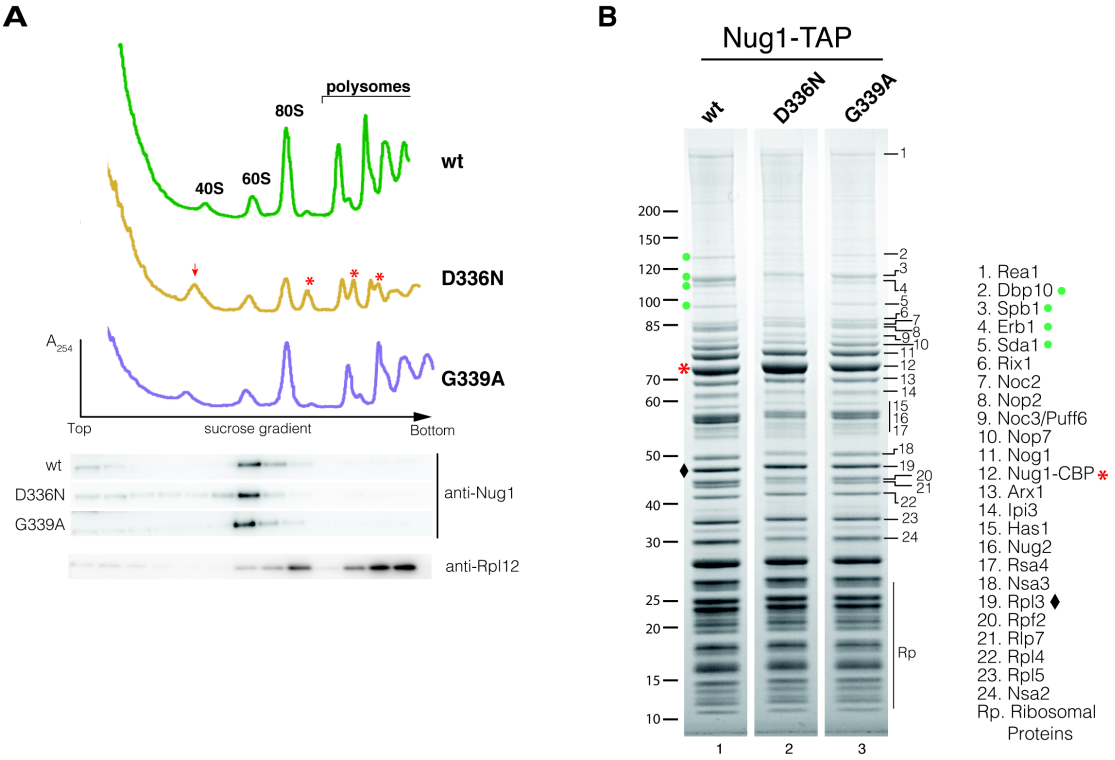

Figure 3.6 Analysis of Nug1 GTPase mutants. (A) The Nug1 nucleotide-binding (D336N) mutant exhibits defects in 60S subunit biogenesis. top: Ribosome and polysome profiles were analyzed by sucrose gradient fractionation of whole cell lysates derived from Nug1 WT, nucleotide-binding (D336N) or hydrolysis (G339A) mutants. A_{254nm} profiles of the fractions collected are depicted and the peaks corresponding to 40S, 60S, 80S, and polysomes are indicated. Red arrow denotes the increase of the 40S subunit and the red asterisks the halfmers; bottom: western blotting of the gradient fractions using antibodies against Nug1 and Rpl12. **(B) Early 60S assembly factors (Dbp10, Sbp1, Erb1) are co-enriching less in affinity purified Nug1 D336N pre-particles.** Nug1 WT and mutants (D336N, G339A) carrying a TAP-tag at the C-terminal end were affinity purified and analyzed by SDS-PAGE and Coomassie staining. The indicated co-enriched bands were identified by mass-spectrometry and/or by comparison with already characterized pre-ribosomal particles. Red asterisks indicate the Nug1 bait protein and green circles the reduced assembly factors. Rpl3 was used as loading control and is depicted with a black diamond.

The fact that both nucleotide-binding and GTP hydrolysis mutants associate with pre-ribosomes, prompted us to analyze the co-purified assembly factors of TAP-tag Nug1 WT and mutants. Such experiments could give insight into which steps during ribosome biogenesis Nug1 GTPase activity is involved in. To this end, Nug1 WT and mutants (D336N, G339A) carrying a TAP-tag at the C-terminal end were affinity purified and analyzed by SDS-PAGE, Coomassie staining and the co-enriched bands were identified by mass-spectrometry. As seen in Figure 3.6 B, the pre-ribosomal particles enriched by WT Nug1 contained a number of nucleolar (Dbp10, Spb1, Erb1, Nop7) and nucleoplasmic (Rea1, Arx1, Rsa4) biogenesis

factors known to function in the 60S biogenesis pathway. Mutant Nug1 proteins (D336N, G339A) co-enriched, in principle, the same assembly factors. However, the levels of the bait Nug1 protein were increased in the case of D336N mutant, compared to WT Nug1, suggesting that the ratio of “free” to “ribosome-bound” Nug1 has changed (the slight increase of bait protein in the mutant was reproducible). Such increase in the bait Nug1 protein was not observed for the catalytic G339A mutant. In addition, the D336N mutant showed reduced levels of assembly factors such as Dbp10, Erb1, Spb1 and Sda1 (Figure 3.6 B). Some of these factors (Dbp10, Erb1 and Spb1) are characterized as early assembly factors, suggesting a possible role for Nug1 GTPase in the early steps of 60S subunit maturation.

Taken together, the nucleotide-binding (D336N) and the catalytic (G339A) mutants are binding to pre-ribosomes, but their association differs slightly as seen in the purified Nug1 pre-ribosomal particles. In addition, I observed that the association of early assembly factors (Dbp10, Erb1 and Spb1) was reduced in the D336N mutant, which could be the reason for the slow growth phenotypes observed.

3.4 Nug1 is involved in the early steps of 60S biogenesis.

To identify the exact step in ribosome biogenesis where Nug1 functions, I affinity purified 60S pre-ribosomes from various maturation stages ranging from early nucleolar (Nsa1), to intermediate nucleoplasmic (Rix1), late nucleoplasmic (Arx1) and cytoplasmic (Arx1; Lsg1) stage (Figure 3.7 A). For that reason, Nsa1, Rix1, Arx1 and Lsg1 were TAP-tagged at the C-terminal end in the Nug1 shuffle strain. These strains were then transformed with a centromeric plasmid expressing the Nug1 WT or mutants (D336N, G339A). The affinity-purified pre-particles were analyzed by SDS-PAGE followed by Coomassie staining or western blotting. The co-enriched assembly factors were identified by mass-spectrometry (Figure 3.7 B, top).

This analysis revealed similar, but not identical, composition of assembly factors in the purified pre-particles (Nsa1, Rix1, Arx1 and Lsg1) when Nug1 WT was compared to the nucleotide-binding (D336N) or catalytic (G339A) mutant. However,

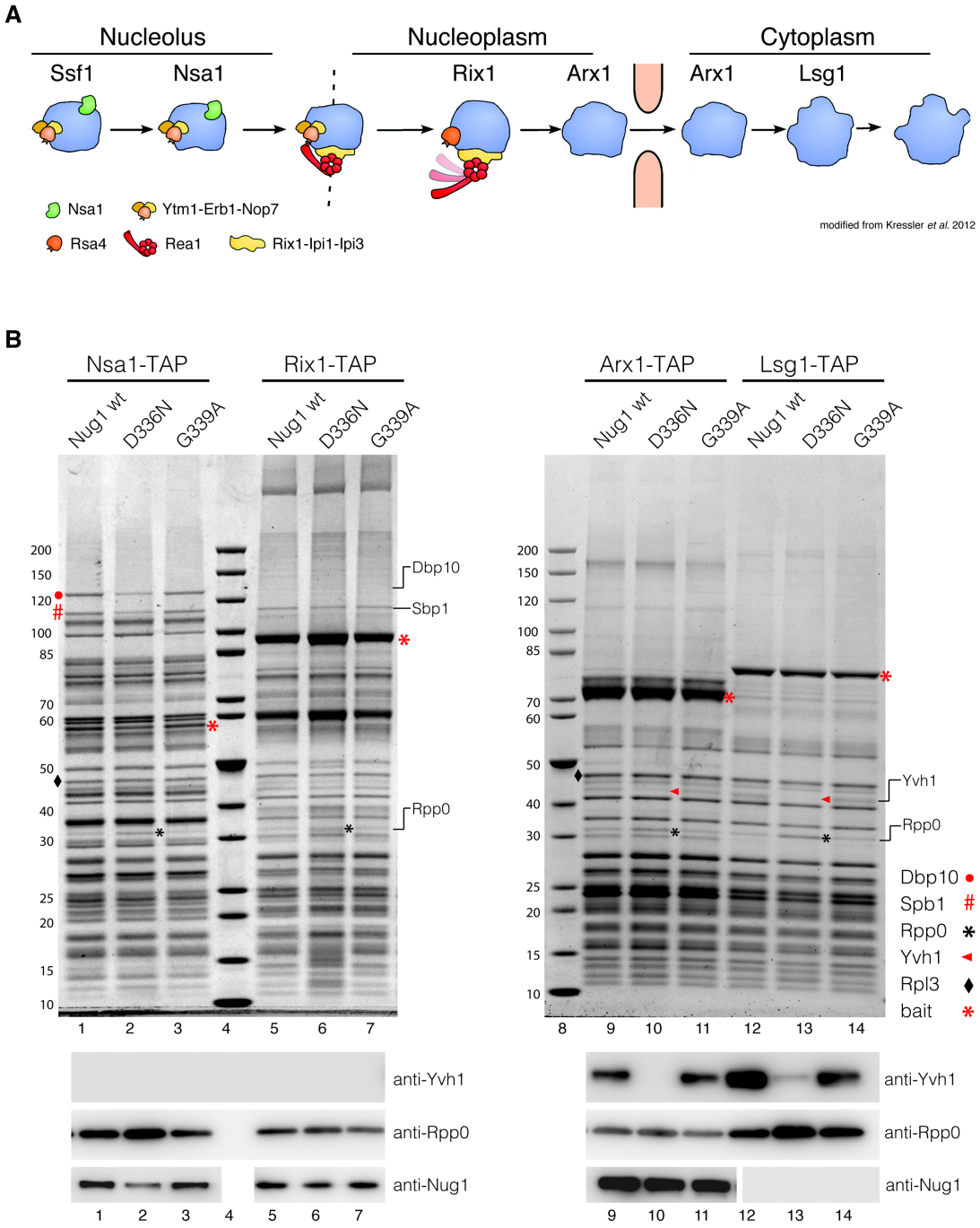

Figure 3.7 The Nug1 nucleotide-binding mutant results in the reduced association of early and late assembly factors. (A) Cartoon depicting representative pre-ribosomal particles from the 60S subunit biogenesis. Ssf1 and Nsa1 bait proteins co-enrich in nucleolar biogenesis factors and Rix1 in early nucleoplasmic. Arx1 co-purifies late nucleoplasmic and early cytoplasmic assembly factors, whereas Lsg1 exclusively cytoplasmic. **(B) Analysis of pre-ribosomal particles from strains expressing Nug1 WT or mutants (D336N, G339A).** top: Tandem affinity purification of the indicated TAP-tagged assembly factors (Nsa1, Rix1, Arx1 and Lsg1) from the Nug1 shuffle strain expressing Nug1 WT or mutants (D336N or G339A). The final TAP eluates were analyzed by SDS-PAGE and Coomassie staining. Rpl3 was used as loading control for each of the individual pre-particles. Red asterisks indicate the baits (Nsa1, Rix1, Arx1 and Lsg1). Red dot, red hash tag, black asterisk, red triangle and black diamond correspond to Dbp10, Spb1, Rpp0, Yvh1 and Rlp3, respectively; bottom: western blotting of the affinity purified pre-ribosomal particles using antibodies against Yvh1, Rpp0 and Nug1.

the early Nsa1 particles showed reduced levels of Dbp10 and Spb1, in the case of Nug1 D336N mutant (Figure 3.7 B, see lanes 1 to 3). Additionally, we observed reduced levels of Rpp0 and loss of Yvh1 in the Arx1 and Lsg1 pre-particles only in the nucleotide-binding mutant of Nug1 (see lanes 12 to 14). Western blotting (Figure 3.7 B, bottom) confirmed the loss of Yvh1 in the Arx1 and Lsg1 pre-particles for the Nug1 D336N mutant and it showed that Rpp0 levels were increased not only in Arx1 and Lsg1 pre-particles, but also in the early Nsa1. Since Yvh1 and Rpp0 participate in the P-stalk formation, our findings suggested a possible role for Nug1 in this pathway.

Yvh1 and Rpp0 together with Mrt4 are involved in the formation of the P-stalk. This is a landmark structure of the mature 60S subunit, which serves as a platform for different elongation factors during translation (see also introduction). Mrt4 is the acidic paralogue of Rpp0 and it is suggested to have overlapping binding sites on the ribosome with Rpp0, i.e in the pre-ribosomes the binding site is occupied by Mrt4 and in the mature 60S subunits by Rpp0. Additionally, it is proposed that Mrt4 is released in an Yvh1-dependent manner (Figure 3.8 A). (Kemmler et al., 2009; Lo et al., 2009; May et al., 2012; Remacha et al., 1995a; Remacha et al., 1995b; Rodriguez-Mateos et al., 2009a; Rodriguez-Mateos et al., 2009b).

The loss of Yvh1 and the enrichment of Rpp0 (figure 3.7 B) in the affinity purified pre-60S particles, prompted us to also analyze Mrt4. To this end, Mrt4 and Yvh1 were TAP-tagged at the C-terminal end in the Nug1 shuffle strain and used as baits for affinity purification of pre-ribosomes when Nug1 WT or mutants (D336N, G339A) were expressed. The co-purified proteins (assembly factors and ribosomal proteins) enriched in Mrt4 or Yvh1 TAP purifications, were analyzed by SDS-PAGE and Coomassie staining (Figure 3.8 B). Here, we observed that both Mrt4 and Yvh1 protein baits associated less with the pre-ribosomes in the Nug1 nucleotide-binding mutant (D336N) (see lanes 3 and 7), as only a subset of assembly factor were co-enriched compared to Nug1 WT or the catalytic G339A mutant. The decreased association of Yvh1 with the pre-ribosomes agreed with the previous findings showing the loss of Yvh1 from the Arx1 and Lsg1 pre-particles.

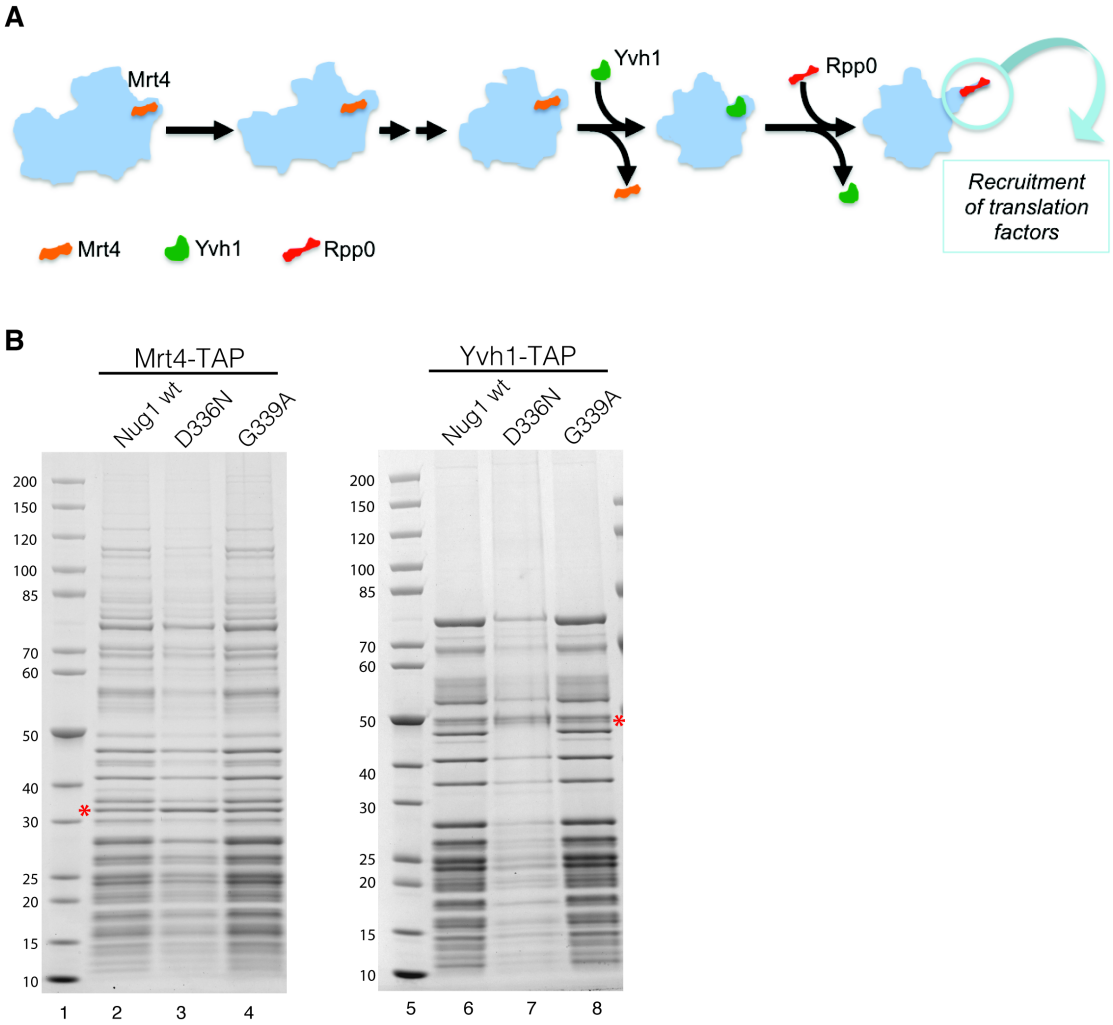

Figure 3.8 Mrt4 and Yvh1 associate less with the pre-ribosomes in the Nug1 D336N mutant. (A) Mrt4, Yvh1 and Rpp0 are involved in the P-stalk formation. Cartoon depicting the P-stalk formation. Mrt4 associates with early pre-ribosomal particles and Yvh1 is responsible for its release. Rpp0 is the paralogue of Mrt4 and binds approximately at the same position as Mrt4, but in the mature ribosome (see also introduction). **(B) The affinity purified Mrt4 and Yvh1 pre-ribosomes are co-enriched with fewer assembly factors when the Nug1 D336N mutant is expressed.** Affinity purified Mrt4 (left panel) and Yvh1 (right panel) pre-ribosomal particles from the Nug1 shuffle strain expressing Nug1 WT or mutants (D336N or G339A). TAP eluates were analyzed by SDS-PAGE and Coomassie staining. Mrt4- and Yvh1- bait proteins are indicated with red asterisks and were used for equal loading of the respective eluates.

As Mrt4 associates earlier with the pre-ribosomes than Yvh1 during 60S subunit biogenesis, I postulated that the decrease observed in the association of Yvh1 is likely the result of a decrease recruitment of Mrt4 in the pre-ribosomes, i.e if less Mrt4 is recruited, then less Yvh1 would be needed for its release.

The reduced association of Mrt4 with pre-ribosomes when Nug1 nucleotide-binding mutant was expressed, together with the reduced levels of Dbp10, Sbp1

and Erb1 seen in early Nsa1 pre-particles, raised the question of whether Nug1 could be involved in the early steps of 60S biogenesis and thus influence the P-stalk formation. To explore whether the presence of Nug1 could affect Mrt4's recruitment/association with early pre-ribosomes, I designed a Nug1 depletion experiment based on the auxin inducible degron system (AID) (Morawska and Ulrich, 2013; Nishimura et al., 2009). In this system, auxin (indole-3-acetic acid; IAA) induces degradation by mediating the interaction of the Aid-degron in the target protein with the substrate recognition domain of the TIR1 (F-box protein, auxin receptor). This interaction leads to ubiquitination of the target and subsequent proteasomal degradation (Figure 3.9 A). In our experiments Nug1 was C-terminally Aid-tagged and the auxin receptor TIR1 was genomically integrated under the constitutive promoter P.*ADH1.*

To verify that the auxin degron system could be used to deplete Nug1, samples of exponentially growing cell cultures were taken at different time points after the addition of auxin and subsequently analyzed by western blot. Nug1-Aid was completely depleted between 30 and 60 minutes (Figure 3.9 B) after auxin treatment. To assess the Nug1 depletion in terms of growth behavior, yeast strains expressing untagged or Aid-tagged Nug1 were spotted in 10-fold serial dilution on auxin-containing YPD plates (Figure 3.9 C). Cells expressing the Nug1-Aid fusion protein did not grow when spotted on auxin-containing plates at both 23 and 30°C, whereas cells expressing the untagged Nug1 exhibited no growth inhibition. Moreover, the effects of Nug1 depletion on ribosome and polysome profiles were analyzed by sucrose gradient fractionation of whole cell lysates derived from auxin-treated and untreated cells (Figure 3.9 D). When cells were treated with auxin a substantial increase in the 40S subunits was observed together with the appearance of halfmers. These findings were similar to the ribosome and polysome profiles obtained for the Nug1 nucleotide-binding mutant (D336N), where increased 40S subunits and halfmers were also observed. However in the Nug1 depletion experiments we observed halfmers also in the case of the untreated cells.

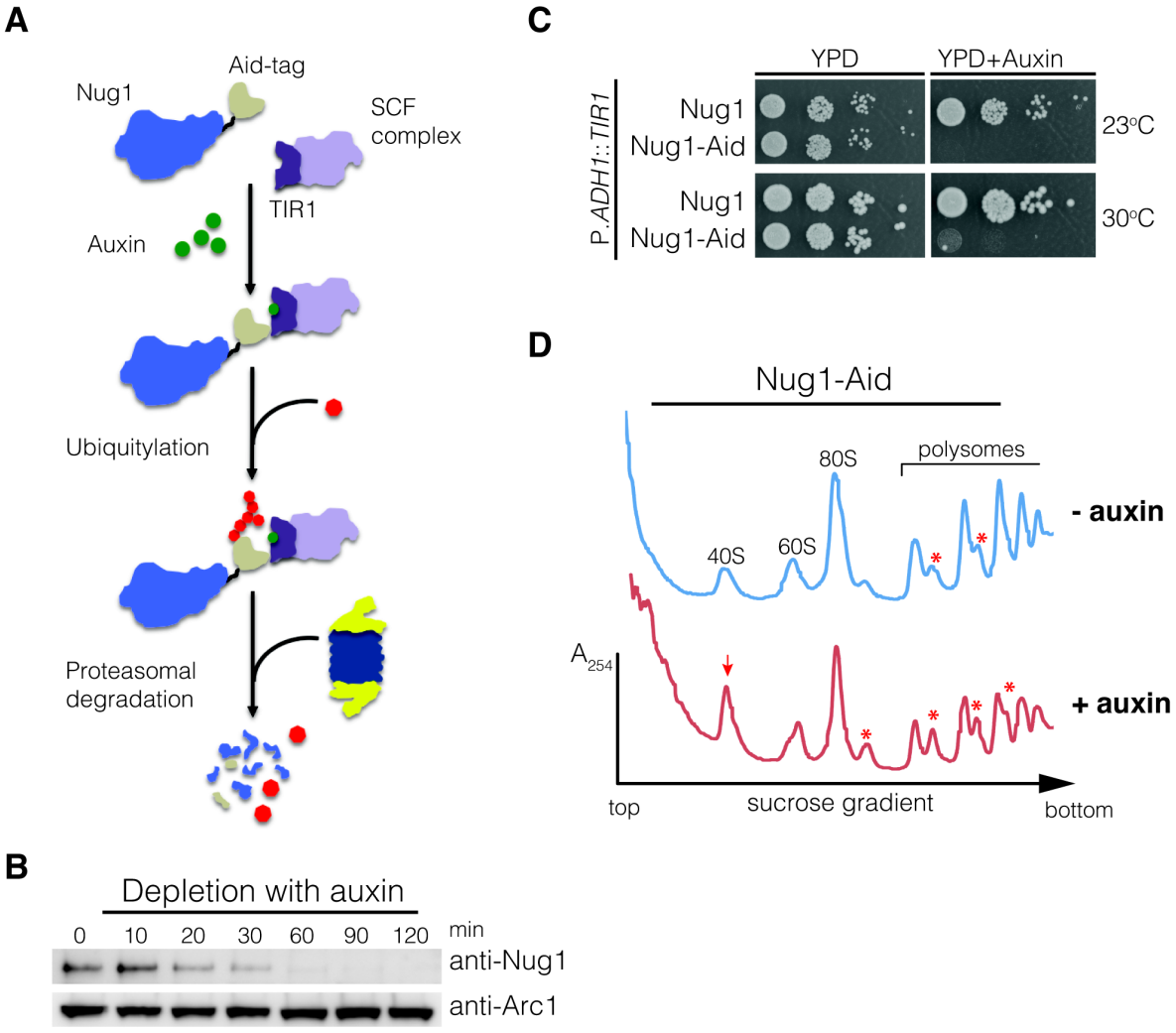

Figure 3.9 Nug1 depletion inhibits cell growth and causes defects in 60S subunit maturation. (A) The auxin-inducible degron system targets proteins for proteasomal degradation. In this system, auxin (indole-3-acetic acid; IAA) induces degradation by mediating the interaction of the Aid-degron (fused with the protein target) with the substrate recognition domain of the TIR1 (F-box protein, auxin receptor). TIR is part of the SCF complex (E3 ubiquitin ligase) and leads to ubiquitination of the target and finally proteasomal degradation. **(B) and (C) Depletion of Nug1 results in growth inhibition.** Nug1 was genomically tagged at the C-terminal end with the Aid-tag. The ubiquitin E3 ligase TIR1 was genomically integrated and expressed under the constitutive *ADH1* promoter (P.*ADH*1). **(B)** Cell culture expressing the Nug1-Aid was treated with 0.5 mM auxin and samples were taken at different time points (t=0, 10, 20, 30, 60, 90 and 120 min). Whole cell lysates were subsequently analyzed by SDS-PAGE and western blotting using an anti-Nug1 antibody. The anti-Arc1 western blot served as loading control. **(C)** Growth analysis of yeast cells expressing Aid-tagged or untagged Nug1 in the *ADH1*::*TIR1* background. Cells were spoted in 10-fold serial dilutions on YPD plates with or without 0.5 mM auxin and incubated at 23 and 30°C for 1 day. **(D) Nug1 depletion results in decreased levels of 60S subunits.** Ribosome and polysome profiles of whole cell lysates derived from auxin-treated and untreated cells were analyzed by sucrose gradient fractionation. A_{254nm} profiles of the fractions collected are depicted and the peaks corresponding to 40S, 60S, 80S, and polysomes are indicated. Red arrow denotes the increase of the 40S subunit and the red asterisks the halfmers.

We believe that this was due to the Aid-tag, although we could not observe any growth defects between tagged and untagged Nug1, as seen in Figure 3.9 C.

To address whether Nug1 could affect Mrt4's recruitment/association with early pre-ribosomes, the assembly factors Ssf1 and Nsa1 were TAP-tagged in the Nug1-Aid strain and pre-particles were affinity purified upon auxin treatment. The final TAP-eluates were analyzed by SDS-PAGE and Coomassie staining, followed by western blotting (Figure 3.10 A) This analysis showed that Mrt4 levels were indeed reduced upon auxin-depletion of Nug1 in both Ssf1 and Nsa1 particles (Figure 3.10 A). Other biogenesis factors including Nsa3 and Tif6 did not change, whereas Rpp0 together with Rpl12 (another component of the P-stalk) were enriched. The decreased levels of pre-ribosome bound Mrt4 would lead to an increased binding of Rpp0 (likely together with Rpl12) as they bind in a mutually exclusive manner on the pre-ribosome. To exclude that the reduced levels of Mrt4 observed in the pre-ribosomes were not due to Mrt4 protein instability, whole cell-lysates were analyzed by western blotting and showed no detectable differences between untreated and auxin-treated cells (Figure 3.10 B). Interestingly, Nsa2 levels were also reduced when Nug1 was depleted. Nsa2 is another assembly factor suggested to localize in close proximity to the 60S stalk (in press *Bassler et al.* 2014) and could also have a role in the P-stalk formation (see next section). Further, in the Nug1 depletion experiments we also observed reduced levels of early assembly factors such as Rrp5, Noc1/Utp9, Dbp10, Spb1 and Drs1 in the Ssf1 and Nsa1 pre-particles as seen by Coomassie staining. Some of these factors (Dbp10, Spb1) were also reduced in the case of Nug1 D336N mutant when Nsa1 pre-particles were analyzed (Figure 3.7 B).

The similar reduction in early assembly factors seen in both the nucleotide-binding mutant (D336N) and when Nug1 was depleted (Figure 3.6, 3.7 and 3.10), suggests that the association of Nug1 with the pre-ribosomes might be affected when the nucleotide-binding ability of the protein is impaired. In addition, these data show that Nug1 is involved in the P-stalk formation. However, one cannot exclude that the early biogenesis factors (Dbp10, Sbp1, Drs1) reduced upon Nug1's depletion are not responsible for the reduced levels of Mrt4 and consequently Yvh1.

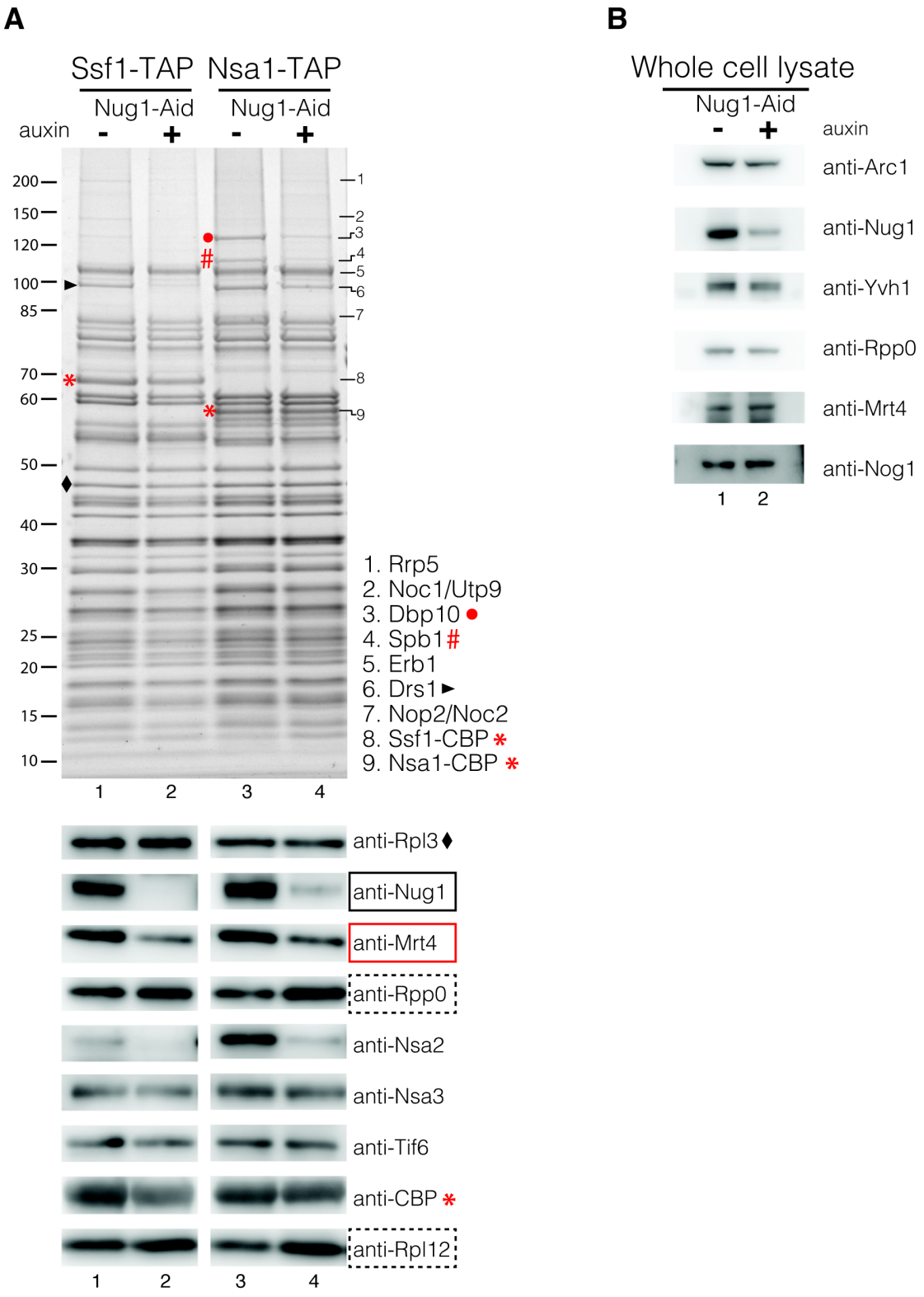

Figure 3.10 Nug1 depletion affects the association of early assembly factors in nucleolar pre-ribosomal particles. (A) The affinity purified Ssf1 and Nsa1 pre-ribosomes exhibit reduced levels of Dbp10, Sbp1, Drs1 and Mrt4 upon depletion of Nug1. top: Affinity purified Ssf1 and Nsa1 pre-particles from yeast cells expressing the fusion Nug1-Aid protein upon treatment with auxin. TAP eluates were analyzed by SDS-PAGE and Coomassie staining. Rpl3 was used as loading control for each pre-particle. Red asterisks indicate the baits (Ssf1 and Nsa1). Red dot, red hash tag, black triangle and black diamond correspond to Dbp10, Spb1, Drs1 and Rpl3, respectively; bottom: western blotting of the affinity purified pre-ribosomal particles using antibodies against Nug1,

Mrt4, Rpp0, Nsa2, Nsa3, Tif6, CBP and Rpl12. **(B) The steady state protein levels of Mrt4 are not affected upon Nug1 auxin-depletion.** Whole cell lysates derived from auxin-treated and untreated cells expressing Nug1-Aid were analyzed by SDS-PAGE and western blotting using antibodies against Nug1, Mrt4, Yvh1, Rpp0, Nog1 and Arc1. The anti-Arc1 western blot served as loading control.

3.5 Nug1 and Dbp10 bind at proximal sites on the pre-ribosomes and physically interact.

From the early biogenesis factors reduced upon Nug1's depletion or in the Nug1 D336N mutant, only Dbp10 exhibits a synthetic lethal interaction with Nug1 (Bassler et al., 2006). The biochemical data from the affinity-purified pre-ribosomes along with this genetic link between Nug1 and Dbp10, led us to address whether the two proteins bind proximal to each other on the pre-ribosome. Therefore UV crosslinking and analysis of cDNA (CRAC) technique was employed, to identify the rRNA interaction sites of Nug1 and Dbp10. For this reason, an HTpA-tag (-6xHIS-TEV-pA) was introduced at the C- or N-terminal end of Nug1 and Dbp10, respectively. The CRAC analysis was performed by Dr. Emma Thomson following essentially the protocol described in (Granneman et al., 2009).

Figure 3.11 A, shows the different interaction sites on the 35S rRNA for both Nug1 and Dbp10. The major crosslinking site for Nug1 corresponds to the base of H89 within the 25S rRNA, which is located on the 60S subunit interface. H89 is functionally important in the mature ribosome, as it is part of the peptidyl-transferase centre (PTC). Additionally, H69 constitutes a minor crosslink site of Nug1 and forms a part of the A and P sites in the mature ribosome. When the 3D volume of the recently published Arx1 pre-ribosome (Leidig et al., 2014) was used as a template to map the crosslinking sites of Nug1, we observed that they are positioned close to each other (Figure 3.11 B). Furthermore, two more minor crosslink sites were identified for Nug1, corresponding to H30 and ES12 that are located on the solvent exposed side of the 60S subunit (Figure 3.11 B).

CRAC analysis of Dbp10 revealed two major sites of crosslink, both found on the 60S intersubunit area. The first site corresponds to a single helix, H64, whereas the second region of crosslinks corresponds to multiple hits from H89 to H92. When

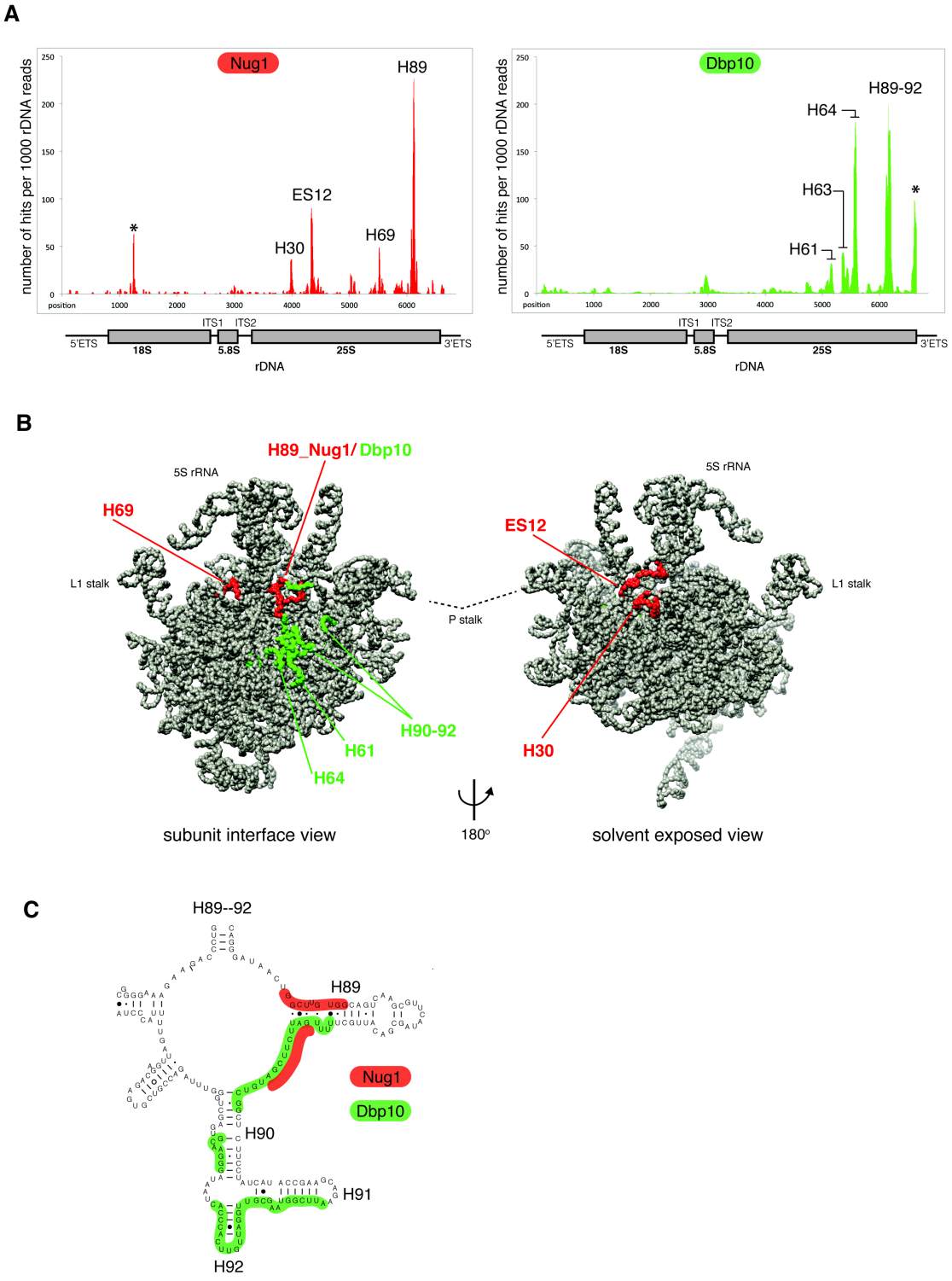

Figure 3.11 Nug1 and Dbp10 bind at proximal sites on the intersubunit area of the 60S subunit. (A) Both Nug1 and Dbp10 were efficiently crosslinking to RNA and the positions of interactions were identified by CRAC. Illumina-Miseq sequencing results were aligned to the yeast 35S rDNA and plotted. The Histogram shows the position and distribution of crosslink sites of Nug1 (red) and Dbp10 (green) on the 35S rRNA. The Y-axis displays the number of times each nucleotide was mapped (hits) per 1000 rDNA reads. Position of mature rRNA sequences and spacers are indicated below the X-axis. The indicated helix (H) numbers above the peaks correspond to helices in the secondary structure of the rRNA. The asterisks indicate frequent contaminants. **(B) Although Nug1 and Dbp10 occupy distinct sites, they are in close proximity.** Mapping the Nug1 (red) and Dbp10 (grenn) crosslink sites on the cryo-EM structure of Arx1 lacking the protein components (PDB

ID: 3J64). **(C) Nug1 and Dbp10 crosslink sites overlap on the base of Helix89.** The interaction sites of both proteins were mapped onto the secondary structure of H89. Nug1 is shown in red and Dbp10 in green.

the crosslinking sites of both Nug1 and Dbp10 proteins were mapped onto the Arx1 pre-ribosome, we observed that while their crosslinking patterns occupy distinct sites, they are in close proximity on the intersubunit face. Interestingly, a small overlap in the H89 could be observed from the hits acquired from both proteins (Figure 3.11 C).

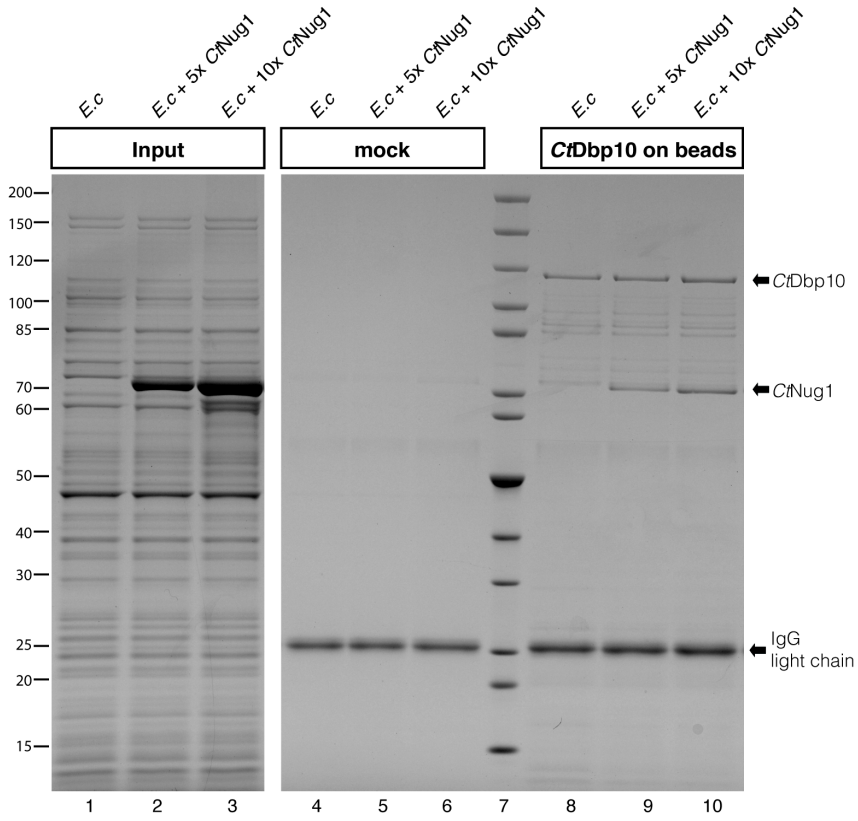

Figure 3.12 *Ct*Nug1 and *Ct*Dbp10 physically interact *in vitro*. Binding assays performed with *Ct*Nug1 and *Ct*Dbp10 proteins. *Ct*Dbp10 carrying an N-terminal FtpA-tag (pA-TEV-FLAG-) was expressed under the *GAL*1 promoter in yeast and affinity purified. The FLAG-*Ct*Dbp10 was immobilized on anti-FLAG beads and incubated with five- or ten-fold excess of recombinantly purified *Ct*Nug1 in the presence of competitor *E. coli* lysate (*E.c*). The bound material was eluted with SDS-sample buffer and analyzed by SDS-PAGE and Coomassie staining. As a negative control (mock), *Ct*Nug1 was incubated with anti-FLAG beads (lanes 4-6). The bands corresponding to *Ct*Dbp10, *Ct*Nug1 and IgG light chain are indicated with arrows.

The fact that Dbp10 and Nug1 were found to bind in close proximity onto the pre-ribosomes, prompted us to investigate a possible physical interaction between the two proteins. For this reason, the *C. thermophilum* homologues of Nug1 and Dbp10 (*Ct*Nug1, *Ct*Dbp10) were utilized and *in vitro* binding assays were performed (Figure 3.12). *Ct*Dbp10 carrying an N-terminal FtpA-tag (pA-TEV-FLAG-) was expressed under the *GAL*1 promoter in yeast and subsequently purified, as described in Material and Methods (see section 5.3.3.4). FLAG-*Ct*Dbp10 was immobilized on anti-FLAG beads and incubated with an excess of purified *Ct*Nug1 in the presence of competitor *E. coli* lysate. From the binding assays performed we could observe an interaction between *Ct*Dbp10 and *Ct*Nug1, suggesting a complex formation between the two proteins, although, one cannot formerly exclude that the interaction seen could be mediated by ribosomal contaminants.

Together our data show that when Nug1 is depleted or when the nucleotide-binding mutant is expressed, the association of Dbp10 with early pre-ribosomes decreases. This, along with proximal binding sites of Dbp10 and Nug1 on the pre-ribosome suggests that the physical interaction observed *in vitro* between these two proteins has a functional relevance and may be involved in the maturation of the PTC.

4. Discussion

This doctoral thesis has revealed for the first time that the circularly permuted Nug1 is a potassium-dependent GTPase that binds at the interface of the 60S subunit close to the PTC. Subsequent mutational analysis in the yeast Nug1 GTPase domain showed that the association of early biogenesis factors with pre-ribosomes is impaired when both GTP/GDP-binding is inhibited or when Nug1 is depleted from cells. Among these early biogenesis factors is the RNA helicase Dbp10, which is genetically linked to Nug1. I could now show that Dbp10 binds at sites close to Nug1 on the pre-ribosome and that both proteins physically interact. Thus, these findings indicate that the Nug1 GTPase, along with the RNA helicase Dbp10, may be involved in rRNA rearrangements at the PTC region during early steps of 60S subunit maturation.

4.1 Nug1 is a circularly permuted GTPase that is stimulated by potassium ions.

To date, five GTPases have been implicated in the 60S subunit maturation in yeast. Three of them, including Nug1, are circularly permuted (cp). The permutation on the GTPase domain does not cause major changes in the overall 3D structure. However, the mechanism of activation and hydrolysis is believed to be different from the canonical GTPases (Levdikov et al., 2004; Shin et al., 2004). Additionally, the circularly permuted GTPases (cpGTPases) involved in ribosome biogenesis carry a hydrophobic substitution after the G3 motif [DxxG**I**]. The presence of this hydrophobic residue suggests an alternative catalytic mechanism, compared to that of GAP-activated GTPases (Kim do et al., 2008). In our experiments, we were able to show that *Ct*Nug1 has low intrinsic GTPase activity (0.05 nucleotide /min) and a nucleotide affinity (Km) in the micromolar range (0.57 µM). Other GTPases including members of the Ras, Rab or Rho subfamilies, also exhibit low intrinsic enzymatic activities (0.02- 0.08 nucleotide /min), but very high nucleotide binding affinities in the picomolar range (pM). It is due to this property that such GTPases depend on GEFs to exchange the bound nucleotide, as well as on GAPs to

stimulate GTP hydrolysis (Barr and Lambright, 2010; Bos et al., 2007; Cherfils and Chardin, 1999; Iwashita and Song, 2008; Sprang, 1997; Vetter and Wittinghofer, 2001).

Likewise, the intrinsically low rate of GTP hydrolysis exhibited by *Ct*Nug1 suggested that its GTPase activity could be subject to regulation. Interestingly, a new group of GTPases, termed 'cation-dependent' has been described that display enhanced activity when certain cations are present (Ash et al., 2012). A comparison between crystal structures of GAP activated GTPases (Ras-like GTPases) and the CD-cpGTPases shows a clear difference in the position of the flexible Switch I region (Figure 4.1). The Switch I in the Ras-like GTPases leaves the bound GTP molecule exposed to the solvent area, rendering it accessible for the GAP protein to reach. Conversely, the Switch I region in CD-cpGTPases covers and almost buries the nucleotide (Ash et al., 2012). In the case of CD-GTPases the cation is coordinated at the equivalent position where the "arginine finger" of GAPs protrudes. Thus, the arginine finger of GAPs or the cation neutralizes the negative charge of the nucleotide phosphates. This results in the stabilization of the transition state during hydrolysis and allows stimulation of GTPase activity. In our experiments we showed that Nug1's enzymatic activity could be stimulated by cations and that potassium ions could specifically trigger its activity, rendering Nug1 a cation-dependent (CD) potassium-selective GTPase.

A common feature of the potassium selective CD-GTPases is the presence of a conserved asparagine in the G1 motif [Gxx**N**xGKS], which has been shown to coordinate the cation (Ash et al., 2012). In our mutational analysis, we showed that the potassium coordination is affected when the conserved asparagine (N322) is substituted with a charged aspartic acid (N322D) or a hydrophobic leucine (N322L). Surprisingly, the uncharged alanine substitution (N322A) (predicted to impair potassium binding) exhibited higher GTPase activity compared to the WT *Ct*Nug1.

As the alanine residue is smaller than asparagine, free space is likely available in the enzymatic pocket allowing the potassium ion to have a higher coordination number, i.e bonding to more atoms around it (potassium ions can be coordinated by four up to eight atoms). A higher state of coordination of the

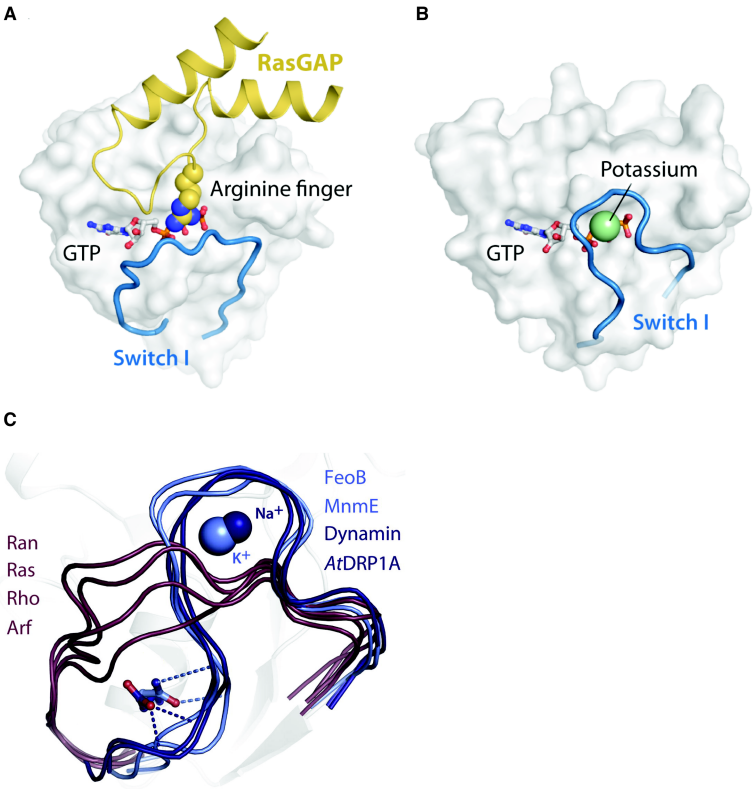

Figure 4.1 Comparison between GAP-activated and cation-dependent GTPases. (A) Switch I position leaves the nucleotide solvent exposed when activation is mediated by GAPs. Ras GTPase in complex with RasGAP (PDB: 1WQ1). Only residues 766-805 from RasGAP are shown in yellow. The arginine finger is depicted in spheres and the GTP as sticks. **(B) Switch I covers the nucleotide when activation is achieved by potassium ions.** G-domain of FeoB (PDB: 3LX5, 3SS8). Switch I in blue, potassium ions (green sphere). **(C) Superposition of the Switch I loop from cation-dependent (cyan-blue) and GAP-activated (red-magenta) GTPases**. Cation-dependent GTPase depicted here are: MnmE (2GJ8), FeoB (3SS8), dynamin-1 (2X2E) and *At*DRP1A (3T34). GAP-activated: Ras (1QRA), Ran (1RRP), Rho (1A2B) and Arf1 (1J2J). Adapted from Miriam-Rose Ash *et al.* 2012.

potassium ion could occur if water molecules present in the solution are surrounding the potassium ion, forming a cell and additionally participating in bond formation with residues forming the enzymatic pocket. Thus, we speculate that the increased GTPase activity observed in the N322A could be due to the presence of additional water molecules. Interestingly, in the case of the CD-GTPase MnmE, seven water molecules have been identified in the enzymatic pocket, where two of them are directly involved in catalysis (Scrima and Wittinghofer, 2006).

Stimulation of *Ct*Nug1's activity was seen when increasing concentrations of potassium ions were used. This is in agreement with the increased enzymatic activities observed when similar experiments were performed with the bacterial CD-GTPases FeoB and MnmE (Ash et al., 2010; Yamanaka et al., 2000). Despite the

stimulatory role of potassium ions seen *in vitro*, the intracellular concentration of potassium is around 200-300 mM in yeast (Arino et al., 2010; Harvey Lodish). This concentration is lower than the one (500 mM) required for maximal stimulation of *Ct*Nug1 *in vitro*, and thus raises the question of whether all *Ct*Nug1 molecules bind potassium ion *in vivo*. Hence, we postulate that the presence of potassium in not a strict requirement for GTPase hydrolysis, but rather an additional *in vivo* "co-factor" for these GTPases to achieve a catalysis-competent state. This hypothesis is supported by crystal structures of the available CD-GTPases that suggest: i) the cation supports the GTP binding, as it forms bonds with the phosphate oxygens and ii) it promotes the conformational changes of the active site around the substrate, by establishing bonds with the backbone residues (Switch I) (Achila et al., 2012; Ash et al., 2010; Ash et al., 2012; Kuhle and Ficner, 2014; Scrima and Wittinghofer, 2006).

It is note-worthy that for some CD-GTPases the maximum activity is achieved not only by the presence of cations, but also by additional mechanisms. Dimerization has been shown to be a prerequisite for activity of MnmE and dynamin (Chappie et al., 2010; Scrima and Wittinghofer, 2006), whereas for RbgA and YqeH CD-GTPases, binding to the ribosome increased their enzymatic activities (Achila et al., 2012; Kolanczyk et al., 2011). Nevertheless, as more crystal structures of CD-GTPases become available, together with detailed biochemical characterization, it becomes evident that the cation-dependency points towards an evolutionary-conserved catalytic mechanism. This is supported by the fact that CD-GTPases are involved in fundamental processes from prokaryotes to eukaryotes, including ribosome biogenesis and translation (Achila et al., 2012; Ash et al., 2012; Kolanczyk et al., 2011; Kuhle and Ficner, 2014). This would suggest that the stimulatory role of GAP proteins was achieved in the common ancestral CD-GTPase by the residues participating in cation coordination. Thus, a complete understanding of this ancestral potassium-dependent GTPase requires further experimentation and structural analysis.

4.2 Mutational analysis on the GTPase domain of the yeast Nug1 reveals a dynamic interplay of assembly factors.

Based on the mutational analysis of *Ct*Nug1's GTPase domain, we could identify the residues important for GTP hydrolysis, nucleotide binding, as well as potassium coordination. Accordingly, the orthologous mutations in the yeast Nug1 were generated in the conserved residues (K293, T320, D336N, G339 and N290) of the GTPase domain. These G-domain mutants were analyzed for *in vivo* effects on ribosome biogenesis along with complimentary Nug1 depletion experiments. Unexpectedly, the GTPase activity of Nug1 exhibited no growth defects and no detectable differences in the composition of purified pre-ribosomal particles. In contrast, when the nucleotide binding ability of Nug1 was impaired (D336N mutant) or when Nug1 was depleted from cells, growth inhibition, defects in 60S subunit maturation and reduced levels of assembly factors associating with pre-ribosomal particles were observed. Specifically, a decrease in the levels of early assembly factors (Dbp10, Spb1, Nop2 and Nsa2), as well as changes in biogenesis factors involved in the P-stalk formation (decrease Mrt4/Yvh1 and increase in Rpp0, Rpl12) were observed.

As the results obtained from the depletion of Nug1 and the D336N mutant were very similar, we postulate that the nucleotide-binding mutant of Nug1 exhibits reduced association with the pre-ribosome and thus causes the same effects as the depletion. In support of this, we have observed a small increase in the levels of the Nug1 bait protein when the D336N mutant was TAP-tagged as compared to the WT. Additionally, we also observed reduced levels of Nug1 D336N in the affinity purified Nsa1 and Rix1 pre-ribosomal particles. A possible explanation for this observation could be, that upon GTP binding conformational changes within the G-domain of Nug1 take place. These changes are then transmitted to the N- or C-terminal domain, affecting its association with the pre-ribosome. Interestingly, the N-terminus of Nug1 mediates binding to the pre-ribosome (Bassler et al., 2001), which could mean that if the conformation of the N-terminus is altered, Nug1's binding to pre-ribosomes will also be affected.

Indeed, the additional domains flanking the GTPase core in cpGTPase have been proposed to stabilize the permuted G-domain, as well as propagate intra-

molecular conformational changes upon GTP binding or hydrolysis (Anand et al., 2006). This could explain why the catalytic G339A mutant associates with pre-ribosomes like the WT Nug1, as they both have the same affinity for GTP and thus adopt the appropriate N-terminal conformation. In contrast, we could postulate that conformational changes in the N-terminal domain are inhibited in the mutant impaired in nucleotide binding (D336N), thus preventing the efficient association of Nug1 with pre-ribosomes.

To learn more about the mechanistic details behind Nug1's function in the pre-ribosome, as well as to confirm possible conformational changes triggered upon nucleotide binding between the N-terminus and the G-domain of Nug1, detailed structural studies will be required. Solving the atomic structure of Nug1 together with detailed cryo-EM analysis of pre-ribosomal particles isolated from cells expressing WT or mutant Nug1 could provide insight into the mechanism of function and its impact on other assembly factors. The tertiary structure prediction of Nug1, obtained using Phyre2 software, is based on the atomic structure of the *B. subtilis* homologue (YlqF) and resolves only the GTPase domain and a small part of the C-terminal end of Nug1. However, the unresolved N-terminal end is of particular interest as it is anchoring Nug1 to the pre-ribosome (Bassler et al., 2006). To date, crystallization trials using the full-length protein or truncated versions have not been successful, likely due to inherent flexibility of the protein or domains of it. Hence, the structural determination of fragments of Nug1 by NMR might be a better approach and will be further pursued in the Hurt laboratory.

When the cryo-EM structure of the Arx1 pre-ribosome was obtained, a number of assembly factors together with a few r-proteins could be fitted in the density map (Bradatsch et al., 2012; Leidig et al., 2014). Although additional masses are present, it is not possible at this stage to fit exactly the predicted structure of the Nug1's GTPase domain. Nevertheless, using RNA-protein crosslinking analysis we were able to determine binding sites of Nug1 on the pre-ribosome. Nug1's major crosslink site was at the base of H89, which is part of the peptidyl-transferase center (PTC) in the mature ribosome. Additionally, significant crosslink hits of Nug1 are close to this area and correspond to H69. Based on the 3D volume of the Arx1 pre-ribosomal particle, both helices undergo conformational

changes during biogenesis in order to acquire the correct position on the mature ribosome. More specifically, H89 appears shorter than in its native state and entirely relocated (Leidig et al., 2014). Interestingly, Dbp10 crosslink sites were also mapped to this area and are in close proximity to Nug1 as seen on the Arx1 pre-ribosome. Unexpectedly, both of these proteins had a partial overlap on the base of H89. This could be due to multiple reasons. However, we postulate that each protein binds to H89 at distinct time points during 60S maturation. Although the exact functional relationship between Dbp10 and Nug1 remains unclear, the fact that these two enzymes bind in such close proximity on the pre-ribosome, at the functionally important PTC, raises the question of whether the GTPase activity of Nug1 influences the ATPase/helicase activity of Dbp10 or vice versa. Interestingly, it has been shown that the GTPase Snu114 regulates unwinding of U4/U6 and therefore spliceosome dynamics by affecting Brr2 RNA helicase activity (Small et al., 2006). Future studies will therefore address whether Nug1 and Dbp10 display a similar relationship.

The evolving PTC appears to be highly complex region during 60S biogenesis as a number of additional assembly factors have been found to bind in its proximity. Nsa2 is such an assembly factor that, like Nug1, has been shown to bind to H89. Recent evidence suggests that Nsa2 is involved in the relocation of H89 through its physical association with Rsa4 and the mechanochemical energy provided by the AAA-ATPase Rea1 (Bassler *et al.* 2014). Furthermore, crystal structures of Rsa4 and Mrt4 can be fitted into the 3D volume of the Arx1 pre-ribosome, which shows that blades from Rsa4's beta-propeller contact the developing P-stalk, where Mrt4 resides. As Rsa4 physically interacts with Nsa2 and Nsa2 in turn binds proximately to Mrt4, it has been suggested that these proteins constitute a group of remodeling factors that act to mature the PTC (Chantha et al., 2006) (Bassler *et al.* 2014, in press). Interestingly, our experiments show that in addition to a decrease in the levels Dbp10, other factors including Nsa2 and Mrt4 were reduced on early pre-ribosomal particles when Nug1 was depleted or when the Nug1 nucleotide-binding (D336N) mutant was expressed. This suggests the possibility of crosstalk between the factors that localize to the developing PTC area. We suggest that H89 is the rRNA link between Nug1 and Nsa2, which could then

transmit the information to the other assembly factors (Figure 4.2). This would explain the observed differences in the components located at the distant P-stalk (reduction in Mrt4/Yvh1 and increase in Rpp0/Rpl12) in the case of Nug1 D336N mutant. Thus, Nug1's nucleotide binding ability might serve as a sensor of dynamic conformational changes on distinct areas of the pre-ribosome. It is tempting to speculate that the formation of structural hallmarks of the mature ribosome including the P-stalk and the PTC region are linked during biogenesis to guarantee the advance to the next step of the pathway. This could be regulated by the "switch function" of Nug1 GTPase that might mediate the crosstalk between Nsa2, Rsa4 and Mrt4 through the rRNA Helix89.

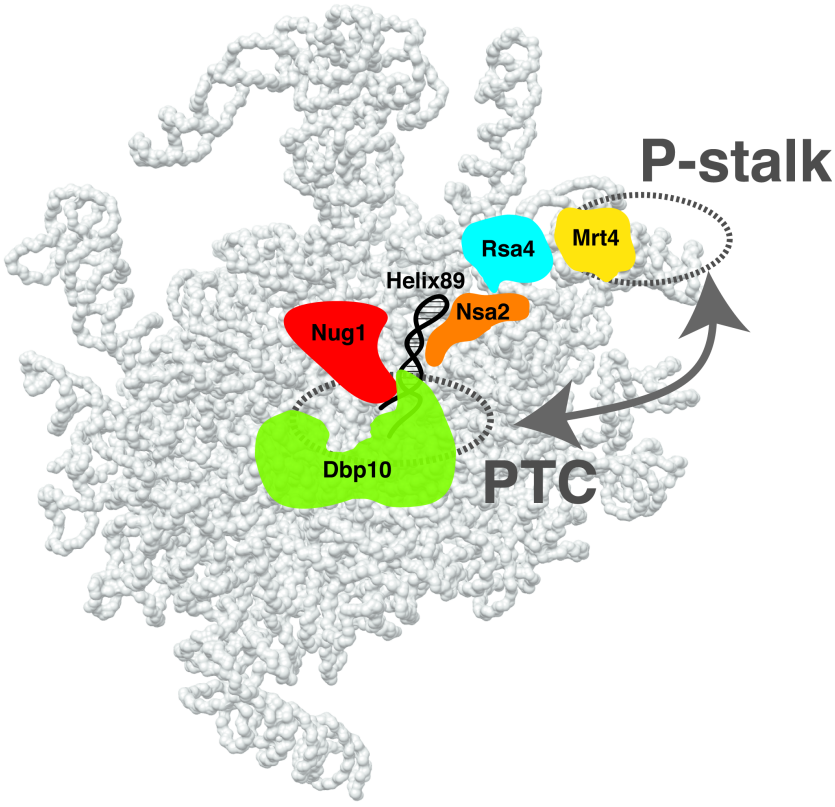

Figure 4.2 Dynamic interplay of assembly factors at the developing PTC region and P-stalk during biogenesis. Cartoon depicting the relative positions of assembly factors based on CRAC analysis (Nug1, Dbp10, Nsa2) and fitting of crystal structures (Nsa2, Rsa4, Mrt4) into the 3D volume of Arx1 pre-ribosome.

If this were true, what role could the Dbp10 helicase play in this area of the pre-ribosome and what is the significance of its interaction with Nug1? Dbp10 is an essential ribosome biogenesis factor in yeast and is predicted to be an ATP-

dependent RNA helicase. Additionally, it displays a synthetic lethal interaction with Nug1 (Bassler et al., 2001), but its function in ribosome biogenesis remains elusive. Interestingly, the bacterial helicase DbpA has been shown to bind to H92 of the 23S rRNA via its C-terminal domain (CTD) in a sequence-specific manner (Diges and Uhlenbeck, 2001; Diges and Uhlenbeck, 2005; Nicol and Fuller-Pace, 1995). It is suggested that anchoring the CTD of DbpA allows the targeting of its catalytic N-terminal ATPase domain to nearby rRNA regions.

Strikingly, footprinting studies in the presence of AMppNp (a non hydrolyzable ATP analog) showed that the catalytic domain of DbpA binds and acts upon the H89 region of rRNA (Karginov and Uhlenbeck, 2004). The fact that the yeast Dbp10 binds at the same position (H92 and H89) in the 25S rRNA as the prokaryotic DbpA does in the 23S rRNA, suggests that their function is conserved. Additionally, C-terminal tagging of Dbp10 is lethal, which further supports the idea that the CTD needs to be available for rRNA binding. Thus an analogous model where Dbp10 plays a role in the unwinding of H89 so other proteins can bind, could be suggested. In yeast, Nug1 would be a potential candidate as we have now shown that it also binds to H89. However, one cannot formerly exclude that Nug1 is already bound and that Dbp10 is involved in the disruption of the interaction between Nug1 and the rRNA or that it affects the binding of Nsa2 on the same helix. It would be interesting to see whether the yeast Dbp10 displays helicase activity and if this activity is required for ribosome biogenesis, as it could participate in the rearrangements predicted above. Further, mutations affecting Dbp10's helicase activity, as well as CRAC analysis of Dbp10 in the Nug1 D336N mutant could shed light on the mechanistic link between Dbp10 and Nug1.

Together, the findings from my doctoral work point towards a dynamic interplay of assembly factors that bind on the 60S subunit interface and link the formation of the PTC and the P-stalk, both structural hallmarks of the mature ribosome. In this interplay, the Nug1 GTPase binds at the base of helix 89 and may act as a molecular switch that mediates crosstalk between the biogenesis factors present in the developing PTC region (Dbp10, Sbp1, Nop2, Nsa2), as well as the ones (Mrt4, Rpp0, Rpl12) localizing at the P-stalk area.

5. Materials and Methods

5.1 Molecular biology methods and techniques

5.1.1 General

Standard molecular biology techniques including Polymerase Chain Reaction (PCR) for DNA fragment amplification, site-directed mutagenesis, DNA digestion with restriction enzymes, ligation of DNA fragments, as well as analysis and purification of DNA fragments via agarose gel-electrophoresis were performed according to protocols from (Edelheit *et al.*, 2009; Inoue *et al.*, 1990; Sambrook *et al.*, 1989).

PCR purification, gel extraction and plasmid preparation were performed using SIGMA-ALDRICH life science GenElute™- PCR Clean-Up, Gel Extraction and HPplasmid Miniprep Kit, respectively, following the manufacturer's instructions. For PCR amplification oligo-nucleotides were ordered from SIGMA-ALDRICH and Phusion or Taq1 DNA polymerase from ThermoScientific (formerly MBI Fermentas). Restriction-digest enzymes from New England BioLabs and ThermoScientific were used. FastAP thermosensitive alkaline phosphatase from ThermoScientific and T4 DNA-ligase from NEB were used. Sequencing reactions were performed by EurofinsMWG-Operon.

5.1.2 Construct and plasmid generation

Chaetomium thermophilum (*C. thermophilum*) genes encoding the proteins of interest (ribosome biogenesis factors) were identified and cloned from cDNA or genomic DNA as previously described (Amlacher *et al.*, 2011). For recombinant expression of thermophilic Nug1, Kap123 and Dbp10 plasmids were generated by cloning PCR-amplified inserts into digested *Escherichia coli (E. coli)* or yeast expression vectors. Specifically, all GTPase domain mutants of *Ct*Nug1 or *Sc*Nug1 were generated by site-directed mutagenesis and subsequently cloned as described above. Truncations in the N- or C- terminus of proteins were PCR generated using the appropriate oligonucleotides. Plasmids used during this study are listed in tableS2.

5.2 Microbiology and genetic methods

5.2.1 Media and Compounds

Luria-Bertani (LB) medium:

0.5 % (w/v) yeast extract (MP)

1 % (w/v) tryptone (MP) and

0.5 % (w/v) NaCl (Sigma)

pH 7.2

YPD medium (yeast peptone dextrose medium):

1 % (w/v) yeast extract (MP)

2 % (w/v) Bacto™peptone (BD)

2 % (w/v) glucose (Merck)

pH 5.5

SDC-X,Y,Z (synthetic dextrose complete):

2 % (w/v) glucose(Merck)

0.67 % (w/v) "yeast nitrogen base without amino acids" (Formedium) complemented with amino acids lacking X,Y,Z required for selection (CSM drop-out, Formedium),

pH 5.5

SRC-X,Y,Z (synthetic raffinose complete):

2 % (w/v) raffinose (MP)

0.67 % (w/v) "yeast nitrogen base without amino acids" (Formedium) complemented with amino acids lacking X,Y,Z required for selection (CSM drop-out, Formedium),

pH 5.5

YPG (yeast peptone galactose media):

1 % (w/v) yeast extract (MP)

2 % (w/v) Bacto™peptone (BD)

2 % (w/v)galactose (Sigma)

pH 5.5

Solid-media were made by mixing 1L of medium with 16,4 gr of agar (BD).

Phosphate-buffered saline (PBS):

10 mM Na_2HPO_4

1.8 mM KH_2PO_2

2.7 mM KCl

137 mM NaCl

5.2.2 *Escherichia coli* and recombinant expression of proteins

Cultivation, transformation and preparation of competent *E. coli* cells were performed according to (Inoue *et al.*, 1990; Sambrook *et al.*, 1989). Chemically-competent *E. coli* DH5α strain [F^-(Φ80dΔ(*lacZ*)M15) *recA1 endA1 gyrA96 thi1 hsdR17*($r_k^-m_k^+$) *supE44 relA1 deoRΔ(lacZYA-argF)* U169] was used for amplification of plasmids, as well as cloning purposes. For heterologous expression of *C. thermophilum* recombinant proteins, the *E. coli* BL21 CodonPlus RIL strain (B F^- *ompT hsdS* (rB^- mB^-) *dcm*$^+$ *Tetr gal I (DE3) endA* Hte [*argU ileY leuW Camr*]) (Stratagene) was used.

In order to select for plasmids, the medium was supplemented with Ampicillin (100 µg/ml), Kanamycin (10 µg/ml) or Chloramphenicol (34 µg/ml) (all from Sigma). The transformants were cultured in liquid medium at 37°C and their growth was monitored spectroscopically at 600nm. When the optic density (OD_{600}) reached 0.4-0.5, expression of recombinant proteins was induced with 0.1 mM IPTG for two or three hours depending on the protein (for *Ct*Nug1 three hours and two hours for *Ct*Kap123). After induction, the cells were harvested by centrifugation at 5000 xg, washed with PBS, flash-frozen in liquid nitrogen, and stored at –20 °C until use.

5.2.3 Transformation and Genomic tagging in *Saccharomyces cerevisiae*

S. cerevisiae transformation was performed with the lithium acetate method as described in (Gietz and Woods, 2006). Gene disruption, N- and C-terminal tagging

of genomic loci were performed by standard PCR-based homologues recombination techniques (Janke *et al.*, 2004; Longtine *et al.*, 1998; Puig *et al.*, 2001). Genomic DNA preparation from yeast cells was done according to (Hoffman and Winston, 1987). The integration efficiency was assessed with antibiotic-resistance-selection using Geneticin (200 *µ*g/ml) (G418, (Wach *et al.*, 1994), Nourseothricin (100 *µ*g/ml) (CloNat,natNT2: (Goldstein and McCusker, 1999) or Hygromycin B (300 *µ*g/ml) (Hyg,(Gonzalez *et al.*, 1978), as well as colony-PCR and western analysis. Yeast strains used and generated during this study are listed in tableS1.

5.2.4 *S. cerevisiae* growth, complementation tests and recombinant expression of proteins

Cultivation of *S. cerevisiae* cells was based on techniques previously described (Sherman, 1998). More specifically, for tandem affinity purifications yeast cells were cultivated at 30°C to an OD_{600} of 1.8-2.3 in a volume of 2 L of the appropriate medium (YPD or SDC-) using 5 L Erlenmeyer flasks containing breakers. Cells were harvested at 4000 rpm for 3 minutes at 4°C (Beckman Coulter Avanti^{TM} J-20XP; rotor: JLA 8.100), washed once with PBS, flash-frozen in liquid nitrogen and stored at -20°C.

For complementation tests, SDC medium was supplemented with 5-fluoro-orotic acid (5'-FOA) at 2 mg/ml concentration. For Auxin-induced depletion assays, media were supplemented with Auxin (Sigma) at a final concentration of 0.5 mM. Auxin depletion was performed in liquid cultures by adding auxin to YPD medium (depletion with auxin was not possible in synthetic media) in a final concentration of 0.5 mM, when OD_{600} was equal to 0.6-0.8.

Heterologous expression of *C. thermophilum* proteins in *S. cerevisiae* was carried out into DS1-2b and W303 strains (see specific examples in result section). For galactose induction, cells were grown in 1L raffinose (SRC-) medium to an OD_{600} of 2 and then shifted to 2L galactose medium (YPG) to induce expression. When the OD_{600} reached 3.5 the cells were harvested by centrifugation at 5000xg and washed with PBS. The cell-pellets were flash-frozen in liquid nitrogen and stored at –20 °C until use.

5.2.5 Complementation test and cell growth behavior with serial dilution analysis.

Complementation tests were performed using the shuffle strains. These strains were generated by disrupting the genomic locus of an essential gene with a selective marker, while providing a copy of that gene in a *URA3* plasmid. The shuffle strains were then transformed with the desired constructs, selected with the appropriate marker and subsequently incubated on plates containing 5'-fluoro-orotic acid (5'-FOA), which is lethal for cells containing the *URA3* gene.

For the complementation tests, yeast cells were selected with the respective marker after transformation and then plated two sequential times on plates containing 5'-FOA and incubated at 30°C. Following this selection dotspot analysis was performed starting with a pre-culture grown on YPD or synthetic medium (SDC) at 30°C for 16 hours (overnight). The next day the culture was diluted and grown up to an OD_{600} of 0.3-0.5. A cell-suspension was spotted on plates in 10-fold serial dilution steps, beginning with the undiluted dot (OD_{600} = 0.3). The volume spotted was 10 or 5 µl for sythetic SDC- and YPD media, respectively. The plates were then incubated at different temperatures (16°C, 23°C, 30°C and 37°C) for a period of time ranging from 2 to 5 days.

5.2.6 Sub-cellular localization of proteins using GFP-tagged constructs

To investigate the sub-cellular localization of proteins, fusion constructs were generated using eGFP and mRFP. Cells were grown in liquid medium at 30°C to mid-logarithmic phase (OD_{600} of 0.3-0.6) and fluorescence microscopy was performed using an Imager Z1 fluorescence microscope (Zeiss) equipped with 63x and 100x lenses, 1.4 Plan-Apo-Chromat oil immersion lens (Zeiss). Analysis was performed with DICIII, HEeGP, and RFP filter sets. All pictures were acquired using the AxioCharmMRm camera (Zeiss) operated by the AxioVision software (Zeiss) and were processed with ImageJ145 and Adobe Photoshop CS4.

5.2.7 Yeast two-hybrid analysis

The yeast two-hybrid system (Chien *et al.*, 1991; Fields and Song, 1989) was

utilized to investigate potential protein-protein interactions. To perform this assay ORFs were cloned in-frame to a GAL4 DNA binding domain (G4_BD, bait) and to a GAL4 transcription activation domain (G4_AD, prey), so that both combinations could be tested. Both plasmid-borne constructs were co-transformed into the reporter strain PJ694A (James *et al.*, 1996). Interaction between the two fusion proteins induced transcription of the reporter genes *HIS3* and *ADE2*, the expression of which could be evaluated by screening on different selective plates. Weak interactions among the tested proteins were visible only on SDC-His plates, whereas strong interactions enabled growth on SDC-Ade. The combination of plasmids bearing SV40_AD and P53_BD served as positive control and were also used to test putative self-activation of the constructs under investigation.

5.3 Biochemical methods.

5.3.1 Whole cell lysate preparation from *E. coli* and yeast.

To assess the expression levels of *C. thermophilum* proteins in *E. coli*, samples of 2 ml of OD_{600} 0.5 were taken before and after induction, cells were pelleted in a tabletop centrifuge, resuspended in 100 µl SDS-loading buffer, boiled at 95°C for 10 minutes and 10 µl were analyzed by SDS-PAGE.

In the case of yeast cells, 3 OD_{600} were harvested, resuspended in 76 µl of 1.85 M NaOH and 770 µl ddH_20 and incubated on ice for 10 minutes. 150 µl of TCA were subsequently added. After incubating the lysate for 10 minutes, it was centrifuged at full-speed for 5 minutes. The supernatant was removed and the pellet was washed with 1 ml of acetone. Spun again and left to dry. 40 µl of 0.1 M NaOH were added together with 40 µl of SDS-loading buffer, boiled at 95°C for 10 minutes and 10 µl were analyzed by means of SDS-PAGE.

5.3.2 SDS-PAGE, staining and western blotting

All protein analysis techniques and methods including SDS-PAGE, Coomassie-staining (R250 or colloidal) and western blotting were performed as previously described (Sambrook *et al.*, 1989). 4-12% Bis-Tris gradient gels

(NuPAGE™), MOPS running buffer, as well as LDS NuPAGE sample buffer (4x) (LifeTechnologies, former Invitrogen) were used for SDS-PAGE analysis. Pre-stained and unstained molecular weight protein standards (MBI Fermentas) were used as a reference.

For western blotting analysis, Protran BA85 nitrocellulose membrane (GE Healthcare) was used. All washing steps were performed with PBS supplemented with 0.1% (v/v) Tween20 (PBST) and nitrocellulose membranes were blocked with 5% nonfat dried milk in PBST. The chemiluminescence reaction was performed using the Immobilon™Western chemiluminescent HRP substrate (Millipore) and the signals were acquired using the ImageQuantLAS4000mini (GE Healthcare) imager. In cases of re-probing, the nitrocellulose membranes were stripped off with Restore™ WesterBlotStrippingBuffer (ThermoScientific), according to manufacturers instructions. Antibodies used in this study are listed in tableS3.

5.3.3 Protein purifications

5.3.3.1 General:

For tandem affinity purification (TAP) of protein complexes, purification of recombinantly expressed proteins (from *E. coli* or yeast strains), as well as for binding assays, the following buffers were prepared and used together with protease inhibitor mix tablets (Sigma*FAST*™ protease Inhibitor Cocktail Tablet):

buffer A:	**buffer B:**
20 mM HEPES, pH=7.5	20 mM HEPES, pH=7.5
150 mM KCl	150 mM NaCl
10 mM NaCl	10 mM KCl
5 mM $MgCl_2$	5 mM $MgCl_2$
1 mM DTT	1 mM DTT

buffer C:

50 mM Tris-HCl, pH=7.5
100 mM KCl
5 mM $MgCl_2$
0.15 % (v/v) Nonident P40
2 mM $CaCl_2$
5 % (v/v) Glycerol

buffer D:

20 mM HEPES, pH=7.5
150 mM KCl
5 mM $MgCl_2$
0.1 % (v/v) Nonident P40
5 % (v/v) Glycerol

5.3.3.2 Tandem affinity purification

Tandem affinity purifications (TAPs) were performed as previously described (Rigaut *et al.*, 1999) with minor modifications. For all steps described bellow buffer C was used, unless otherwise stated.

For lysis, yeast cell pellets were thawed, resuspended in 25 ml of buffer C supplemented with 1 mM DTT and combined with equal volume of 0.5 mm glass beads. The mixture of lysate and beads was transferred into a ball mill (Fritsch Pulverisette) for mechanical cell disruption. Lysis was performed at 4°C using a three-cycle program (bead-beating for 4 minutes at 500 rpm separated by 1 minute pause). After lysis, glass beads were removed with a 50 ml syringe, and the cell lysate was pre-cleared at 4000 rpm, for 10 min at 4°C, to remove non-lysed cells and remaining glass beads. The pre-cleared lysate was then spun in an analytical centrifuge (Beckman Avanti^{TM} J-25I; rotor: JA25-50) at 16000 rpm for 20 minutes at 4°C, in order to separate the soluble fraction from the cell debris.

A 300 µl slurry of IgG-Sepharose beads (GE-Healthcare), were equilibrated, added to the lysate and incubated for 1.5 hours at 4°C on a rotating wheel. After binding, IgG-beads were collected by centrifugation at 1500 rpm for 2 minutes at 4°C and washed twice. First, a 10 ml batch wash was carried out, after which the beads were collected and transferred to 2.5 ml columns from MoBiTec. The second washing step was performed inside the columns with 15 ml of buffer (gravity flow). For TEV cleavage, 10 µl of TEV-protease, 7.5 µl of 100 mM DTT and 750 µl of buffer C were added to the IgG-beads and incubated for 1.5 hours at 16°C on a rotating wheel. The TEV-eluate was collected and beads were washed with additional 250 µl to

reach a final volume of 1 ml. The resulting eluate was then added to 200 µl of pre-equilibrated Calmodulin affinity slurry (Sigma) and incubated for 1 hour at 4°C. After binding, the resin was washed with 15 ml of buffer and elution was carried out at 30°C for 30 minutes with 600 µl of elution buffer containing 10 mM EGTA and 10 mM Tris-Hcl, pH=8. Prior to SDS-PAGE and western blotting analysis, the protein samples were TCA-precipitated and resuspended in 2x Laemmli buffer (Laemmli, 1970).

5.3.3.3 CtNug1 purification from E. coli

Cell pellets containing the *Ct*Nug1-6xHIS-tag were thawed, resuspended in 20 ml of buffer A supplemented with 250 mM KCl, lysed by high pressure cavitation homogenizer (microfluidizer) and centrifuged at 18000rpm for 20 minutes at 4°C (Beckman Avanti^{TM} J-25I; rotor: JA25-50). The supernatant was incubated with 1 ml of pre-equilibrated SP sepharose cation exchange beads (Sigma) at 4 °C for 1 hour. After binding, beads were collected by centrifugation (1500 rpm for 2 minutes) and washed with buffer A (250 mM KCl). A second wash was performed inside 20 ml gravity-flow columns with 20ml of buffer A (250 mM KCl). Elution was then performed with buffer A supplemented with 600 mM KCl.

The eluate was then slowly diluted to a final KCl concentration of 400 mM. 500 µl of pre-equilibrated Ni-NTA agarose beads (Machery-Nagel) were added and incubated at 4 °C for 1 hour. After Ni-NTA binding, the beads were washed with buffer A (400 mM), and *Ct*Nug1 was eluted twice from the beads with 500 mM Imidazole in buffer A (containing 250 mM KCl and no DTT). This eluate was then used for size exclusion chromatography with Superdex^{TM}200 10/300 (GE Healthcare) on an ÄktaPurifier System (GE Healthcare). The same purification scheme was followed for the *Ct*Nug1 G-domain mutants.For crystallization trials, Superdex^{TM}200 HiLoad^{TM}16/60 (GE Healthcare) was used and the fractions containing *Ct*Nug1 were concentrated with Amicon Ultra spin columns (Millipore). For certain trials 2 mM of nucleotide (GTP, GDP or GMppNp), 20 mM NaF and 2 mM $AlCl_3$ were added into the concentrated protein and incubated for 10 minutes at room

temperature. After centrifugation, the soluble protein was retrieved and introduced to the crystallization platform where Phoenix RE nano-liter crystallization robot and the Rigaku Minstrel HT imaging system were used.

5.3.3.4 CtDbp10 purification from yeast

*Ct*Dbp10 was purified with the previously described Tandem affinity purification protocol (section 5.3.3.2) with the following modifications. 500 µl pre-equilibrated IgG-Sepharose slurry (GE-Healthcare) were added to the lysate and incubated for 1 hour at 4°C on a rotating wheel. After binding, IgG-beads were collected by centrifugation at 1500 rpm for 2 minutes at 4°C and washed twice. First, a 10 ml batch wash was carried out, after which the beads were collected and transferred to 2.5 ml columns from MoBiTec. The second washing step was performed inside the columns with 15 ml of buffer (gravity flow). For TEV cleavage, 10 µl of TEV-protease, 7.5 µl of 100 mM DTT and 750 µl of buffer C were added to the IgG-beads and incubated for 1.5 hours at 16°C on a rotating wheel. The TEV-eluate was collected and beads were washed with additional 250 µl to reach a final volume of 1 ml. The resulting eluate was then added to 300 µl of pre-equilibrated anti-FLAG slurry (Sigma) and incubated for 1 hour at 4°C. After binding the resin was washed with 15 ml of buffer and elution was carried out with 600 µl of 2xFLAG peptide (Sigma) at 4°C for 1 hour.

5.3.3.5 GST Affinity Purification

For binding assays GST-tagged constructs were generated. Cell pellets containing GST-tagged proteins were lysed with buffer B as described in section 5.3.3.3. The supernatant was incubated with 200 µl of pre-equilibrated Glutathione-Sepharose 4B (Sigma) slurry at 4 °C for 1 hour. After binding, beads were collected by centrifugation (1500 rpm for 2 minutes) and washed with buffer B. A second wash was performed inside 2.5 ml gravity-flow columns with buffer B, this time supplemented with 300 mM KCl (high salt wash). Elution of the bound proteins was performed with TEV cleavage (10 µl

of TEV-protease, 7.5 µl of 100 mM DTT and 750 µl of buffer B for 1.5 hours at 16°C on a rotating wheel).

5.3.3.6 Binding assays

All binding assays were performed with buffer D. Bait-proteins were immobilized on Glutathione-Sepharose4B or anti-FLAG beads (both from Sigma) and prey-proteins (Ni^+-eluates) were added in a 5 to 20 times excess (estimation based on SDS-PAGE) (see individual experiments in the result section). To avoid non-specific binding, *E. coli* BL21 lysate was used as a competitor in each reaction and GST-bound to glutathione beads or empty anti-FLAG beads were used as controls. Reactions were assembled in microbio/spin colums (BioRad) and incubated for 45 minutes at 16°C on a shaking (500rpm) thermomixer (Eppendorf). After binding, the flow-through was collected and beads were washed with buffer D. Elution of the bound material was achived by boiling the beads at 95°C with 2x LDS NuPAGE sample buffer (LifeTechnologies) or by TEV-cleavage. Detection of binding was assessed by SDS-PAGE followed by coomassie staining.

5.3.4 Single-turnover GTPase assays

Single turnover experiments were performed as previously described (Peluso *et al.*, 2001). In brief, varying amounts of proteins (0.1, 0.25, 0.5, 1, 2, 5 µM) were incubated with a final concentration of 100 nM GTP containing 750 nCi of γ^{32}P-labeled GTP (Hartman Analytic 6000 Ci/mmol). Samples of 5 µl were taken at different time points (t=0, 10, 30, 60, 120 and 180 minutes) rapidly mixed with 90 µl of perchloric acid (1M), directly neutralized with 30 µl volumes of potassium acetate (8 M) and stored in liquid nitrogen. When all time points were collected, samples were thawed and centrifuge at 14,000rpm for 10 min at room temperature. 2 µl of each sample were loaded on Polygram Cel 300 PEI TLC plates (Macherey-Nagel), developed in 350 mM KH_2PO_4 buffer inside a thin-layer chromatography chamber for 45–60 min. After developing, the TLC plates were blow-dried, exposed overnight on a

Phosphorimager screen (BAS-MS 2040 Fujifilm) and scanned with a FLA-7000 (Fujifilm). ImageJ was used for all quantifications of Phosphorimager screens and for each time point the amount of GTP and free phosphate were determined after subtraction of background signal. Single turnover assays were performed in subsaturating GTP concentrations (100 nM) in the presence *Ct*Nug1 (0.1-5 µM). Fraction of GTP was plotted as a function of time. K_{obs} (observed rate constants) values were calculated for each concentration by fitting obtained time courses to equation (1)

(1) $$Frac\ (GTP) = (a - b)\exp(Kobs\ t) + b$$

Frac (GTP) is the fraction of GTP at each time point, **a** is the fraction of GTP at the beginning of the reaction, **b** the fraction of GTP at the end of the time course, t➔∞ and $\mathbf{K_{obs}}$ is the observed rate constant. The affinity of the protein for GTP was determined from the dependence of the observed reaction rate on protein concentration according to equation (2)

(2) $$\mathrm{Kobs} = Kmax\frac{[Nug1]}{K_{1/2}+[Nug1]}$$

$\mathbf{K_{obs}}$ is the observed rate constant at a particular protein concentration, $\mathbf{K_{max}}$ is the maximal rate constant with saturating protein concentration, $\mathbf{K_{1/2}}$ is the protein concentration that provides half the maximal rate. The K_m and K_{cat} values were determined using GraphPad PRISM.

5.3.5 Fluorescence-based nucleotide binding assays

The nucleotide-binding assays were performed using the fluorescently labeled nucleotides, such as mant-GTP, mant-GDP and mant-GMppNp (JenaBioscience). Reactions of 100 µl were performed in 96 well-plates, with 1 µM of recombinant protein incubated with 0.5 µM of mant-nucleotides in buffer A for 10 min at 30°C. The reaction mixture was then excited at 355 nm with a xenon lamp, and emission spectra were recorded between 385 and

600 nm with a 5-nm increment step using a Synergy 4 spectrophotometer (BioTek). All data were processed with Office Excel.

5.3.6 Ribosome and polysome profile analysis with sucrose gradients

buffer E:

50 mM Tris-HCl, pH=7.5

100 mM KCl

12 mM $MgCl_2$

0.1 mg/ml Cycloheximide

In order to analyze ribosomal profiles from *S. cerevisiae*, sucrose density gradients (10-45% w/v in buffer E) were poured in polyallomer centrifuge tubes (Beckman, 14x95mm, for SW40 rotor) and mixed by the GRADIENT MASTER^{TM}107ip (BioComp) following the manufacturers instructions. A yeast culture of 100 ml was grown up to an OD_{600} 0.5-0.8 and cycloheximide was then added to a final concentration of 0.1 mg/ml. The yeast cells were then incubated on ice for 10 minutes, harvested at 2500 rpm for 3 minutes at 4°C and washed with 20 ml of buffer containing cycloheximide. The yeast pellet was resuspended in approximately 1 ml and an equal volume of 0.5 mm glass beads was added. The lysis was performed by repeated cycles of vortexing and resting on ice (each cycle was 30 seconds vortexing and 30 seconds pause on ice, repeated 5 times). The lysate was then collected and the glass beads were washed with 250 µl of buffer. The supernatant was retrieved after centrifugation in a cooling tabletop centrifuge at 14000 rpm for 10 minutes at 4°C.

An Equivalent of 5-10 OD_{260} were loaded onto the sucrose gradient, after measuring the OD_{260} from diluted (1/10) samples with Nanodrop2000 (ThermoScientific). The ultra-centrifugation was performed using the SW40 rotor (Beckman) at 27000 rpm for 16 hours at 4°C. Thereafter, sucrose gradients were fractionated and analyzed based on their UV profiles (λ= 254

nm) using the ProTeamLC gradient system. Finally, each fraction was TCA-precipitated and analyzed by SDS-PAGE and western blotting.

5.3.7 UV cross-linking and cDNA analysis (CRAC)

The CRAC experiments were performed as previously described (Granneman et al., 2009) using a 6xHis-TEV-ProtA tag either in the N- or C-terminal end of *Ct*Dbp10 and *Ct*Nug1, respectively. Cultures were grown in SDC medium to OD_{600} 0.8 and cells were UV-irradiated in the Megatron UV chamber1 at a dose of 1.6 J cm^{-2} for 3 minutes and processed as described (Granneman et al., 2009; Granneman et al., 2011). The cDNAs originating from *Ct*Nug1 and *Ct*Dbp10 CRAC experiments were sequenced on the Illumina MiSeq system (single-end 50b), according to manufacturer's procedures. Illumina sequencing data were aligned to the yeast genome using Novoalign (http://www.novocraft.com). Downstream analyses were performed using the pyCRAC tool suite (Webb et al., 2014) and the UCSF Chimera (Pettersen *et al.*, 2004). For detailed protocols refer to: http://sandergranneman.bio.ed.ac.uk

5.3.8 *In silico* analysis and homology modeling.

To assess the conservation and domain-composition of *C. thermophilum* proteins, sequences from prokaryotic and eukaryotic orthologues (e.g. *Bacilus subtilis*, *Saccharomyces cerevisiae*, *Neurospora crassa*, *Schizosaccharomyces pombe*, *Drosophila melanogaster*) were aligned with ClustalW2 (Larkin *et al.*, 2007). Secondary-structure predictions, tertiary-structure models and homology modeling were performed using I-Tasser (Roy *et al.*, 2010) and Phyre2 (Kelley and Sternberg, 2009) online tools (http://zhanglab.ccmb.med.umich.edu/I-TASSER/) (http://www.sbg.bio.ic.ac.uk/phyre2/html/page.cgi?id=index). Visualization and manipulation of tertiary structure models was done with UCSF Chimera (Pettersen *et al.*, 2004) and PyMOL (Version 1.2r3pre, Schrödinger, LLC).

Table S1. Yeast strains used in this study

Name	Genotype	Reference
*NUG*1 shuffle (Y3879)	W303 *MATa nug1::kanMX6 pRS316-NUG1*	Kressler D.
*NUG*1 shuffle Ssf1-TAP	W303 *MATa nug1::kanMX6, SSF1-TAP:: natNT2*	this study
*NUG*1 shuffle TAP-Dbp10	W303 *MATa nug1::kanMX6, DBP10-TAP:: natNT2*	this study
*NUG*1 shuffle Rix-TAP	DS1-2b *MAT*alpha *nug1::natNT2, RIX1-TAP::TRP1*	Thoms M.
*NUG*1 shuffle Nsa1-TAP	DS1-2b *MAT*alpha *nug1::natNT2, NSA1-TAP::TRP1*	Thoms M.
*NUG*1 shuffle Arx1-TAP	DS1-2b *MAT*alpha *nug1::natNT2, ARX1-TAP::TRP1*	Thoms M.
*NUG*1 shuffle Lsg1-TAP	DS1-2b *MAT*alpha *nug1::natNT2, LSG1-TAP::TRP1*	Thoms M.
*NUG*1 shuffle Mrt4-TAP	W303 *MATa nug1::kanMX6 pRS316-NUG1, MRT4-TAP:: HIS3MX6*	Thoms M.
*NUG*1 shuffle Yvh1-TAP	W303 *MATa nug1::kanMX6 pRS316-NUG1, YVH1-TAP::HIS3MX6*	Thoms M.
Ssf1-TAP, Nsa2-FLAG	W303 *MATa nug1::kanMX6, SSF1-TAP:: natNT2, NSA2-L-FLAG*::*HIS3MX6*	this study
Nsa1-TAP, Nsa2-FLAG	DS1-2b *MAT*alpha*, NSA*1-TAP::*TRP*1, *NSA2-L-FLAG*::*HIS3MX6*	this study
Nsa1-TAP, Nug1-FLAG	DS1-2b *MAT*alpha*, NSA*1-TAP::*TRP*1, *NUG1-FLAG::natNT2*	this study
Nsa1-TAP, Mrt4-FLAG	DS1-2b *MAT*alpha*, NSA*1-TAP::*TRP*1, *MRT4-FLAG*::*HIS3MX6*	this study
Nug1-AID, Ssf1-TAP	W303 *MAT*alpha, PADH1-*OsTIR*-9xmyc::*TRP*1, *NUG1-FLAG-AID::HIS3MX6, SSF1-TAP::URA3*	Thoms M.
Nug1-AID, Nsa1-TAP	W303 *MAT*alpha, PADH1-*OsTIR*-9xmyc::*TRP*1, *NUG1-FLAG-AID::HIS3MX6, NSA1-TAP::URA3*	Thoms M.
Nug1-AID, Rix1-TAP	W303 *MAT*alpha, PADH1-*OsTIR*-9xmyc::*TRP*1, *NUG1-FLAG-AID::HIS3MX6, RIX1-TAP::URA3*	Thoms M.
Nug1-AID, Arx1-TAP	W303 *MAT*alpha, PADH1-*OsTIR*-9xmyc::*TRP*1, *NUG1-FLAG-AID::HIS3MX6, ARX1-TAP::URA3*	Thoms M.
Nug1-AID, Lsg1-TAP	W303 *MAT*alpha, PADH1-*OsTIR*-9xmyc::*TRP*1, *NUG1-FLAG-AID::HIS3MX6, LSG1-TAP::URA3*	Thoms M.

TableS2. Plasmids used in this study

Plasmid	Relative information	Reference
pRS314	CEN, *TRP1*	Sikorski & Hieter, 1989
pRS315	CEN, *LEU2*	Sikorski & Hieter, 1989
pRS316	CEN, *URA3*	Sikorski & Hieter, 1989
YCplac22	CEN, *TRP1*	Gietz & Sugino, 1988
YCplac111	CEN, *LEU2*	Gietz & Sugino, 1988
YCplac22-*NUG*1	CEN, *TRP1*, P*NUG1*, *NUG1*	this study
YCplac22-*nug1 K293A*	CEN, *TRP1*, P*NUG1*, *nug1 K293A*	this study
YCplac22-*nug1 K293N*	CEN, *TRP1*, P*NUG1*, *nug1 K293N*	this study
YCplac22-*nug1 S294A*	CEN, *TRP1*, P*NUG1*, *nug1 S294A*	this study
YCplac22-*nug1 S294N*	CEN, *TRP1*, P*NUG1*, *nug1 S294N*	this study
YCplac22-*nug1 T320AT321A*	CEN, *TRP1*, P*NUG1*, *nug1 T320AT321A*	this study
YCplac22-*nug1 D336A*	CEN, *TRP1*, P*NUG1*, *nug1 D336A*	this study
YCplac22-*nug1 D336N*	CEN, *TRP1*, P*NUG1*, *nug1 D336N*	this study
YCplac22-*nug1 D336W*	CEN, *TRP1*, P*NUG1*, *nug1 D336W*	this study
YCplac22-*nug1 G339A*	CEN, *TRP1*, P*NUG1*, *nug1 G339A*	this study
YCplac22-*nug1 N290A*	CEN, *TRP1*, P*NUG1*, *nug1 N290A*	this study
YCplac22-*nug1 N290D*	CEN, *TRP1*, P*NUG1*, *nug1 N290D*	this study
YCplac22-*nug1 N290L*	CEN, *TRP1*, P*NUG1*, *nug1 N290L*	this study
YCplac22-*nug1 N290Q*	CEN, *TRP1*, P*NUG1*, *nug1 N290Q*	this study
YCplac22-*NUG*1-TAP	CEN, *TRP1*, P*NUG1*, *NUG1*-CBP-TEV-pA	this study
YCplac22-*nug1 K293A*-TAP	CEN, *TRP1*, P*NUG1*, *nug1 K293A*-CBP-TEV-pA	this study
YCplac22-*nug1 K293N*-TAP	CEN, *TRP1*, P*NUG1*, *nug1 K293N*-CBP-TEV-pA	this study
YCplac22-*nug1 S294A*-TAP	CEN, *TRP1*, P*NUG1*, *nug1 S294A*-CBP-TEV-pA	this study
YCplac22-*nug1 S294N*-TAP	CEN, *TRP1*, P*NUG1*, *nug1 S294N*-CBP-TEV-pA	this study
YCplac22-*nug1 T320AT321A*-TAP	CEN, *TRP1*, P*NUG1*, *nug1 T320AT321A*-CBP-TEV-pA	this study
YCplac22-*nug1 D336A*-TAP	CEN, *TRP1*, P*NUG1*, *nug1 D336A*-CBP-TEV-pA	this study

YCplac22-*nug1 D336N*-TAP	CEN, *TRP1*, P*NUG1*, *nug1 D336N*-CBP-TEV-pA	this study
YCplac22-*nug1 D336W*-TAP	CEN, *TRP1*, P*NUG1*, *nug1 D336W*-CBP-TEV-pA	this study
YCplac22-*nug1 G339A*-TAP	CEN, *TRP1*, P*NUG1*, *nug1 G339A*-CBP-TEV-pA	this study
YCplac22-*nug1 N290A*-TAP	CEN, *TRP1*, P*NUG1*, *nug1 N290A*-CBP-TEV-pA	this study
YCplac22-*nug1 N290D*-TAP	CEN, *TRP1*, P*NUG1*, *nug1 N290D*-CBP-TEV-pA	this study
YCplac22-*nug1 N290L*-TAP	CEN, *TRP1*, P*NUG1*, *nug1 N290L*-CBP-TEV-pA	this study
YCplac22-*nug1 N290Q*-TAP	CEN, *TRP1*, P*NUG1*, *nug1 N290Q*-CBP-TEV-pA	this study
YCplac22-*NUG*1-FLAG	CEN, *TRP1*, P*NUG1*, *NUG1- FLAG*	this study
YCplac22-*nug1 K293A*- FLAG	CEN, *TRP1*, P*NUG1*, *nug1 K293A- FLAG*	this study
YCplac22-*nug1 K293N*- FLAG	CEN, *TRP1*, P*NUG1*, *nug1 K293N- FLAG*	this study
YCplac22-*nug1 S294A*- FLAG	CEN, *TRP1*, P*NUG1*, *nug1 S294A- FLAG*	this study
YCplac22-*nug1 S294N*- FLAG	CEN, *TRP1*, P*NUG1*, *nug1 S294N- FLAG*	this study
YCplac22-*nug1 T320AT321A*- FLAG	CEN, *TRP1*, P*NUG1*, *nug1 T320AT321A- FLAG*	this study
YCplac22-*nug1 D336A*- FLAG	CEN, *TRP1*, P*NUG1*, *nug1 D336A- FLAG*	this study
YCplac22-*nug1 D336N*- FLAG	CEN, *TRP1*, P*NUG1*, *nug1 D336N- FLAG*	this study
YCplac22-*nug1 D336W*- FLAG	CEN, *TRP1*, P*NUG1*, *nug1 D336W- FLAG*	this study
YCplac22-*nug1 G339A*- FLAG	CEN, *TRP1*, P*NUG1*, *nug1 G339A- FLAG*	this study
YCplac22-*nug1 N290A*- FLAG	CEN, *TRP1*, P*NUG1*, *nug1 N290A- FLAG*	this study
YCplac22-*nug1 N290D*- FLAG	CEN, *TRP1*, P*NUG1*, *nug1 N290D- FLAG*	this study
YCplac22-*nug1 N290L*- FLAG	CEN, *TRP1*, P*NUG1*, *nug1 N290L- FLAG*	this study
YCplac22-*nug1 N290Q*- FLAG	CEN, *TRP1*, P*NUG1*, *nug1 N290Q- FLAG*	this study
YCplac111-*NUG*1- FLAG	CEN, *LEU2*, P*NUG1*, *NUG1- FLAG*	this study
YCplac111-*nug1 K293A*- FLAG	CEN, *LEU2*, P*NUG1*, *nug1 K293A- FLAG*	this study
YCplac111-*nug1 D336N* - FLAG	CEN, *LEU2*, P*NUG1*, *nug1 D336N- FLAG*	this study
YCplac111-*nug1 G339A* - FLAG	CEN, *LEU2*, P*NUG1*, *nug1 G339A- FLAG*	this study
YCplac111-*nug1 N290A* - FLAG	CEN, *LEU2*, P*NUG1*, *nug1 N290A- FLAG*	this study
YCplac22-*nug1 N290Q* - FLAG	CEN, *LEU2*, P*NUG1*, *nug1 N290*Q- *FLAG*	this study
YCplac22-*NUG*1-eGFP	CEN, *TRP1*, P*NUG1*, *NUG1*- eGFP	this study
YCplac22-*nug1 K293A*- eGFP	CEN, *TRP1*, P*NUG1*, *nug1 K293A*- eGFP	this study

YCplac22-*nug1 K293N*- eGFP	CEN, *TRP1*, P*NUG1*, *nug1 K293N*- eGFP	this study
YCplac22-*nug1 S294A*- eGFP	CEN, *TRP1*, P*NUG1*, *nug1 S294A*- eGFP	this study
YCplac22-*nug1 S294N*- eGFP	CEN, *TRP1*, P*NUG1*, *nug1 S294N*- eGFP	this study
YCplac22-*nug1 T320AT321A*- eGFP	CEN, *TRP1*, P*NUG1*, *nug1 T320AT321A*- eGFP	this study
YCplac22-*nug1 D336A*- eGFP	CEN, *TRP1*, P*NUG1*, *nug1 D336A*- eGFP	this study
YCplac22-*nug1 D336N*- eGFP	CEN, *TRP1*, P*NUG1*, *nug1 D336N*- eGFP	this study
YCplac22-*nug1 D336W*- eGFP	CEN, *TRP1*, P*NUG1*, *nug1 D336W*- eGFP	this study
YCplac22-*nug1 G339A*- eGFP	CEN, *TRP1*, P*NUG1*, *nug1 G339A*- eGFP	this study
YCplac22-*nug1 N290A*- eGFP	CEN, *TRP1*, P*NUG1*, *nug1 N290A*- eGFP	this study
YCplac22-*nug1 N290D*- eGFP	CEN, *TRP1*, P*NUG1*, *nug1 N290D*- eGFP	this study
YCplac22-*nug1 N290L*- eGFP	CEN, *TRP1*, P*NUG1*, *nug1 N290L*- eGFP	this study
YCplac22-*nug1 N290Q*- eGFP	CEN, *TRP1*, P*NUG1*, *nug1 N290Q*- eGFP	this study
YCplac22-*nug1 ΔN (1-13)*	CEN, *TRP1*, P*NUG1*, *nug1 ΔN (1-13)*	this study
YCplac22-*nug1 ΔN (1-35)*	CEN, *TRP1*, P*NUG1*, *nug1 ΔN (1-35)*	this study
YCplac22-*nug1 ΔN (1-54)*	CEN, *TRP1*, P*NUG1*, *nug1 ΔN (1-54)*	this study
YCplac22-*nug1 ΔN (1-99)*	CEN, *TRP1*, P*NUG1*, *nug1 ΔN (1-99)*	this study
YCplac22-*nug1 ΔN (1-123)*	CEN, *TRP1*, P*NUG1*, *nug1 ΔN (1-123)*	this study
YCplac22-*nug1 ΔN (1-171)*	CEN, *TRP1*, P*NUG1*, *nug1 ΔN (1-171)*	this study
YCplac22-*nug1 ΔN (1-13)*- eGFP	CEN, *TRP1*, P*NUG1*, *nug1 ΔN (1-13)*- eGFP	this study
YCplac22-*nug1 ΔN (1-35)*- eGFP	CEN, *TRP1*, P*NUG1*, *nug1 ΔN (1-35)*- eGFP	this study
YCplac111-*nug1 ΔN (1-13)*- eGFP	CEN, *LEU2*, P*NUG1*, *nug1 ΔN (1-13)*- eGFP	this study
YCplac111-*nug1 ΔN (1-35)*- eGFP	CEN, *LEU2*, P*NUG1*, *nug1 ΔN (1-35)*- eGFP	this study
YCplac22-Ct*NUG*1	CEN, *TRP1*, P*NUG1*, Ct*NUG*1	this study
pADH111-*CtNUG*1	CEN, *LEU2*, PADH1, Ct*NUG*1	this study
pADH181-*CtNUG*1	2µ, *LEU2*, PADH1, pA-TEV-Ct*NUG*1	this study
pRS314-RSA4	CEN, *TRP1*, PRSA4, *RSA4* TRSA4	Ulbrich *et al.* 2009
pRS315-rsa4-1	CEN, *TRP1*, PRSA4 *rsa4-1* Q12P, K355R, D423N, F436L TRSA4	Ulbrich *et al.* 2009
YEplacLeu2d-Ct*DBP*10	2µ, P*GAL1-10*, TRP, *LEU2*d, pA-TEV-*FLAG*-Ct*DBP*10	this study
YCplac111-HTpA-*DBP10*	CEN, *LEU2*, PNOP53, *6xHIS-TEV-pA-DBP*10	this study

YCplac111-*NUG1-HTpA*	CEN, *LEU2*, P*NUG1*, *NUG*1-6xHIS-TEV-pA	this study
pGADT7	2µ, *LEU2*, PADH1, N-terminal G4AD-HA	Clontech Laboratories, Inc.
pGBKT7	2µ, *TRP1*, PADH1, N-terminal G4BD-c-myc	Clontech Laboratories, Inc.
pFA6a-kanMX6	for genomic deletion disruption	Longtine *et al.*, 1998
pFA6a-HIS3MX4	for genomic deletion disruption	Longtine *et al.*, 1998
pFA6a-natNT2	for genomic deletion disruption	Janke *et al.*, 2004
pET24b-Ct*NUG*1-6xHIS	f1 origin, T7 promoter, pBR322 origin, Kan*R*, Ct*NUG*1-6xHIS	this study
pET24b-Ct*nug*1-K325A-6xHIS	f1 origin, T7 promoter, pBR322 origin, Kan*R*, Ct*nug*1-K325A-6xHIS	this study
pET24b-Ct*nug*1-S326A-6xHIS	f1 origin, T7 promoter, pBR322 origin, Kan*R*, Ct*nug*1-S326A-6xHIS	this study
pET24b-Ct*nug*1-S326N-6xHIS	f1 origin, T7 promoter, pBR322 origin, Kan*R*, Ct*nug*1-S326N-6xHIS	this study
pET24b-Ct*nug*1-K325AS326N -6xHIS	f1 origin, T7 promoter, pBR322 origin, Kan*R*, Ct*nug*1-K325AS326N -6xHIS	this study
pET24b-Ct*nug*1-T356A-6xHIS	f1 origin, T7 promoter, pBR322 origin, Kan*R*, Ct*nug*1-T356A-6xHIS	this study
pET24b-Ct*nug*1-T357A -6xHIS	f1 origin, T7 promoter, pBR322 origin, Kan*R*, Ct*nug*1-T357A -6xHIS	this study
pET24b-Ct*nug*1-T356AT376A-6xHIS	f1 origin, T7 promoter, pBR322 origin, Kan*R*, Ct*nug*1-T356AT376A-6xHIS	this study
pET24b-Ct*nug*1-D372N-6xHIS	f1 origin, T7 promoter, pBR322 origin, Kan*R*, Ct*nug*1-D372N-6xHIS	this study
pET24b-Ct*nug*1-D372W-6xHIS	f1 origin, T7 promoter, pBR322 origin, Kan*R*, Ct*nug*1-D372W-6xHIS	this study
pET24b-Ct*nug*1-G375A-6xHIS	f1 origin, T7 promoter, pBR322 origin, Kan*R*, Ct*nug*1-G375A-6xHIS	this study
pET24b-Ct*nug*1-I376K-6xHIS	f1 origin, T7 promoter, pBR322 origin, Kan*R*, Ct*nug*1-I376K-6xHIS	this study
pET24b-Ct*nug*1-I376Q-6xHIS	f1 origin, T7 promoter, pBR322 origin, Kan*R*, Ct*nug*1-I376Q-6xHIS	this study
pET24b-C*tnug*1ΔN (1-17)-6xHIS	f1 origin, T7 promoter, pBR322 origin, Kan*R*, Ct*nug*1ΔN (1-17)-6xHIS	this study
pET24b-Ct*nug*1ΔN (1-42)-6xHIS	f1 origin, T7 promoter, pBR322 origin, Kan*R*, Ct*nug*1ΔN (1-42)-	this study

	6xHIS	
pET24b-C*tnug*1ΔN (1-52)-6xHIS	f1 origin, T7 promoter, pBR322 origin, Kan*R*, Ct*nug*1ΔN (1-52)-6xHIS	this study
pET24b-Ct*nug*1ΔC (501-558)-6xHIS	f1 origin, T7 promoter, pBR322 origin, Kan*R*, Ct*nug*1ΔC (501-558)-6xHIS	this study
pET24b-Ct*nug*1ΔC (537-558)-6xHIS	f1 origin, T7 promoter, pBR322 origin, Kan*R*, Ct*nug*1 ΔC (537-558)-6xHIS	this study
pET24b-Ct*nug*1 ΔN (1-17) ΔC (402-558)-6xHIS	f1 origin, T7 promoter, pBR322 origin, Kan*R*, Ct*nug*1 ΔN (1-17) ΔC (402-558)-6xHIS	this study
pET24b-Ct*nug*1 ΔN (1-17) ΔC (423-558)-6xHIS	f1 origin, T7 promoter, pBR322 origin, Kan*R*, Ct*nug*1 ΔN (1-17) ΔC (423-558)-6xHIS	this study
pET24b-Ct*nug*1 ΔN (1-17) ΔC (490-558)-6xHIS	f1 origin, T7 promoter, pBR322 origin, Kan*R*, Ct*nug*1 ΔN (1-17) ΔC (490-558)-6xHIS	this study
pET24b-Ct*nug*1 ΔN (1-61) ΔC (490-558)-6xHIS	f1 origin, T7 promoter, pBR322 origin, Kan*R*, Ct*nug*1 ΔN (1-61) ΔC (490-558)-6xHIS	this study
pET24b-Ct*nug*1 ΔN (1-61) ΔC (536-558)-6xHIS	f1 origin, T7 promoter, pBR322 origin, Kan*R*, Ct*nug*1 ΔN (1-61) ΔC (536-558)-6xHIS	this study
pET24b-Ct*nug*1 ΔN (1-84) ΔC (471-558)-6xHIS	f1 origin, T7 promoter, pBR322 origin, Kan*R*, Ct*nug*1 ΔN (1-84) ΔC (471-558)-6xHIS	this study
pET24b-Ct*nug*1 ΔN (1-98) ΔC (402-558)-6xHIS	f1 origin, T7 promoter, pBR322 origin, Kan*R*, Ct*nug*1 ΔN (1-98) ΔC (402-558)-6xHIS	this study
pET24b-Ct*nug*1 ΔN (1-98) ΔC (490-558)-6xHIS	f1 origin, T7 promoter, pBR322 origin, Kan*R*, Ct*nug*1 ΔN (1-98) ΔC (490-558)-6xHIS	this study
pET24b-Ct*nug*1 ΔN (1-98) ΔC (536-558)-6xHIS	f1 origin, T7 promoter, pBR322 origin, Kan*R*, Ct*nug*1 ΔN (1-98) ΔC (536-558)-6xHIS	this study
pET24b-Ct*nug*1 ΔN (1-152) ΔC (508-558)-6xHIS	f1 origin, T7 promoter, pBR322 origin, Kan*R*, Ct*nug*1 ΔN (1-152) ΔC (508-558)-6xHIS	this study
pET24b-Ct*nug*1 ΔN (1-189) ΔC (499-558)-6xHIS	f1 origin, T7 promoter, pBR322 origin, Kan*R*, Ct*nug*1 ΔN (1-189) ΔC (499-558)-6xHIS	this study

pET24b-Ct*nug*1 ΔN (1-189) ΔC (502-558)-6xHIS	f1 origin, T7 promoter, pBR322 origin, Kan*R*, Ct*nug*1 ΔN (1-189) ΔC (502-558)-6xHIS	this study
pET24b-Ct*nug*1 ΔN (1-190) ΔC (499-558)-6xHIS	f1 origin, T7 promoter, pBR322 origin, Kan*R*, Ct*nug*1 ΔN (1-190) ΔC (499-558)-6xHIS	this study
pET24b-Ct*nug*1 ΔN (1-190) ΔC (502-558)-6xHIS	f1 origin, T7 promoter, pBR322 origin, Kan*R*, Ct*nug*1 ΔN (1-190) ΔC (502-558)-6xHIS	this study
pET24b-Ct*nug*1 ΔN (1-196) ΔC (499-558)-6xHIS	f1 origin, T7 promoter, pBR322 origin, Kan*R*, Ct*nug*1ΔC (501-558)-6xHIS	this study
pET24b-Ct*nug*1 ΔN (1-199) ΔC (508-558)-6xHIS	f1 origin, T7 promoter, pBR322 origin, Kan*R*, Ct*nug*1ΔC (501-558)-6xHIS	this study
pET15b-Ct*KAP*123-GST	f1 origin, T7 promoter, pBR322 origin, Amp*R*, Ct*KAP*123-TEV-GST	this study
pET24d-6xHIS-Ct*KAP*123	f1 origin, T7 promoter, pBR322 origin, Kan*R*, 6xHIS-Ct*KAP*123	this study
pProEX1-GST-TEV-Ct*DBP*10	TRC promoter, Amp*R*, GST-TEV-Ct*DBP*10	this study

TableS3. Antibodies used in this study

Antibody	Dilution	Reference	Secondary α- used
α-Nog1	1: 30000	Saveanu et al., 2003	α-rabbit
α-Nug1	1: 1000	Altvater et al., 2012	α-rabbit
α-Nug2	1: 10000	Saveanu et al., 2003	α-rabbit
α-Rsa4	1: 10000	De la Cruz et al., 2005	α-rabbit
α-Nsa2	1: 10000	Lebreton et al., 2006	α-rabbit
α-Yvh1	1: 4000	Altvater et al., 2012	α-rabbit
α-Mrt4	1: 1000	María Rodríguez et al., 2009	α-rabbit
α-Tif6	1: 10000	Senger et al., 2001	α-rabbit
α-Rpp0	1:10	María Rodríguez et al., 2009	α-mouse
α-Rpl3	1: 5000	Bussiere et al. 2012	α-mouse
α-Rpl12	1:10	Vilella MD et al., 1991	α-rabbit
α-Rpl35	1: 35000	Frey et al., 2001	α-rabbit
α-Rpl24	1: 15000	Saveanu et al., 2003	α-rabbit
α-Rps3		Steffen Frey et al., 2001	α-rabbit
α-Arc1	1: 20000	Simos et al., 1996	α-rabbit
α-CBP	1: 70000	Polyclonal, Open Biosystems	α-rabbit
α-GFP	1: 3000	Monoclonal, Roche	α-rabbit
α-HA	1: 1000	Covance / HISS diagnostics	α-mouse
α-FLAG	1: 10000	Monoclonal, Sigma, HRP-conjugated	
α-ProteinA	1: 15000	Peroxidase anti-peroxidase complex antibody, DAKO, HRP-conjugated	
goat-anti-mouse	1: 3000	BioRad, HRP-conjugated	
mouse-anti-rabbit	1: 3000	BioRad, HRP-conjugated	

Table S4. Figure Index

Figure	Tittle
Figure 1.1	The ribosome
Figure 1.2	Comparison between prokaryotic and eukaryotic ribosome composition
Figure 1.3	Structural hallmarks of the ribosomal subunits
Figure 1.4	Simplified outlook of ribosome biogenesis in yeast
Figure 1.5	Schematic representation of the rDNA operon in yeast
Figure 1.6	Schematic representation of C/D and H/ACA box snoRNAs.
Figure 1.7	Schematic representation of 35S rRNA processing
Figure 1.8	Early steps in ribosome biogenesis, the 90S pre-particle
Figure 1.9	The 40S subunit maturation
Figure 1.10	A simplified view of the complex and dynamic pre-60S ribosome maturation
Figure 1.11	Schematic representation of the last cytoplasmic events covering the 60S maturation.
Figure 1.12	Schematic representation of the P-stalk formation during 60S subunit maturation.
Figure 1.13	The nuclear pore complex
Figure 1.14	Nuclear export of pre-40S and pre-60S particles
Figure 1.15	Nucleocytoplasmic transport is mediated by specialized translocating proteins.
Figure 1.16	ATP-dependent RNA helicases
Figure 1.17	Domain organization and structure of an AAA-ATPase
Figure 1.18	General overview of the G domain organization
Figure 1.19	Domain organization of Nug1.
Figure 3.1	*Ct*Nug1 complements the otherwise lethal *nug1*Δ strain
Figure 3.2	Nug1 exhibits an intrinsic GTPase activity *in vitro*.
Figure 3.3	The GTPase activity of *Ct*Nug1 is stimulated by potassium ions.

Abbreviations

3D	three-dimensional
5'FOA	5' fluoro-arotic acid
aa	amino acid
Å	Ångström
ABC	ATP-binding cassette
ADP	Adenosine diphosphate
ATP	Adenosine triphosphate
AAA-ATPase	ATPases Associated with diverse cellular Activities
B.subtilis (Bs	*Bacillus subtilis*
CBP	Calmodulin-binding peptide
cDNA	complementary DNA
cdGTPases	cation-dependent GTPases
CP	Central protuberance
cpGTPases	circularly permuted GTPases
CRAC	cross-linking ans cDNA analysis
C.thermophy	*Chaetomium Thermophilum*
DAPI	4´-6-Diamidin-2-phenylindol
DMSO	dimethyl sulfoxide acid
DNA	deoxyribonucleic acid
DTT	dithiothreitol
E.coli (*Ec*)	*Escherichia coli*
EDTA	ethylenediaminetetraacetic
EGTA	ethylene glycol-bis(**β** -aminoethylether)-N, N, N´, N´
EM	electron microscopy
ES	expansion segments
ETS	external transcribed spacer
FG	phenylalanine-glycine
GAL	galactose
GAP	GTPase-activating protein
GDP	guanosine diphosphate
GDIs	guanine nucleotide dissociation inhibitors
GEF	guanine nucleotide exchange factor
GFP	green fluorescent protein
GNL3L	guanine nucleotide binding protein-like 3
GSH	glutathione
GST	glutathione S-transferase
GTP	guanosine triphosphate
H	helix
HIS	histidine
hnRNPs	heterogeneous nuclear ribonucleoprotein particle
IgG	immunoglobulin G
ITS	Internal transcribed spacer
Kap	karyopherin
Kb	kilobase
kDa	kilodalton
LSU	large subunit
mAU	milli absorbance unit
mant-	methyl-anthraniloyl
mM	millimolar
mDa	Megadalton
MIDAS	metal-ion-dependent-adhesion-site

MIDO	MIDAS-interaction domain
Min	minutes
Ml	mililitter
µM	micromolar
mol	moles
MOPS	4- and 3-Morpholinepropanesulfonic acid
mRNA	messenger ribonucleoprotein acid
mRNP	messenger ribonucleoprotein particle
MS	mass spectrometry
Mtr2	mRNA transport 2
N.Crassa (*Nc*)	*Neurospora crassa*
NE	nuclear envelope
NES	nuclear export signal
NLS	nuclear localization signal
nm	nanometer
NORs	nucleolar organizer regions
NPC	nuclear pore complex
NS	nucleostemin
Nup	nucleoporin
OD	optical density
ORF	open reading frame
PAGE	polyacrylamide gel electrophoresis
PBS	phosphate-buffered saline
PCR	Polymerase chain reaction
Pol (I, II, III)	Polymerase (I, II, III)
P-proteins	Phospho-proteins
ProtA	protein A
PTC	peptyl-transferase center
PVDF	polyvinylidene difluoride
Ran	RAS-related nuclear protein
rDNA	ribosomal DNA
RNA	ribonucleic acid
RNP	ribonucleoprotein particle
rRNA	ribosomal RNA
S	Svedberg unit
S.cerevisiae (*Sc*)	*Saccharomyces cerevisiae*
S.pompe (*Sp*)	*Schizosaccharomyces pombe*
SDS	sodium dodecyl sulfate
SDS-PAGE	SDS polyacrylamide gel electrophoresis
SL	synthetic lethal
snoRNA	small nucleolar RNA
snoRNP	small nucleolar RNP
SSU	small subunit
SV40	simian virus 40
TAP	tandem affinity purification
TCA	tri-chloro-acetic acid
TEV	Tobacco etch virus protease
tRNA	transfer RNA
UTR	untranslated region
UV	ultra violett
WT	Wild-type
Ψ	pseudouridine

Publications

Yoshitaka Matsuo, Sander Granneman, Matthias Thoms, Rizos-Georgios Manikas, David Tollervey & Ed Hurt (2014). Coupled GTPase and remodelling ATPase activities form a checkpoint for ribosome export. *Nature*, 112–116.

References

Achila, D., M. Gulati, N. Jain, and R.A. Britton. 2012. Biochemical characterization of ribosome assembly GTPase RbgA in Bacillus subtilis. *The Journal of biological chemistry*. 287:8417-8423.

Aitchison, J.D., and M.P. Rout. 2012. The yeast nuclear pore complex and transport through it. *Genetics*. 190:855-883.

Amlacher, S., P. Sarges, D. Flemming, V. van Noort, R. Kunze, D.P. Devos, M. Arumugam, P. Bork, and E. Hurt. 2011. Insight into structure and assembly of the nuclear pore complex by utilizing the genome of a eukaryotic thermophile. *Cell*. 146:277-289.

Anand, B., S.K. Verma, and B. Prakash. 2006. Structural stabilization of GTP-binding domains in circularly permuted GTPases: implications for RNA binding. *Nucleic acids research*. 34:2196-2205.

Andersen, C.B., T. Becker, M. Blau, M. Anand, M. Halic, B. Balar, T. Mielke, T. Boesen, J.S. Pedersen, C.M. Spahn, T.G. Kinzy, G.R. Andersen, and R. Beckmann. 2006. Structure of eEF3 and the mechanism of transfer RNA release from the E-site. *Nature*. 443:663-668.

Arino, J., J. Ramos, and H. Sychrova. 2010. Alkali metal cation transport and homeostasis in yeasts. *Microbiology and molecular biology reviews : MMBR*. 74:95-120.

Ash, M.R., A. Guilfoyle, R.J. Clarke, J.M. Guss, M.J. Maher, and M. Jormakka. 2010. Potassium-activated GTPase reaction in the G Protein-coupled ferrous iron transporter B. *The Journal of biological chemistry*. 285:14594-14602.

Ash, M.R., M.J. Maher, J.M. Guss, and M. Jormakka. 2011a. The initiation of GTP hydrolysis by the G-domain of FeoB: insights from a transition-state complex structure. *PloS one*. 6:e23355.

Ash, M.R., M.J. Maher, J.M. Guss, and M. Jormakka. 2011b. A suite of Switch I and Switch II mutant structures from the G-protein domain of FeoB. *Acta crystallographica. Section D, Biological crystallography*. 67:973-980.

Ash, M.R., M.J. Maher, J. Mitchell Guss, and M. Jormakka. 2012. The cation-dependent G-proteins: in a class of their own. *FEBS letters*. 586:2218-2224.

Ban, N., P. Nissen, J. Hansen, P.B. Moore, and T.A. Steitz. 2000. The complete atomic structure of the large ribosomal subunit at 2.4 A resolution. *Science*. 289:905-920.

Barr, F., and D.G. Lambright. 2010. Rab GEFs and GAPs. *Current opinion in cell biology*. 22:461-470.

Bashan, A., and A. Yonath. 2008. Correlating ribosome function with high-resolution structures. *Trends in microbiology*. 16:326-335.

Bassler, J., P. Grandi, O. Gadal, T. Lessmann, E. Petfalski, D. Tollervey, J. Lechner, and E. Hurt. 2001. Identification of a 60S preribosomal particle that is closely linked to nuclear export. *Molecular cell*. 8:517-529.

Bassler, J., M. Kallas, and E. Hurt. 2006. The NUG1 GTPase reveals and N-terminal RNA-binding domain that is essential for association with 60 S pre-ribosomal particles. *The Journal of biological chemistry*. 281:24737-24744.

Bassler, J., M. Kallas, B. Pertschy, C. Ulbrich, M. Thoms, and E. Hurt. 2010. The AAA-ATPase Rea1 drives removal of biogenesis factors during multiple stages of 60S ribosome assembly. *Molecular cell*. 38:712-721.

Bassler, J., I. Klein, C. Schmidt, M. Kallas, E. Thomson, M.A. Wagner, B. Bradatsch, G. Rechberger, H. Strohmaier, E. Hurt, and H. Bergler. 2012. The conserved Bud20 zinc finger protein is a new component of the ribosomal 60S subunit export machinery. *Molecular and cellular biology*. 32:4898-4912.

Basu, U., K. Si, H. Deng, and U. Maitra. 2003. Phosphorylation of mammalian eukaryotic translation initiation factor 6 and its Saccharomyces cerevisiae homologue Tif6p: evidence that phosphorylation of Tif6p regulates its nucleocytoplasmic distribution and is required for yeast cell growth. *Molecular and cellular biology*. 23:6187-6199.

Bataille, N., T. Helser, and H.M. Fried. 1990. Cytoplasmic transport of ribosomal subunits microinjected into the Xenopus laevis oocyte nucleus: a generalized, facilitated process. *The Journal of cell biology*. 111:1571-1582.

Ben-Shem, A., N. Garreau de Loubresse, S. Melnikov, L. Jenner, G. Yusupova, and M. Yusupov. 2011. The structure of the eukaryotic ribosome at 3.0 A resolution. *Science*. 334:1524-1529.

Ben-Shem, A., L. Jenner, G. Yusupova, and M. Yusupov. 2010. Crystal structure of the eukaryotic ribosome. *Science*. 330:1203-1209.

Bernstein, K.A., S. Granneman, A.V. Lee, S. Manickam, and S.J. Baserga. 2006. Comprehensive mutational analysis of yeast DEXD/H box RNA helicases involved in large ribosomal subunit biogenesis. *Molecular and cellular biology*. 26:1195-1208.

Bleichert, F., and S.J. Baserga. 2007. The long unwinding road of RNA helicases. *Molecular cell*. 27:339-352.

Bos, J.L., H. Rehmann, and A. Wittinghofer. 2007. GEFs and GAPs: critical elements in the control of small G proteins. *Cell*. 129:865-877.

Bourne, H.R., D.A. Sanders, and F. McCormick. 1990. The GTPase superfamily: a conserved switch for diverse cell functions. *Nature*. 348:125-132.

Bradatsch, B., J. Katahira, E. Kowalinski, G. Bange, W. Yao, T. Sekimoto, V. Baumgartel, G. Boese, J. Bassler, K. Wild, R. Peters, Y. Yoneda, I. Sinning, and E. Hurt. 2007. Arx1 functions as an unorthodox nuclear export receptor for the 60S preribosomal subunit. *Molecular cell*. 27:767-779.

Bradatsch, B., C. Leidig, S. Granneman, M. Gnadig, D. Tollervey, B. Bottcher, R. Beckmann, and E. Hurt. 2012. Structure of the pre-60S ribosomal subunit with nuclear export factor Arx1 bound at the exit tunnel. *Nature structural & molecular biology*. 19:1234-1241.

Butler, D.K., and R.L. Metzenberg. 1990. Expansion and contraction of the nucleolus organizer region of Neurospora: changes originate in both proximal and distal segments. *Genetics*. 126:325-333.

Caldarola, S., M.C. De Stefano, F. Amaldi, and F. Loreni. 2009. Synthesis and function of ribosomal proteins--fading models and new perspectives. *The FEBS journal*. 276:3199-3210.

Chandramouli, P., M. Topf, J.F. Menetret, N. Eswar, J.J. Cannone, R.R. Gutell, A. Sali, and C.W. Akey. 2008. Structure of the mammalian 80S ribosome at 8.7 A resolution. *Structure*. 16:535-548.

Chantha, S.C., B.S. Emerald, and D.P. Matton. 2006. Characterization of the plant Notchless homolog, a WD repeat protein involved in seed development. *Plant molecular biology*. 62:897-912.

Chappie, J.S., S. Acharya, M. Leonard, S.L. Schmid, and F. Dyda. 2010. G domain dimerization controls dynamin's assembly-stimulated GTPase activity. *Nature*. 465:435-440.

Cherfils, J., and P. Chardin. 1999. GEFs: structural basis for their activation of small GTP-binding proteins. *Trends in biochemical sciences*. 24:306-311.

Chien, C.T., P.L. Bartel, R. Sternglanz, and S. Fields. 1991. The two-hybrid system: a method to identify and clone genes for proteins that interact with a protein of interest. *Proceedings of the National Academy of Sciences of the United States of America*. 88:9578-9582.

Choi, C.H. 2005. ABC transporters as multidrug resistance mechanisms and the development of chemosensitizers for their reversal. *Cancer cell international*. 5:30.

Cingolani, G., J. Bednenko, M.T. Gillespie, and L. Gerace. 2002. Molecular basis for the recognition of a nonclassical nuclear localization signal by importin beta. *Molecular cell*. 10:1345-1353.

Cook, A., F. Bono, M. Jinek, and E. Conti. 2007. Structural biology of nucleocytoplasmic transport. *Annual review of biochemistry*. 76:647-671.
Cordin, O., J. Banroques, N.K. Tanner, and P. Linder. 2006. The DEAD-box protein family of RNA helicases. *Gene*. 367:17-37.
Cronshaw, J.M., A.N. Krutchinsky, W. Zhang, B.T. Chait, and M.J. Matunis. 2002. Proteomic analysis of the mammalian nuclear pore complex. *The Journal of cell biology*. 158:915-927.
Dasso, M. 2002. The Ran GTPase: theme and variations. *Current biology : CB*. 12:R502-508.
Decatur, W.A., X.H. Liang, D. Piekna-Przybylska, and M.J. Fournier. 2007. Identifying effects of snoRNA-guided modifications on the synthesis and function of the yeast ribosome. *Methods in enzymology*. 425:283-316.
Dechampesme, A.M., O. Koroleva, I. Leger-Silvestre, N. Gas, and S. Camier. 1999. Assembly of 5S ribosomal RNA is required at a specific step of the pre-rRNA processing pathway. *The Journal of cell biology*. 145:1369-1380.
Demoinet, E., A. Jacquier, G. Lutfalla, and M. Fromont-Racine. 2007. The Hsp40 chaperone Jjj1 is required for the nucleo-cytoplasmic recycling of preribosomal factors in Saccharomyces cerevisiae. *Rna*. 13:1570-1581.
Denning, D.P., S.S. Patel, V. Uversky, A.L. Fink, and M. Rexach. 2003. Disorder in the nuclear pore complex: the FG repeat regions of nucleoporins are natively unfolded. *Proceedings of the National Academy of Sciences of the United States of America*. 100:2450-2455.
Deutschbauer, A.M., D.F. Jaramillo, M. Proctor, J. Kumm, M.E. Hillenmeyer, R.W. Davis, C. Nislow, and G. Giaever. 2005. Mechanisms of haploinsufficiency revealed by genome-wide profiling in yeast. *Genetics*. 169:1915-1925.
Devos, D., S. Dokudovskaya, R. Williams, F. Alber, N. Eswar, B.T. Chait, M.P. Rout, and A. Sali. 2006. Simple fold composition and modular architecture of the nuclear pore complex. *Proceedings of the National Academy of Sciences of the United States of America*. 103:2172-2177.
Diges, C.M., and O.C. Uhlenbeck. 2001. Escherichia coli DbpA is an RNA helicase that requires hairpin 92 of 23S rRNA. *The EMBO journal*. 20:5503-5512.
Diges, C.M., and O.C. Uhlenbeck. 2005. Escherichia coli DbpA is a 3' --> 5' RNA helicase. *Biochemistry*. 44:7903-7911.
Dinman, J.D. 2005. 5S rRNA: Structure and Function from Head to Toe. *International journal of biomedical science : IJBS*. 1:2-7.
Dong, J., R. Lai, J.L. Jennings, A.J. Link, and A.G. Hinnebusch. 2005. The novel ATP-binding cassette protein ARB1 is a shuttling factor that stimulates 40S and 60S ribosome biogenesis. *Molecular and cellular biology*. 25:9859-9873.
Dong, J., R. Lai, K. Nielsen, C.A. Fekete, H. Qiu, and A.G. Hinnebusch. 2004. The essential ATP-binding cassette protein RLI1 functions in translation by promoting preinitiation complex assembly. *The Journal of biological chemistry*. 279:42157-42168.
Dragon, F., J.E. Gallagher, P.A. Compagnone-Post, B.M. Mitchell, K.A. Porwancher, K.A. Wehner, S. Wormsley, R.E. Settlage, J. Shabanowitz, Y. Osheim, A.L. Beyer, D.F. Hunt, and S.J. Baserga. 2002. A large nucleolar U3 ribonucleoprotein required for 18S ribosomal RNA biogenesis. *Nature*. 417:967-970.
Dresios, J., P. Panopoulos, and D. Synetos. 2006. Eukaryotic ribosomal proteins lacking a eubacterial counterpart: important players in ribosomal function. *Molecular microbiology*. 59:1651-1663.
Eckert-Boulet, N., and M. Lisby. 2009. Regulation of rDNA stability by sumoylation. *DNA repair*. 8:507-516.
Edelheit, O., A. Hanukoglu, and I. Hanukoglu. 2009. Simple and efficient site-directed mutagenesis using two single-primer reactions in parallel to generate mutants for protein structure-function studies. *BMC biotechnology*. 9:61.
Erzberger, J.P., and J.M. Berger. 2006. Evolutionary relationships and structural mechanisms of AAA+ proteins. *Annual review of biophysics and biomolecular structure*. 35:93-114.
Fatica, A., D. Tollervey, and M. Dlakic. 2004. PIN domain of Nob1p is required for D-site cleavage in 20S pre-rRNA. *Rna*. 10:1698-1701.
Faza, M.B., Y. Chang, L. Occhipinti, S. Kemmler, and V.G. Panse. 2012. Role of Mex67-Mtr2 in the nuclear export of 40S pre-ribosomes. *PLoS genetics*. 8:e1002915.
Fei, J., J.E. Bronson, J.M. Hofman, R.L. Srinivas, C.H. Wiggins, and R.L. Gonzalez, Jr. 2009. Allosteric collaboration between elongation factor G and the ribosomal L1 stalk directs tRNA

movements during translation. *Proceedings of the National Academy of Sciences of the United States of America*. 106:15702-15707.
Ferreira-Cerca, S., I. Kiburu, E. Thomson, N. LaRonde, and E. Hurt. 2014. Dominant Rio1 kinase/ATPase catalytic mutant induces trapping of late pre-40S biogenesis factors in 80S-like ribosomes. *Nucleic acids research*. 42:8635-8647.
Ferreira-Cerca, S., G. Poll, P.E. Gleizes, H. Tschochner, and P. Milkereit. 2005. Roles of eukaryotic ribosomal proteins in maturation and transport of pre-18S rRNA and ribosome function. *Molecular cell*. 20:263-275.
Ferreira-Cerca, S., V. Sagar, T. Schafer, M. Diop, A.M. Wesseling, H. Lu, E. Chai, E. Hurt, and N. LaRonde-LeBlanc. 2012. ATPase-dependent role of the atypical kinase Rio2 on the evolving pre-40S ribosomal subunit. *Nature structural & molecular biology*. 19:1316-1323.
Fields, S., and O. Song. 1989. A novel genetic system to detect protein-protein interactions. *Nature*. 340:245-246.
Frickey, T., and A.N. Lupas. 2004. Phylogenetic analysis of AAA proteins. *Journal of structural biology*. 146:2-10.
Fromont-Racine, M., B. Senger, C. Saveanu, and F. Fasiolo. 2003. Ribosome assembly in eukaryotes. *Gene*. 313:17-42.
Gadal, O., D. Strauss, J. Braspenning, D. Hoepfner, E. Petfalski, P. Philippsen, D. Tollervey, and E. Hurt. 2001a. A nuclear AAA-type ATPase (Rix7p) is required for biogenesis and nuclear export of 60S ribosomal subunits. *The EMBO journal*. 20:3695-3704.
Gadal, O., D. Strauss, J. Kessl, B. Trumpower, D. Tollervey, and E. Hurt. 2001b. Nuclear export of 60s ribosomal subunits depends on Xpo1p and requires a nuclear export sequence-containing factor, Nmd3p, that associates with the large subunit protein Rpl10p. *Molecular and cellular biology*. 21:3405-3415.
Galani, K., T.A. Nissan, E. Petfalski, D. Tollervey, and E. Hurt. 2004. Rea1, a dynein-related nuclear AAA-ATPase, is involved in late rRNA processing and nuclear export of 60 S subunits. *The Journal of biological chemistry*. 279:55411-55418.
Gall, J.G. 1967. Octagonal nuclear pores. *The Journal of cell biology*. 32:391-399.
Gallagher, J.E., D.A. Dunbar, S. Granneman, B.M. Mitchell, Y. Osheim, A.L. Beyer, and S.J. Baserga. 2004. RNA polymerase I transcription and pre-rRNA processing are linked by specific SSU processome components. *Genes & development*. 18:2506-2517.
Garbarino, J.E., and I.R. Gibbons. 2002. Expression and genomic analysis of midasin, a novel and highly conserved AAA protein distantly related to dynein. *BMC genomics*. 3:18.
Garcia, I., and O.C. Uhlenbeck. 2008. Differential RNA-dependent ATPase activities of four rRNA processing yeast DEAD-box proteins. *Biochemistry*. 47:12562-12573.
Geerlings, T.H., A.W. Faber, M.D. Bister, J.C. Vos, and H.A. Raue. 2003. Rio2p, an evolutionarily conserved, low abundant protein kinase essential for processing of 20 S Pre-rRNA in Saccharomyces cerevisiae. *The Journal of biological chemistry*. 278:22537-22545.
Gelperin, D., L. Horton, J. Beckman, J. Hensold, and S.K. Lemmon. 2001. Bms1p, a novel GTP-binding protein, and the related Tsr1p are required for distinct steps of 40S ribosome biogenesis in yeast. *Rna*. 7:1268-1283.
Gietz, R.D., and R.A. Woods. 2006. Yeast transformation by the LiAc/SS Carrier DNA/PEG method. *Methods in molecular biology*. 313:107-120.
Gleizes, P.E., J. Noaillac-Depeyre, I. Leger-Silvestre, F. Teulieres, J.Y. Dauxois, D. Pommet, M.C. Azum-Gelade, and N. Gas. 2001. Ultrastructural localization of rRNA shows defective nuclear export of preribosomes in mutants of the Nup82p complex. *The Journal of cell biology*. 155:923-936.
Goldstein, A.L., and J.H. McCusker. 1999. Three new dominant drug resistance cassettes for gene disruption in Saccharomyces cerevisiae. *Yeast*. 15:1541-1553.
Gonzalez, A., A. Jimenez, D. Vazquez, J.E. Davies, and D. Schindler. 1978. Studies on the mode of action of hygromycin B, an inhibitor of translocation in eukaryotes. *Biochimica et biophysica acta*. 521:459-469.
Gorbalenya, A.E., and E.V. Koonin. 1993. Helicases - Amino-Acid-Sequence Comparisons and Structure-Function-Relationships. *Current opinion in structural biology*. 3:419-429.
Grandi, P., V. Rybin, J. Bassler, E. Petfalski, D. Strauss, M. Marzioch, T. Schafer, B. Kuster, H. Tschochner, D. Tollervey, A.C. Gavin, and E. Hurt. 2002. 90S pre-ribosomes include the 35S pre-rRNA, the U3 snoRNP, and 40S subunit processing factors but predominantly lack 60S synthesis factors. *Molecular cell*. 10:105-115.

Granneman, S., and S.J. Baserga. 2004. Ribosome biogenesis: of knobs and RNA processing. *Experimental cell research*. 296:43-50.

Granneman, S., and S.J. Baserga. 2005. Crosstalk in gene expression: coupling and co-regulation of rDNA transcription, pre-ribosome assembly and pre-rRNA processing. *Current opinion in cell biology*. 17:281-286.

Granneman, S., K.A. Bernstein, F. Bleichert, and S.J. Baserga. 2006a. Comprehensive mutational analysis of yeast DEXD/H box RNA helicases required for small ribosomal subunit synthesis. *Molecular and cellular biology*. 26:1183-1194.

Granneman, S., G. Kudla, E. Petfalski, and D. Tollervey. 2009. Identification of protein binding sites on U3 snoRNA and pre-rRNA by UV cross-linking and high-throughput analysis of cDNAs. *Proceedings of the National Academy of Sciences of the United States of America*. 106:9613-9618.

Granneman, S., C. Lin, E.A. Champion, M.R. Nandineni, C. Zorca, and S.J. Baserga. 2006b. The nucleolar protein Esf2 interacts directly with the DExD/H box RNA helicase, Dbp8, to stimulate ATP hydrolysis. *Nucleic acids research*. 34:3189-3199.

Granneman, S., E. Petfalski, A. Swiatkowska, and D. Tollervey. 2010. Cracking pre-40S ribosomal subunit structure by systematic analyses of RNA-protein cross-linking. *The EMBO journal*. 29:2026-2036.

Granneman, S., E. Petfalski, and D. Tollervey. 2011. A cluster of ribosome synthesis factors regulate pre-rRNA folding and 5.8S rRNA maturation by the Rat1 exonuclease. *The EMBO journal*. 30:4006-4019.

Greber, B.J., D. Boehringer, C. Montellese, and N. Ban. 2012. Cryo-EM structures of Arx1 and maturation factors Rei1 and Jjj1 bound to the 60S ribosomal subunit. *Nature structural & molecular biology*. 19:1228-1233.

Hackmann, A., T. Gross, C. Baierlein, and H. Krebber. 2011. The mRNA export factor Npl3 mediates the nuclear export of large ribosomal subunits. *EMBO reports*. 12:1024-1031.

Hage, A.E., and D. Tollervey. 2004. A surfeit of factors: why is ribosome assembly so much more complicated in eukaryotes than bacteria? *RNA biology*. 1:10-15.

Hakulinen, N., O. Turunen, J. Janis, M. Leisola, and J. Rouvinen. 2003. Three-dimensional structures of thermophilic beta-1,4-xylanases from Chaetomium thermophilum and Nonomuraea flexuosa. Comparison of twelve xylanases in relation to their thermal stability. *European journal of biochemistry / FEBS*. 270:1399-1412.

Hall, A. 1990. The cellular functions of small GTP-binding proteins. *Science*. 249:635-640.

Hanson, P.I., and S.W. Whiteheart. 2005. AAA+ proteins: Have engine, will work. *Nat Rev Mol Cell Bio*. 6:519-529.

Harnpicharnchai, P., J. Jakovljevic, E. Horsey, T. Miles, J. Roman, M. Rout, D. Meagher, B. Imai, Y. Guo, C.J. Brame, J. Shabanowitz, D.F. Hunt, and J.L. Woolford, Jr. 2001. Composition and functional characterization of yeast 66S ribosome assembly intermediates. *Molecular cell*. 8:505-515.

Harvey Lodish, A.B., S Lawrence Zipursky, Paul Matsudaira, David Baltimore, and James Darnell. Molecular Cell Biology. 4th edition.

Hedges, J., M. West, and A.W. Johnson. 2005. Release of the export adapter, Nmd3p, from the 60S ribosomal subunit requires Rpl10p and the cytoplasmic GTPase Lsg1p. *The EMBO journal*. 24:567-579.

Henras, A.K., J. Soudet, M. Gerus, S. Lebaron, M. Caizergues-Ferrer, A. Mougin, and Y. Henry. 2008. The post-transcriptional steps of eukaryotic ribosome biogenesis. *Cellular and molecular life sciences : CMLS*. 65:2334-2359.

Henry, Y., H. Wood, J.P. Morrissey, E. Petfalski, S. Kearsey, and D. Tollervey. 1994. The 5' end of yeast 5.8S rRNA is generated by exonucleases from an upstream cleavage site. *The EMBO journal*. 13:2452-2463.

Hill, T.A., J. Broadhvest, R.K. Kuzoff, and C.S. Gasser. 2006. Arabidopsis SHORT INTEGUMENTS 2 is a mitochondrial DAR GTPase. *Genetics*. 174:707-718.

Ho, J.H., and A.W. Johnson. 1999. NMD3 encodes an essential cytoplasmic protein required for stable 60S ribosomal subunits in Saccharomyces cerevisiae. *Molecular and cellular biology*. 19:2389-2399.

Ho, J.H., G. Kallstrom, and A.W. Johnson. 2000a. Nascent 60S ribosomal subunits enter the free pool bound by Nmd3p. *Rna*. 6:1625-1634.

Ho, J.H., G. Kallstrom, and A.W. Johnson. 2000b. Nmd3p is a Crm1p-dependent adapter protein for nuclear export of the large ribosomal subunit. *The Journal of cell biology*. 151:1057-1066.

Hoelz, A., E.W. Debler, and G. Blobel. 2011. The structure of the nuclear pore complex. *Annual review of biochemistry*. 80:613-643.

Holzel, M., M. Rohrmoser, M. Schlee, T. Grimm, T. Harasim, A. Malamoussi, A. Gruber-Eber, E. Kremmer, W. Hiddemann, G.W. Bornkamm, and D. Eick. 2005. Mammalian WDR12 is a novel member of the Pes1-Bop1 complex and is required for ribosome biogenesis and cell proliferation. *The Journal of cell biology*. 170:367-378.

Hung, N.J., and A.W. Johnson. 2006. Nuclear recycling of the pre-60S ribosomal subunit-associated factor Arx1 depends on Rei1 in Saccharomyces cerevisiae. *Molecular and cellular biology*. 26:3718-3727.

Hurt, E., S. Hannus, B. Schmelzl, D. Lau, D. Tollervey, and G. Simos. 1999. A novel in vivo assay reveals inhibition of ribosomal nuclear export in ran-cycle and nucleoporin mutants. *The Journal of cell biology*. 144:389-401.

Inoue, H., H. Nojima, and H. Okayama. 1990. High efficiency transformation of Escherichia coli with plasmids. *Gene*. 96:23-28.

Isgro, T.A., and K. Schulten. 2007. Association of nuclear pore FG-repeat domains to NTF2 import and export complexes. *Journal of molecular biology*. 366:330-345.

Iwashita, S., and S.Y. Song. 2008. RasGAPs: a crucial regulator of extracellular stimuli for homeostasis of cellular functions. *Molecular bioSystems*. 4:213-222.

Iyer, L.M., D.D. Leipe, E.V. Koonin, and L. Aravind. 2004. Evolutionary history and higher order classification of AAA+ ATPases. *Journal of structural biology*. 146:11-31.

James, P., J. Halladay, and E.A. Craig. 1996. Genomic libraries and a host strain designed for highly efficient two-hybrid selection in yeast. *Genetics*. 144:1425-1436.

Janke, C., M.M. Magiera, N. Rathfelder, C. Taxis, S. Reber, H. Maekawa, A. Moreno-Borchart, G. Doenges, E. Schwob, E. Schiebel, and M. Knop. 2004. A versatile toolbox for PCR-based tagging of yeast genes: new fluorescent proteins, more markers and promoter substitution cassettes. *Yeast*. 21:947-962.

Jankowsky, E., and H. Bowers. 2006. Remodeling of ribonucleoprotein complexes with DExH/D RNA helicases. *Nucleic acids research*. 34:4181-4188.

Jankowsky, E., and M.E. Fairman. 2007. RNA helicases--one fold for many functions. *Current opinion in structural biology*. 17:316-324.

Jentsch, S., and S. Rumpf. 2007. Cdc48 (p97): a "molecular gearbox" in the ubiquitin pathway? *Trends in biochemical sciences*. 32:6-11.

Kappel, L., M. Loibl, G. Zisser, I. Klein, G. Fruhmann, C. Gruber, S. Unterweger, G. Rechberger, B. Pertschy, and H. Bergler. 2012. Rlp24 activates the AAA-ATPase Drg1 to initiate cytoplasmic pre-60S maturation. *The Journal of cell biology*. 199:771-782.

Karbstein, K., and J.A. Doudna. 2006. GTP-dependent formation of a ribonucleoprotein subcomplex required for ribosome biogenesis. *Journal of molecular biology*. 356:432-443.

Karbstein, K., S. Jonas, and J.A. Doudna. 2005. An essential GTPase promotes assembly of preribosomal RNA processing complexes. *Molecular cell*. 20:633-643.

Karginov, F.V., and O.C. Uhlenbeck. 2004. Interaction of Escherichia coli DbpA with 23S rRNA in different functional states of the enzyme. *Nucleic acids research*. 32:3028-3032.

Kelley, L.A., and M.J. Sternberg. 2009. Protein structure prediction on the Web: a case study using the Phyre server. *Nature protocols*. 4:363-371.

Kemmler, S., L. Occhipinti, M. Veisu, and V.G. Panse. 2009. Yvh1 is required for a late maturation step in the 60S biogenesis pathway. *The Journal of cell biology*. 186:863-880.

Kim do, J., J.Y. Jang, H.J. Yoon, and S.W. Suh. 2008. Crystal structure of YlqF, a circularly permuted GTPase: implications for its GTPase activation in 50 S ribosomal subunit assembly. *Proteins*. 72:1363-1370.

Kispal, G., K. Sipos, H. Lange, Z. Fekete, T. Bedekovics, T. Janaky, J. Bassler, D.J. Aguilar Netz, J. Balk, C. Rotte, and R. Lill. 2005. Biogenesis of cytosolic ribosomes requires the essential iron-sulphur protein Rli1p and mitochondria. *The EMBO journal*. 24:589-598.

Kolanczyk, M., M. Pech, T. Zemojtel, H. Yamamoto, I. Mikula, M.A. Calvaruso, M. van den Brand, R. Richter, B. Fischer, A. Ritz, N. Kossler, B. Thurisch, R. Spoerle, J. Smeitink, U. Kornak, D. Chan, M. Vingron, P. Martasek, R.N. Lightowlers, L. Nijtmans, M. Schuelke, K.H. Nierhaus, and S. Mundlos. 2011. NOA1 is an essential GTPase required for mitochondrial protein synthesis. *Molecular biology of the cell*. 22:1-11.

Kressler, D., E. Hurt, and J. Bassler. 2010. Driving ribosome assembly. *Biochimica et biophysica acta*. 1803:673-683.

Kressler, D., D. Roser, B. Pertschy, and E. Hurt. 2008. The AAA ATPase Rix7 powers progression of ribosome biogenesis by stripping Nsa1 from pre-60S particles. *The Journal of cell biology*. 181:935-944.

Kruiswijk, T., R.J. Planta, and J.M. Krop. 1978. The course of the assembly of ribosomal subunits in yeast. *Biochimica et biophysica acta*. 517:378-389.

Kufel, J., B. Dichtl, and D. Tollervey. 1999. Yeast Rnt1p is required for cleavage of the pre-ribosomal RNA in the 3' ETS but not the 5' ETS. *Rna*. 5:909-917.

Kuhle, B., and R. Ficner. 2014. A monovalent cation acts as structural and catalytic cofactor in translational GTPases. *The EMBO journal*.

La Touche, G.J. 1948. A Chætomium-like Thermophile Fungus. *Nature*. Volume 161:pp. 320.

Laemmli, U.K. 1970. Cleavage of structural proteins during the assembly of the head of bacteriophage T4. *Nature*. 227:680-685.

Lafontaine, D.L., C. Bousquet-Antonelli, Y. Henry, M. Caizergues-Ferrer, and D. Tollervey. 1998. The box H + ACA snoRNAs carry Cbf5p, the putative rRNA pseudouridine synthase. *Genes & development*. 12:527-537.

Lafontaine, D.L., and D. Tollervey. 2001. The function and synthesis of ribosomes. *Nature reviews. Molecular cell biology*. 2:514-520.

Lamanna, A.C., and K. Karbstein. 2009. Nob1 binds the single-stranded cleavage site D at the 3'-end of 18S rRNA with its PIN domain. *Proceedings of the National Academy of Sciences of the United States of America*. 106:14259-14264.

Larkin, M.A., G. Blackshields, N.P. Brown, R. Chenna, P.A. McGettigan, H. McWilliam, F. Valentin, I.M. Wallace, A. Wilm, R. Lopez, J.D. Thompson, T.J. Gibson, and D.G. Higgins. 2007. Clustal W and Clustal X version 2.0. *Bioinformatics*. 23:2947-2948.

Lebaron, S., C. Froment, M. Fromont-Racine, J.C. Rain, B. Monsarrat, M. Caizergues-Ferrer, and Y. Henry. 2005. The splicing ATPase prp43p is a component of multiple preribosomal particles. *Molecular and cellular biology*. 25:9269-9282.

Lebaron, S., C. Papin, R. Capeyrou, Y.L. Chen, C. Froment, B. Monsarrat, M. Caizergues-Ferrer, M. Grigoriev, and Y. Henry. 2009. The ATPase and helicase activities of Prp43p are stimulated by the G-patch protein Pfa1p during yeast ribosome biogenesis. *The EMBO journal*. 28:3808-3819.

Lebaron, S., C. Schneider, R.W. van Nues, A. Swiatkowska, D. Walsh, B. Bottcher, S. Granneman, N.J. Watkins, and D. Tollervey. 2012. Proofreading of pre-40S ribosome maturation by a translation initiation factor and 60S subunits. *Nature structural & molecular biology*. 19:744-753.

Lebreton, A., C. Saveanu, L. Decourty, J.C. Rain, A. Jacquier, and M. Fromont-Racine. 2006. A functional network involved in the recycling of nucleocytoplasmic pre-60S factors. *The Journal of cell biology*. 173:349-360.

Leger-Silvestre, I., P. Milkereit, S. Ferreira-Cerca, C. Saveanu, J.C. Rousselle, V. Choesmel, C. Guinefoleau, N. Gas, and P.E. Gleizes. 2004. The ribosomal protein Rps15p is required for nuclear exit of the 40S subunit precursors in yeast. *The EMBO journal*. 23:2336-2347.

Leidig, C., M. Thoms, I. Holdermann, B. Bradatsch, O. Berninghausen, G. Bange, I. Sinning, E. Hurt, and R. Beckmann. 2014. 60S ribosome biogenesis requires rotation of the 5S ribonucleoprotein particle. *Nature communications*. 5:3491.

Leipe, D.D., Y.I. Wolf, E.V. Koonin, and L. Aravind. 2002. Classification and evolution of P-loop GTPases and related ATPases. *Journal of molecular biology*. 317:41-72.

Levdikov, V.M., E.V. Blagova, J.A. Brannigan, L. Cladiere, A.A. Antson, M.N. Isupov, S.J. Seror, and A.J. Wilkinson. 2004. The crystal structure of YloQ, a circularly permuted GTPase essential for Bacillus subtilis viability. *Journal of molecular biology*. 340:767-782.

Linder, P. 2006. Dead-box proteins: a family affair--active and passive players in RNP-remodeling. *Nucleic acids research*. 34:4168-4180.

Lindstrom, M.S. 2009. Emerging functions of ribosomal proteins in gene-specific transcription and translation. *Biochemical and biophysical research communications*. 379:167-170.

Liu, F., A. Putnam, and E. Jankowsky. 2008. ATP hydrolysis is required for DEAD-box protein recycling but not for duplex unwinding. *Proceedings of the National Academy of Sciences of the United States of America*. 105:20209-20214.

Lo, K.Y., Z. Li, F. Wang, E.M. Marcotte, and A.W. Johnson. 2009. Ribosome stalk assembly requires the dual-specificity phosphatase Yvh1 for the exchange of Mrt4 with P0. *The Journal of cell biology*. 186:849-862.

Locher, K.P. 2009. Review. Structure and mechanism of ATP-binding cassette transporters. *Philosophical transactions of the Royal Society of London. Series B, Biological sciences*. 364:239-245.
Longtine, M.S., A. McKenzie, 3rd, D.J. Demarini, N.G. Shah, A. Wach, A. Brachat, P. Philippsen, and J.R. Pringle. 1998. Additional modules for versatile and economical PCR-based gene deletion and modification in Saccharomyces cerevisiae. *Yeast*. 14:953-961.
Ma, H., and T. Pederson. 2008. Nucleostemin: a multiplex regulator of cell-cycle progression. *Trends in cell biology*. 18:575-579.
Mansfeld, J., S. Guttinger, L.A. Hawryluk-Gara, N. Pante, M. Mall, V. Galy, U. Haselmann, P. Muhlhausser, R.W. Wozniak, I.W. Mattaj, U. Kutay, and W. Antonin. 2006. The conserved transmembrane nucleoporin NDC1 is required for nuclear pore complex assembly in vertebrate cells. *Molecular cell*. 22:93-103.
Matsuo, Y., S. Granneman, M. Thoms, R.G. Manikas, D. Tollervey, and E. Hurt. 2014. Coupled GTPase and remodelling ATPase activities form a checkpoint for ribosome export. *Nature*. 505:112-116.
Matsuo, Y., T. Morimoto, M. Kuwano, P.C. Loh, T. Oshima, and N. Ogasawara. 2006. The GTP-binding protein YlqF participates in the late step of 50 S ribosomal subunit assembly in Bacillus subtilis. *The Journal of biological chemistry*. 281:8110-8117.
Matsuo, Y., T. Oshima, P.C. Loh, T. Morimoto, and N. Ogasawara. 2007. Isolation and characterization of a dominant negative mutant of Bacillus subtilis GTP-binding protein, YlqF, essential for biogenesis and maintenance of the 50 S ribosomal subunit. *The Journal of biological chemistry*. 282:25270-25277.
Maximiliano Juri Ayub, W.J.L., Johan Hoebeke and Cristian R. Smulski. 2012. Ribosomes from Trypanosomatids: Unique Structural and Functional Properties, Cell-Free Protein Synthesis.
May, K.L., X.P. Li, F. Martinez-Azorin, J.P. Ballesta, P. Grela, M. Tchorzewski, and N.E. Tumer. 2012. The P1/P2 proteins of the human ribosomal stalk are required for ribosome binding and depurination by ricin in human cells. *The FEBS journal*. 279:3925-3936.
Melnikov, S., A. Ben-Shem, N. Garreau de Loubresse, L. Jenner, G. Yusupova, and M. Yusupov. 2012. One core, two shells: bacterial and eukaryotic ribosomes. *Nature structural & molecular biology*. 19:560-567.
Meng, L., Q. Zhu, and R.Y. Tsai. 2007. Nucleolar trafficking of nucleostemin family proteins: common versus protein-specific mechanisms. *Molecular and cellular biology*. 27:8670-8682.
Menne, T.F., B. Goyenechea, N. Sanchez-Puig, C.C. Wong, L.M. Tonkin, P.J. Ancliff, R.L. Brost, M. Costanzo, C. Boone, and A.J. Warren. 2007. The Shwachman-Bodian-Diamond syndrome protein mediates translational activation of ribosomes in yeast. *Nature genetics*. 39:486-495.
Meyer, A.E., N.J. Hung, P. Yang, A.W. Johnson, and E.A. Craig. 2007. The specialized cytosolic J-protein, Jjj1, functions in 60S ribosomal subunit biogenesis. *Proceedings of the National Academy of Sciences of the United States of America*. 104:1558-1563.
Milkereit, P., O. Gadal, A. Podtelejnikov, S. Trumtel, N. Gas, E. Petfalski, D. Tollervey, M. Mann, E. Hurt, and H. Tschochner. 2001. Maturation and intranuclear transport of pre-ribosomes requires Noc proteins. *Cell*. 105:499-509.
Miller, O.L., Jr., and B.R. Beatty. 1969. Visualization of nucleolar genes. *Science*. 164:955-957.
Moore, P.B. 2009. The ribosome returned. *Journal of biology*. 8:8.
Moore, P.B. 2012. How Should We Think About the Ribosome? *Annu Rev Biophys*. 41:1-19.
Moore, P.B., and T.A. Steitz. 2003. After the ribosome structures: how does peptidyl transferase work? *Rna*. 9:155-159.
Morawska, M., and H.D. Ulrich. 2013. An expanded tool kit for the auxin-inducible degron system in budding yeast. *Yeast*. 30:341-351.
Mosammaparast, N., and L.F. Pemberton. 2004. Karyopherins: from nuclear-transport mediators to nuclear-function regulators. *Trends in cell biology*. 14:547-556.
Moy, T.I., and P.A. Silver. 1999. Nuclear export of the small ribosomal subunit requires the ran-GTPase cycle and certain nucleoporins. *Genes & development*. 13:2118-2133.
Moy, T.I., and P.A. Silver. 2002. Requirements for the nuclear export of the small ribosomal subunit. *Journal of cell science*. 115:2985-2995.

Neuwald, A.F., L. Aravind, J.L. Spouge, and E.V. Koonin. 1999. AAA+: A class of chaperone-like ATPases associated with the assembly, operation, and disassembly of protein complexes. *Genome research*. 9:27-43.

Nicol, S.M., and F.V. Fuller-Pace. 1995. The "DEAD box" protein DbpA interacts specifically with the peptidyltransferase center in 23S rRNA. *Proceedings of the National Academy of Sciences of the United States of America*. 92:11681-11685.

Nilsson, J., K. Weis, and J. Kjems. 2002. The C-terminal extension of the small GTPase Ran is essential for defining the GDP-bound form. *Journal of molecular biology*. 318:583-593.

Nishimura, K., T. Fukagawa, H. Takisawa, T. Kakimoto, and M. Kanemaki. 2009. An auxin-based degron system for the rapid depletion of proteins in nonplant cells. *Nature methods*. 6:917-922.

Nissan, T.A., J. Bassler, E. Petfalski, D. Tollervey, and E. Hurt. 2002. 60S pre-ribosome formation viewed from assembly in the nucleolus until export to the cytoplasm. *The EMBO journal*. 21:5539-5547.

Nissan, T.A., K. Galani, B. Maco, D. Tollervey, U. Aebi, and E. Hurt. 2004. A pre-ribosome with a tadpole-like structure functions in ATP-dependent maturation of 60S subunits. *Molecular cell*. 15:295-301.

Nissen, P., J. Hansen, N. Ban, P.B. Moore, and T.A. Steitz. 2000. The structural basis of ribosome activity in peptide bond synthesis. *Science*. 289:920-930.

Ofengand, J. 2002. Ribosomal RNA pseudouridines and pseudouridine synthases. *FEBS letters*. 514:17-25.

Panse, V.G., D. Kressler, A. Pauli, E. Petfalski, M. Gnadig, D. Tollervey, and E. Hurt. 2006. Formation and nuclear export of preribosomes are functionally linked to the small-ubiquitin-related modifier pathway. *Traffic*. 7:1311-1321.

Pante, N., and M. Kann. 2002. Nuclear pore complex is able to transport macromolecules with diameters of about 39 nm. *Molecular biology of the cell*. 13:425-434.

Parenteau, J., M. Durand, G. Morin, J. Gagnon, J.F. Lucier, R.J. Wellinger, B. Chabot, and S.A. Elela. 2011. Introns within ribosomal protein genes regulate the production and function of yeast ribosomes. *Cell*. 147:320-331.

Parsyan, A., Y. Svitkin, D. Shahbazian, C. Gkogkas, P. Lasko, W.C. Merrick, and N. Sonenberg. 2011. mRNA helicases: the tacticians of translational control. *Nature reviews. Molecular cell biology*. 12:235-245.

Patel, S.S., B.J. Belmont, J.M. Sante, and M.F. Rexach. 2007. Natively unfolded nucleoporins gate protein diffusion across the nuclear pore complex. *Cell*. 129:83-96.

Peluso, P., S.O. Shan, S. Nock, D. Herschlag, and P. Walter. 2001. Role of SRP RNA in the GTPase cycles of Ffh and FtsY. *Biochemistry*. 40:15224-15233.

Perez-Fernandez, J., P. Martin-Marcos, and M. Dosil. 2011. Elucidation of the assembly events required for the recruitment of Utp20, Imp4 and Bms1 onto nascent pre-ribosomes. *Nucleic acids research*. 39:8105-8121.

Perez-Fernandez, J., A. Roman, J. De Las Rivas, X.R. Bustelo, and M. Dosil. 2007. The 90S preribosome is a multimodular structure that is assembled through a hierarchical mechanism. *Molecular and cellular biology*. 27:5414-5429.

Pertschy, B., C. Saveanu, G. Zisser, A. Lebreton, M. Tengg, A. Jacquier, E. Liebminger, B. Nobis, L. Kappel, I. van der Klei, G. Hogenauer, M. Fromont-Racine, and H. Bergler. 2007. Cytoplasmic recycling of 60S preribosomal factors depends on the AAA protein Drg1. *Molecular and cellular biology*. 27:6581-6592.

Peters, R. 2005. Translocation through the nuclear pore complex: selectivity and speed by reduction-of-dimensionality. *Traffic*. 6:421-427.

Peters, R. 2009. Functionalization of a nanopore: the nuclear pore complex paradigm. *Biochimica et biophysica acta*. 1793:1533-1539.

Pettersen, E.F., T.D. Goddard, C.C. Huang, G.S. Couch, D.M. Greenblatt, E.C. Meng, and T.E. Ferrin. 2004. UCSF Chimera--a visualization system for exploratory research and analysis. *Journal of computational chemistry*. 25:1605-1612.

Pugh, T.J., S.D. Weeraratne, T.C. Archer, D.A. Pomeranz Krummel, D. Auclair, J. Bochicchio, M.O. Carneiro, S.L. Carter, K. Cibulskis, R.L. Erlich, H. Greulich, M.S. Lawrence, N.J. Lennon, A. McKenna, J. Meldrim, A.H. Ramos, M.G. Ross, C. Russ, E. Shefler, A. Sivachenko, B. Sogoloff, P. Stojanov, P. Tamayo, J.P. Mesirov, V. Amani, N. Teider, S. Sengupta, J.P. Francois, P.A. Northcott, M.D. Taylor, F. Yu, G.R. Crabtree, A.G. Kautzman, S.B. Gabriel, G. Getz, N. Jager, D.T. Jones, P. Lichter, S.M. Pfister, T.M. Roberts, M. Meyerson, S.L. Pomeroy, and Y.J. Cho.

2012. Medulloblastoma exome sequencing uncovers subtype-specific somatic mutations. *Nature*. 488:106-110.

Puig, O., F. Caspary, G. Rigaut, B. Rutz, E. Bouveret, E. Bragado-Nilsson, M. Wilm, and B. Seraphin. 2001. The tandem affinity purification (TAP) method: a general procedure of protein complex purification. *Methods*. 24:218-229.

Rabut, G., V. Doye, and J. Ellenberg. 2004. Mapping the dynamic organization of the nuclear pore complex inside single living cells. *Nature cell biology*. 6:1114-1121.

Ramakrishnan, V. 2002. Ribosome structure and the mechanism of translation. *Cell*. 108:557-572.

Raska, I., P.J. Shaw, and D. Cmarko. 2006. New insights into nucleolar architecture and activity. *Int Rev Cytol*. 255:177-+.

Ray, P., U. Basu, A. Ray, R. Majumdar, H. Deng, and U. Maitra. 2008. The Saccharomyces cerevisiae 60 S ribosome biogenesis factor Tif6p is regulated by Hrr25p-mediated phosphorylation. *The Journal of biological chemistry*. 283:9681-9691.

Reichow, S.L., T. Hamma, A.R. Ferre-D'Amare, and G. Varani. 2007. The structure and function of small nucleolar ribonucleoproteins. *Nucleic acids research*. 35:1452-1464.

Remacha, M., A. Jimenez-Diaz, B. Bermejo, M.A. Rodriguez-Gabriel, E. Guarinos, and J.P. Ballesta. 1995a. Ribosomal acidic phosphoproteins P1 and P2 are not required for cell viability but regulate the pattern of protein expression in Saccharomyces cerevisiae. *Molecular and cellular biology*. 15:4754-4762.

Remacha, M., A. Jimenez-Diaz, C. Santos, E. Briones, R. Zambrano, M.A. Rodriguez Gabriel, E. Guarinos, and J.P. Ballesta. 1995b. Proteins P1, P2, and P0, components of the eukaryotic ribosome stalk. New structural and functional aspects. *Biochemistry and cell biology = Biochimie et biologie cellulaire*. 73:959-968.

Ribbeck, K., and D. Gorlich. 2002. The permeability barrier of nuclear pore complexes appears to operate via hydrophobic exclusion. *The EMBO journal*. 21:2664-2671.

Riddick, G., and I.G. Macara. 2005. A systems analysis of importin-{alpha}-{beta} mediated nuclear protein import. *The Journal of cell biology*. 168:1027-1038.

Rigaut, G., A. Shevchenko, B. Rutz, M. Wilm, M. Mann, and B. Seraphin. 1999. A generic protein purification method for protein complex characterization and proteome exploration. *Nature biotechnology*. 17:1030-1032.

Rocak, S., and P. Linder. 2004. DEAD-box proteins: the driving forces behind RNA metabolism. *Nature reviews. Molecular cell biology*. 5:232-241.

Rodriguez-Mateos, M., D. Abia, J.J. Garcia-Gomez, A. Morreale, J. de la Cruz, C. Santos, M. Remacha, and J.P. Ballesta. 2009a. The amino terminal domain from Mrt4 protein can functionally replace the RNA binding domain of the ribosomal P0 protein. *Nucleic acids research*. 37:3514-3521.

Rodriguez-Mateos, M., J.J. Garcia-Gomez, R. Francisco-Velilla, M. Remacha, J. de la Cruz, and J.P. Ballesta. 2009b. Role and dynamics of the ribosomal protein P0 and its related trans-acting factor Mrt4 during ribosome assembly in Saccharomyces cerevisiae. *Nucleic acids research*. 37:7519-7532.

Rout, M.P., J.D. Aitchison, A. Suprapto, K. Hjertaas, Y. Zhao, and B.T. Chait. 2000. The yeast nuclear pore complex: composition, architecture, and transport mechanism. *The Journal of cell biology*. 148:635-651.

Roy, A., A. Kucukural, and Y. Zhang. 2010. I-TASSER: a unified platform for automated protein structure and function prediction. *Nature protocols*. 5:725-738.

Sambrook, J., E.F. Fritsch, and T. Maniatis. 1989. Molecular cloning : a laboratory manual. Cold Spring Harbor Laboratory Press, Cold Spring Harbor, N.Y.

Saveanu, C., D. Bienvenu, A. Namane, P.E. Gleizes, N. Gas, A. Jacquier, and M. Fromont-Racine. 2001. Nog2p, a putative GTPase associated with pre-60S subunits and required for late 60S maturation steps. *The EMBO journal*. 20:6475-6484.

Schafer, T., B. Maco, E. Petfalski, D. Tollervey, B. Bottcher, U. Aebi, and E. Hurt. 2006. Hrr25-dependent phosphorylation state regulates organization of the pre-40S subunit. *Nature*. 441:651-655.

Schafer, T., D. Strauss, E. Petfalski, D. Tollervey, and E. Hurt. 2003. The path from nucleolar 90S to cytoplasmic 40S pre-ribosomes. *The EMBO journal*. 22:1370-1380.

Schmitt, M.E., and D.A. Clayton. 1993. Nuclear RNase MRP is required for correct processing of pre-5.8S rRNA in Saccharomyces cerevisiae. *Molecular and cellular biology*. 13:7935-7941.

Scrima, A., and A. Wittinghofer. 2006. Dimerisation-dependent GTPase reaction of MnmE: how potassium acts as GTPase-activating element. *The EMBO journal*. 25:2940-2951.
Seiser, R.M., A.E. Sundberg, B.J. Wollam, P. Zobel-Thropp, K. Baldwin, M.D. Spector, and D.E. Lycan. 2006. Ltv1 is required for efficient nuclear export of the ribosomal small subunit in Saccharomyces cerevisiae. *Genetics*. 174:679-691.
Senger, B., D.L. Lafontaine, J.S. Graindorge, O. Gadal, A. Camasses, A. Sanni, J.M. Garnier, M. Breitenbach, E. Hurt, and F. Fasiolo. 2001. The nucle(ol)ar Tif6p and Efl1p are required for a late cytoplasmic step of ribosome synthesis. *Molecular cell*. 8:1363-1373.
Shajani, Z., M.T. Sykes, and J.R. Williamson. 2011. Assembly of bacterial ribosomes. *Annual review of biochemistry*. 80:501-526.
Sherman, F. 1998. An Introduction to the Genetics and Molecular Biology of the Yeast Saccharomyces cerevisiae. *The Encyclopedia of Molecular Biology and Molecular Medicine,*. Vol. 6:pp. 302-325.
Shin, D.H., Y. Lou, J. Jancarik, H. Yokota, R. Kim, and S.H. Kim. 2004. Crystal structure of YjeQ from Thermotoga maritima contains a circularly permuted GTPase domain. *Proceedings of the National Academy of Sciences of the United States of America*. 101:13198-13203.
Small, E.C., S.R. Leggett, A.A. Winans, and J.P. Staley. 2006. The EF-G-like GTPase Snu114p regulates spliceosome dynamics mediated by Brr2p, a DExD/H box ATPase. *Molecular cell*. 23:389-399.
Sorokin, A.V., E.R. Kim, and L.P. Ovchinnikov. 2007. Nucleocytoplasmic transport of proteins. *Biochemistry. Biokhimiia*. 72:1439-1457.
Spingola, M., L. Grate, D. Haussler, and M. Ares, Jr. 1999. Genome-wide bioinformatic and molecular analysis of introns in Saccharomyces cerevisiae. *Rna*. 5:221-234.
Sprang, S.R. 1997. G proteins, effectors and GAPs: structure and mechanism. *Current opinion in structural biology*. 7:849-856.
Stage-Zimmermann, T., U. Schmidt, and P.A. Silver. 2000. Factors affecting nuclear export of the 60S ribosomal subunit in vivo. *Molecular biology of the cell*. 11:3777-3789.
Staley, J.P., and J.L. Woolford, Jr. 2009. Assembly of ribosomes and spliceosomes: complex ribonucleoprotein machines. *Current opinion in cell biology*. 21:109-118.
Stavru, F., G. Nautrup-Pedersen, V.C. Cordes, and D. Gorlich. 2006. Nuclear pore complex assembly and maintenance in POM121- and gp210-deficient cells. *The Journal of cell biology*. 173:477-483.
Steitz, T.A. 2008a. Structural insights into the functions of the large ribosomal subunit, a major antibiotic target. *The Keio journal of medicine*. 57:1-14.
Steitz, T.A. 2008b. A structural understanding of the dynamic ribosome machine. *Nature reviews. Molecular cell biology*. 9:242-253.
Strom, A.C., and K. Weis. 2001. Importin-beta-like nuclear transport receptors. *Genome biology*. 2:REVIEWS3008.
Strunk, B.S., C.R. Loucks, M. Su, H. Vashisth, S. Cheng, J. Schilling, C.L. Brooks, 3rd, K. Karbstein, and G. Skiniotis. 2011. Ribosome assembly factors prevent premature translation initiation by 40S assembly intermediates. *Science*. 333:1449-1453.
Strunk, B.S., M.N. Novak, C.L. Young, and K. Karbstein. 2012. A translation-like cycle is a quality control checkpoint for maturing 40S ribosome subunits. *Cell*. 150:111-121.
Takai, Y., T. Sasaki, and T. Matozaki. 2001. Small GTP-binding proteins. *Physiological reviews*. 81:153-208.
Tang, L., A. Sahasranaman, J. Jakovljevic, E. Schleifman, and J.L. Woolford, Jr. 2008. Interactions among Ytm1, Erb1, and Nop7 required for assembly of the Nop7-subcomplex in yeast preribosomes. *Molecular biology of the cell*. 19:2844-2856.
Terry, L.J., and S.R. Wente. 2009. Flexible gates: dynamic topologies and functions for FG nucleoporins in nucleocytoplasmic transport. *Eukaryotic cell*. 8:1814-1827.
Thomson, E., S. Ferreira-Cerca, and E. Hurt. 2013. Eukaryotic ribosome biogenesis at a glance. *Journal of cell science*. 126:4815-4821.
Tollervey, D., H. Lehtonen, R. Jansen, H. Kern, and E.C. Hurt. 1993. Temperature-sensitive mutations demonstrate roles for yeast fibrillarin in pre-rRNA processing, pre-rRNA methylation, and ribosome assembly. *Cell*. 72:443-457.
Trabuco, L.G., E. Schreiner, J. Eargle, P. Cornish, T. Ha, Z. Luthey-Schulten, and K. Schulten. 2010. The role of L1 stalk-tRNA interaction in the ribosome elongation cycle. *Journal of molecular biology*. 402:741-760.

Tran, E.J., and S.R. Wente. 2006. Dynamic nuclear pore complexes: life on the edge. *Cell*. 125:1041-1053.
Trapman, J., and R.J. Planta. 1976. Maturation of ribosomes in yeast. I Kinetic analysis by labelling of high molecular weight rRNA species. *Biochimica et biophysica acta*. 442:265-274.
Trapman, J., R.J. Planta, and H.A. Raue. 1976. Maturation of ribosomes in yeast. II. Position of the low molecular weight rRNA species in the maturation process. *Biochimica et biophysica acta*. 442:275-284.
Trapman, J., J. Retel, and R.J. Planta. 1975. Ribosomal precursor particles from yeast. *Experimental cell research*. 90:95-104.
Traub, P., K. Hosokawa, G.R. Craven, and M. Nomura. 1967. Structure and function of E. coli ribosomes, IV. Isolation and characterization of functionally active ribosomal proteins. *Proceedings of the National Academy of Sciences of the United States of America*. 58:2430-2436.
Tschochner, H., and E. Hurt. 2003. Pre-ribosomes on the road from the nucleolus to the cytoplasm. *Trends in cell biology*. 13:255-263.
Tucker, P.A., and L. Sallai. 2007. The AAA+ superfamily--a myriad of motions. *Current opinion in structural biology*. 17:641-652.
Udem, S.A., and J.R. Warner. 1972. Ribosomal RNA synthesis in Saccharomyces cerevisiae. *Journal of molecular biology*. 65:227-242.
Udem, S.A., and J.R. Warner. 1973. The cytoplasmic maturation of a ribosomal precursor ribonucleic acid in yeast. *The Journal of biological chemistry*. 248:1412-1416.
Uicker, W.C., L. Schaefer, and R.A. Britton. 2006. The essential GTPase RbgA (YlqF) is required for 50S ribosome assembly in Bacillus subtilis. *Molecular microbiology*. 59:528-540.
Ulbrich, C., M. Diepholz, J. Bassler, D. Kressler, B. Pertschy, K. Galani, B. Bottcher, and E. Hurt. 2009. Mechanochemical removal of ribosome biogenesis factors from nascent 60S ribosomal subunits. *Cell*. 138:911-922.
Vale, R.D. 2000. AAA proteins. Lords of the ring. *The Journal of cell biology*. 150:F13-19.
van Hoof, A., P. Lennertz, and R. Parker. 2000. Three conserved members of the RNase D family have unique and overlapping functions in the processing of 5S, 5.8S, U4, U5, RNase MRP and RNase P RNAs in yeast. *The EMBO journal*. 19:1357-1365.
Vanrobays, E., J.P. Gelugne, M. Caizergues-Ferrer, and D.L. Lafontaine. 2004. Dim2p, a KH-domain protein required for small ribosomal subunit synthesis. *Rna*. 10:645-656.
Vanrobays, E., J.P. Gelugne, P.E. Gleizes, and M. Caizergues-Ferrer. 2003. Late cytoplasmic maturation of the small ribosomal subunit requires RIO proteins in Saccharomyces cerevisiae. *Molecular and cellular biology*. 23:2083-2095.
Vanrobays, E., P.E. Gleizes, C. Bousquet-Antonelli, J. Noaillac-Depeyre, M. Caizergues-Ferrer, and J.P. Gelugne. 2001. Processing of 20S pre-rRNA to 18S ribosomal RNA in yeast requires Rrp10p, an essential non-ribosomal cytoplasmic protein. *The EMBO journal*. 20:4204-4213.
Venema, J., and D. Tollervey. 1999. Ribosome synthesis in Saccharomyces cerevisiae. *Annual review of genetics*. 33:261-311.
Verstraeten, N., M. Fauvart, W. Versees, and J. Michiels. 2011. The universally conserved prokaryotic GTPases. *Microbiology and molecular biology reviews : MMBR*. 75:507-542, second and third pages of table of contents.
Vetter, I.R., C. Nowak, T. Nishimoto, J. Kuhlmann, and A. Wittinghofer. 1999. Structure of a Ran-binding domain complexed with Ran bound to a GTP analogue: implications for nuclear transport. *Nature*. 398:39-46.
Vetter, I.R., and A. Wittinghofer. 2001. The guanine nucleotide-binding switch in three dimensions. *Science*. 294:1299-1304.
Wach, A., A. Brachat, R. Pohlmann, and P. Philippsen. 1994. New heterologous modules for classical or PCR-based gene disruptions in Saccharomyces cerevisiae. *Yeast*. 10:1793-1808.
Walker, J.E., M. Saraste, M.J. Runswick, and N.J. Gay. 1982. Distantly related sequences in the alpha- and beta-subunits of ATP synthase, myosin, kinases and other ATP-requiring enzymes and a common nucleotide binding fold. *The EMBO journal*. 1:945-951.
Warner, J.R. 1999. The economics of ribosome biosynthesis in yeast. *Trends in biochemical sciences*. 24:437-440.
Warner, J.R., and K.B. McIntosh. 2009. How common are extraribosomal functions of ribosomal proteins? *Molecular cell*. 34:3-11.

Waterhouse, A.M., J.B. Procter, D.M. Martin, M. Clamp, and G.J. Barton. 2009. Jalview Version 2--a multiple sequence alignment editor and analysis workbench. *Bioinformatics*. 25:1189-1191.

Webb, S., R.D. Hector, G. Kudla, and S. Granneman. 2014. PAR-CLIP data indicate that Nrd1-Nab3-dependent transcription termination regulates expression of hundreds of protein coding genes in yeast. *Genome biology*. 15:R8.

Wegierski, T., E. Billy, F. Nasr, and W. Filipowicz. 2001. Bms1p, a G-domain-containing protein, associates with Rcl1p and is required for 18S rRNA biogenesis in yeast. *Rna*. 7:1254-1267.

Weis, K. 2003. Regulating access to the genome: nucleocytoplasmic transport throughout the cell cycle. *Cell*. 112:441-451.

Wente, S.R., and M.P. Rout. 2010. The nuclear pore complex and nuclear transport. *Cold Spring Harbor perspectives in biology*. 2:a000562.

West, M., J.B. Hedges, A. Chen, and A.W. Johnson. 2005. Defining the order in which Nmd3p and Rpl10p load onto nascent 60S ribosomal subunits. *Molecular and cellular biology*. 25:3802-3813.

Wilson, D.N., and K.H. Nierhaus. 2005. Ribosomal proteins in the spotlight. *Critical reviews in biochemistry and molecular biology*. 40:243-267.

Wool, I.G. 1996. Extraribosomal functions of ribosomal proteins. *Trends in biochemical sciences*. 21:164-165.

Yamamoto, H., Y. Qin, J. Achenbach, C. Li, J. Kijek, C.M. Spahn, and K.H. Nierhaus. 2014. EF-G and EF4: translocation and back-translocation on the bacterial ribosome. *Nature reviews. Microbiology*. 12:89-100.

Yamanaka, K., J. Hwang, and M. Inouye. 2000. Characterization of GTPase activity of TrmE, a member of a novel GTPase superfamily, from Thermotoga maritima. *Journal of bacteriology*. 182:7078-7082.

Yao, W., D. Roser, A. Kohler, B. Bradatsch, J. Bassler, and E. Hurt. 2007. Nuclear export of ribosomal 60S subunits by the general mRNA export receptor Mex67-Mtr2. *Molecular cell*. 26:51-62.

Yao, Y., E. Demoinet, C. Saveanu, P. Lenormand, A. Jacquier, and M. Fromont-Racine. 2010. Ecm1 is a new pre-ribosomal factor involved in pre-60S particle export. *Rna*. 16:1007-1017.

Yarunin, A., V.G. Panse, E. Petfalski, C. Dez, D. Tollervey, and E.C. Hurt. 2005. Functional link between ribosome formation and biogenesis of iron-sulfur proteins. *The EMBO journal*. 24:580-588.

Yokoyama, T., and T. Suzuki. 2008. Ribosomal RNAs are tolerant toward genetic insertions: evolutionary origin of the expansion segments. *Nucleic acids research*. 36:3539-3551.

Yonath, A. 2002. The search and its outcome: high-resolution structures of ribosomal particles from mesophilic, thermophilic, and halophilic bacteria at various functional states. *Annual review of biophysics and biomolecular structure*. 31:257-273.

Zakalskiy, A., G. Hogenauer, T. Ishikawa, E. Wehrschutz-Sigl, F. Wendler, D. Teis, G. Zisser, A.C. Steven, and H. Bergler. 2002. Structural and enzymatic properties of the AAA protein Drg1p from Saccharomyces cerevisiae. Decoupling of intracellular function from ATPase activity and hexamerization. *The Journal of biological chemistry*. 277:26788-26795.

Zemp, I., and U. Kutay. 2007. Nuclear export and cytoplasmic maturation of ribosomal subunits. *FEBS letters*. 581:2783-2793.

Zemp, I., F. Wandrey, S. Rao, C. Ashiono, E. Wyler, C. Montellese, and U. Kutay. 2014. CK1delta and CK1epsilon are components of human 40S subunit precursors required for cytoplasmic 40S maturation. *Journal of cell science*. 127:1242-1253.

Zemp, I., T. Wild, M.F. O'Donohue, F. Wandrey, B. Widmann, P.E. Gleizes, and U. Kutay. 2009. Distinct cytoplasmic maturation steps of 40S ribosomal subunit precursors require hRio2. *The Journal of cell biology*. 185:1167-1180.

Zhang, B., and T.R. Cech. 1997. Peptide bond formation by in vitro selected ribozymes. *Nature*. 390:96-100.

Zhang, J., P. Harnpicharnchai, J. Jakovljevic, L. Tang, Y. Guo, M. Oeffinger, M.P. Rout, S.L. Hiley, T. Hughes, and J.L. Woolford, Jr. 2007. Assembly factors Rpf2 and Rrs1 recruit 5S rRNA and ribosomal proteins rpL5 and rpL11 into nascent ribosomes. *Genes & development*. 21:2580-2592.